ABSTRACT

Title of Document: DISCRETE AND POLYMERIC COMPLEXES COMPRISING BIS-*NOR*-*SECO*-CB[10] AND OLIGOAMMONIUM IONS

Regan C. Nally, Ph.D., 2009

Directed By: Professor Lyle D. Isaacs
Department of Chemistry and Biochemistry

Supramolecular architectures composed of multiple components are challenging to produce, as the enthalpic gain must be greater than the entropic penalty of strict geometrical arrangements. Therefore, it is the goal of supramolecular chemists to strategically design and synthesize molecules that will exhibit selectivity toward formation of a particular complex. This dissertation describes the formation of supramolecular architectures of increasing size and is organized in the following way.

Chapter 1 introduces the reader to the field of supramolecular polymer chemistry.

Chapter 2 describes the synthesis of a series of monovalent ditopic guests (**II-1 – II-6**) and their complexation properties toward double cavity cucurbituril host bis-*ns*-CB[10]. We observed the preferential formation of 1:1, 2:2, and oligomeric

complexes rather than the desired n:n supramolecular polymers. Guest **II-7** which contains a longer biphenyl spacer successfully precludes the formation of the 1:1 complex but results in the formation of the 2:2 complex (bis-*ns*-CB[10]$_2$•**II-7**$_2$) rather than supramolecular polymer. Guest **II-8** is heterovalent and ditopic and is shown to reversibly form 2:2 and 1:2 complexes (bis-*ns*-CB[10]$_2$•**II-8**$_2$ and bis-*ns*-CB[10]•**II-8**$_2$) in response to changes in host:guest stoichiometry. Lastly, this equilibrium can be manipulated by the addition of exogenous CB[6] which selectively targets the hexanediammonium ion binding region of **II-8** and delivers the penta-molecular complex bis-*ns*-CB[10]•**II-8**$_2$•CB[6]$_2$.

Chapter 3 describes the formation of a main chain supramolecular polymer from a mixture of poly(diallyldimethylammonium chloride) (**III-1**) and bis-*ns*-CB[10]. The bis-*ns*-CB[10] molecular container behaves as a molecular handcuff, bringing together two ends of individual polymers to form **III-1**$_n$• bis-*ns*-CB[10]$_m$, resulting in an extension of the length of polymer. The effect of bis-*ns*-CB[10] on the physical properties of the polymer was investigated using viscometry in aqueous solution. A decrease in the η_{rel} was observed upon increasing concentrations of bis-*ns*-CB[10] to a solution of **III-1**. Atomic force microscopy (AFM), and diffusion-ordered spectroscopy (DOSY) were performed to probe the mode of interaction between polymer **III-1** and bis-*ns*-CB[10]. Collectively, the data supports the two roles for bis-*ns*-CB[10]: 1) as a deaggregation agent, and 2) as a molecular handcuff that non-covalently links individual polymer strands resulting in overall extension of the polymer.

DISCRETE AND POLYMERIC COMPLEXES COMPRISING BIS-*NOR*-*SECO*-CB[10] AND OLIGOAMMONIUM IONS

By

Regan C. Nally

Dissertation submitted to the Faculty of the Graduate School of the
University of Maryland, College Park, in partial fulfillment
of the requirements for the degree of
Doctor of Philosophy
2009

Advisory Committee:
Professor Lyle Isaacs, Chair
Professor Jeffery Davis
Professor Steven Rokita
Associate Professor Andrei Vedernikov
Associate Professor Sheryl Ehrman, Dean's Representative

Dedication

To Peter

Acknowledgements

A sincere thank you to Lyle, for your persistence in expectations of scientific quality, instruction and guidance over the years, and for all that you have taught me, from experimental techniques to writing.

I am grateful for the outstanding teachers I had my first year- Dr. Davis, Dr. Vedernikov, Dr. DeShong, and Dr. Falvey.

A thank you to all members of the Isaacs lab, past and present. You have each helped to create much laughter and memories, mental stimulation and emotional support. Jason Lagona for taking the time to teach me much of what he had learned through his experiences. My partner in crime, Showme Ghosh, thanks for your continual pranks, napkin chemistry discussions and friendship. Wei-Hao, you especially helped me get through the first year, and also I should thank you for your compound that became the basis of the work in this dissertation! Jing Wu, thank you for positive conversations and strength to battle the boys and friendship of course. Motor- your late night singing was pleasing to the ears. Jimmy and Derick, a troublesome duo, thank you for the tech support and making me feel my age. Becky, thanks for always lending a hand and keeping the sarcasm to a maximum.

Out of the lab but still in the building…thank you Yiu-fai and Yinde for assistance on the NMR spectrometers and experimental suggestions. Karen Gaskell and Aldo for getting the AFM up and running and assisting me with imaging.

I would like to thank the Scherman lab for making me feel at home when I was in England and to Oren Scherman for his guidance during this time of collaboration.

Thank you fellow residents of the nuthouse for all the wine and whine tolerance, Jeffrey Sosa, Akito Kawahara, Cass Taylor, and for the late night bug collecting and other michevious endeavors.

Thank you to my mom, dad, sister, and brother (Mary, Dan, Shannon, and Daniel) for offering a relaxing getaway, full of good food, cheer, and music. And for more than I can ever write, in many ways you got me here.

The folks at Fungi Perfecti and friends from Oly, thanks for the magic that is you.

Whitney Bauer, I'm indebted to your ability to turn any situation into laughter, you have provided much relief and absolute fun, and Cora too!

And to you and for you, Peter Pessiki, what a long, strange trip it's been. You taught me to "… prefer the folly of enthusiasm to the indifference of wisdom." – Anatole France. Your excitement for life is contagious. Can't thank you enough for your undying charm, positive support, homegrown food deliveries, monstrously huge heart, and more, and on and on.

Table of Contents

List of Tables

Chapter 1

Chapter 2

List of Charts

Chapter 1

Chapter 2

List of Figures

Chapter 1

Chapter 2

Chapter 4

List of Schemes

Chapter 1

Chapter 2

List of Abbreviations

Ac	acetyl
AFM	atomic force microscopy
anh.	anhydrous
aq.	aqueous
br. s	broad singlet
t-Bu	tertiary butyl
calcd	calculated
conc	concentration
CPK	Corey, Pauling and Koltun
d	doublet
dd	doublet of doublets
dec	decomposition
DMSO	dimethyl sulfoxide
DNA	deoxyribonucleic acid
EI	electron ionization
EtOAc	ethyl acetate
FAB	fast atom bombardment
h	hour(s)
HR-MS	high resolution mass spectroscopy
Hz	hertz
IR	infrared
J	coupling constant

m	multiplet
m	meta
M^+	molecular ion
m/z	mass-to-charge ratio
MHz	megahertz
min	minute(s)
M.p.	melting point
MS	mass spectroscopy
NMR	nuclear magnetic resonance
o	ortho
OAc	acetate
p	para
Ph	phenyl
PTSA	*p*-toluenesulfonic acid
q	quartet
R_f	retention factor
RT	room temperature
s	second(s)
t	triplet
TFA	trifluoroacetic acid
TLC	thin layer chromatography
TMS	trimethylsilyl

I. Chapter 1: Literature Review of Supramolecular Polymers

1.1 Introduction.

Supramolecular Chemistry is the chemistry of non-covalent interactions and the assemblage of macromolecular structures as a result of these interactions. A molecule comprised of covalently bonded atoms can interact with other molecules through weaker, reversible, non-covalent means: hydrogen-bonds, $\pi - \pi$ interactions, metal coordination, hydrophobic forces, van der Waals forces and other electrostatic effects. It is these forces between molecular entities that "build" larger structures and translate to the bulk properties of the material. Supramolecular chemistry, as a defined discipline, has surged since the work of Lehn, Cram, and Pedersen on molecular recognition. They were awarded with a Nobel Prize in Chemistry in 1987 for their investigation of crown ethers and cryptands as cationic receptors. These host-guest complexes were studied for their selectivity toward particular cationic species and biologically active molecules; the structure specific interactions mimicked enzyme-substrate complementarity. Following the pioneering work of Lehn, Cram, and Pedersen, many research groups have made molecular recognition the focus of their work. As a result, the scope of supramolecular chemistry has broadened to include applications in biology and materials science.

1.2 Natural and Synthetic examples of Supramolecular Structures.

Supramolecular structures are ubiquitous in natural and synthetic systems. Nature utilizes reversible, non-covalent interactions to mediate changes in the conformation of a molecule. This situation-specific adaptability allows molecular structures to be adjusted in order to meet the demands of an organism. One example from nature is that of the hemoglobin protein, whose monomeric polypeptide units self-assemble via non-covalent forces (hydrophobic effect, hydrogen bonds).[1] The family of hemoglobin proteins display repetition of an α- and β- subunit, ranging in size from dimers to assemblies of 180 subunits.[2] Chemists have been awestruck at the molecular complexity inherent in biological systems and have been successful in devising relatively simple non-natural systems as a means to understand this complexity. Julius Rebek, Jr. has synthesized a number of recognition units, each unique in their shape and function. One of his earliest receptors is depicted in Figure I-1.

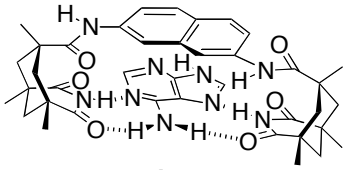

I-1

Figure I-1. Molecular recognition between receptor and adenine, introduced by Rebek.

Using Kemp's triacid as a basis for the construction of this receptor, hydrogen bonding and π – π interactions are responsible for its binding to adenine molecules. Adenosine and other adenine derivatives were able to be extracted from an aqueous solution into chloroform due to non-covalent interactions with the receptor. This work is significant because aqueous media offers strong competition for hydrogen-bonding, but the high affinity of the receptor for adenine enables the transportation of adenosine across organic liquid membranes.[3]

1.3 Introduction to Supramolecular Polymers.

1.3.1 Definition of Supramolecular Polymers.

Polymers are macromolecules built up from the linking together of much smaller molecules. The smaller molecules are termed monomers or repeat units. Staudinger introduced the term "macromolecules" in the early 1920's to describe the structural formulas for polyisoprene (natural rubber), polystyrene, and polyoxymethylene.[4,5] Shortly after, non-covalent interactions of covalent polymers was a focus of extensive study, as the secondary structure imparted by these non-covalent interactions greatly effected the properties of the polymer.

Polymers have and continue to contribute significantly to the materials sector of industry. They possess versatile mechanical and physical properties and have been used in the construction of textiles, rubbers, and plastics. Their importance in the development of technologies cannot be underestimated. Analogous in structure to covalent polymers, whose repeat units are linked through covalent bonds, are

polymers whose monomeric units are linked through non-covalent interactions are known as supramolecular polymers (Figure I-2).

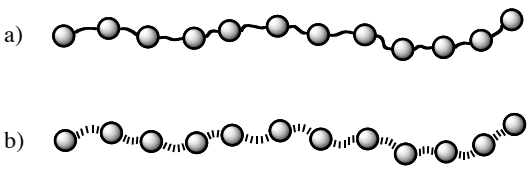

Figure I-2. Schematic representation of a covalent polymer (a) and supramolecular polymer (b).

The formation of these polymers are reversible and are therefore under thermodynamic control. As is often the case, nature has a working example of a supramolecular polymer for chemists to marvel at, the self-assembly of the tobacco mosaic virus, whereby 2130 molecules of a coat protein assemble into a rod like helical structure along one strand of RNA.[6,7] Although synthetic systems have not yet achieved as high a level of complexity as natural systems, the size alone of supramolecular polymers approach those of biological macromolecules. Supramolecular polymers have been the target in a number of research labs for at least the past two decades, beginning with a description by Lehn and co-workers in 1990.[8]

1.3.2 Motivation for Supramolecular Polymer Research.

The attraction to this field of research is rooted in the potential applications of these supramolecular polymeric systems. Polymers, generally covalent polymers, have had a tremendous influence on the advancement of materials. Polymers can

possess a range of materials properties and their versatility has allowed them to produce clothing, food wares, prosthetic body parts, automotive components, building materials and an endless score of other objects. As a material, they possess valuable properties (strength, flexibility, resistance to temperature fluctuation). However, upon melting they can become highly viscous as a result of entanglement of their linear strands, making them difficult to apply to surfaces. In order to reduce the viscosity of the polymeric material for application onto a surface, high temperatures and pressures are often required. Supramolecular polymers may offer a solution to this problem. Due to their dynamic nature, they are sensitive to changes in temperature, concentration, solvent, pH, and to chemical stimulus, all of which can disrupt or encourage the forces that hold the monomers intact. Supramolecular polymers therefore, are stimuli-responsive materials that concomitantly possess low-viscosity melts which facilitates their handling. The mechanical properties of supramolecular polymers are a result of the variable strength and directionality of their reversible bonds. Foreseeable applications are in the realm of thermoplastic elastomers, superglues, hot melts, self-healing rubbers, inks, and coatings.[9-11]

1.4 Types of Supramolecular Polymers.

Supramolecular polymers can assume a variety of spatial arrangements, contingent upon the geometry and valency of the repeat units and the presence of supramolecular interactions leading to secondary and tertiary architectures. For

example, the assembly of linear difunctional monomers can form a linear main chain supramolecular polymer as shown in Figure I-3a – c.

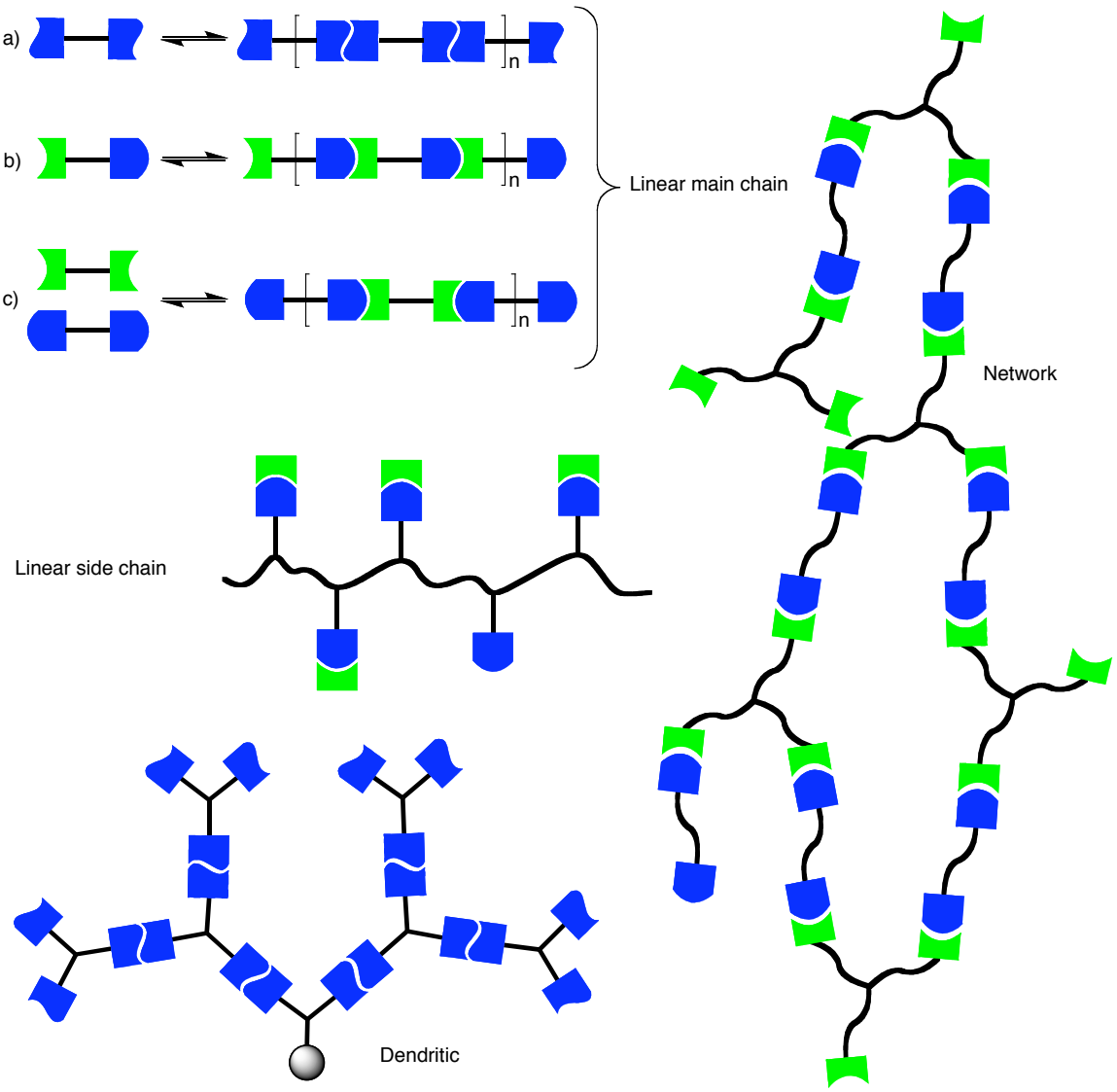

Figure I-3. Schematic representation of supramolecular polymer topologies.

Other possible topologies include side chain, network, and dendritic. Assemblies of linear monomers can form secondary or tertiary structures that take on a helical or tubular shape. To simplify a polymer system, one can describe the ditopic monomers

in terms of the types of sticky ends (functionality responsible for adjoining monomers together) it contains. For example, the monomer shown in Figure 3a can be represented as an A—A type repeat unit, leading to an A—(A•••A)$_n$—A polymer. The monomer in Figure 3b can be represented as an A—B type structure, producing an A—(B•••B—A•••A)$_n$—B supramolecular polymer. The combination of two homotopic A—A type and B—B type monomers, depicted in Figure I-3c, gives rise to an A—(A•••B—B•••A)$_n$—A supramolecular polymer. The formation of these structures will now be addressed.

1.5 Factors Controlling Supramolecular Polymer Formation.

1.5.1 Ring-Chain Equilibrium.

Monomeric units with end functionality may assemble in an open or closed fashion. Open assemblies refer to the addition of successive repeat units at the end of a growing chain and lead to polymer formation. Closed assemblies on the other hand, refer to discrete complexes with satisfied internal binding sites. Common structures are cyclic dimers, trimers, etc. (Figure I-4b).

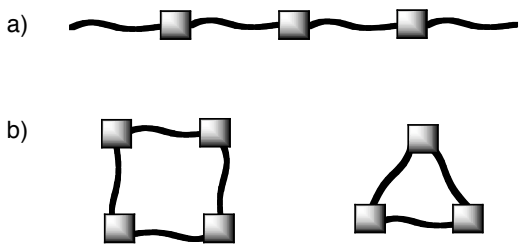

Figure I-4. Schematic representation of an open (a) and closed (b) assemblies.

Not always is there a clear-cut differentiation between closed and open assemblies, due to the reversible interactions of monomers. For this reason, the rings (closed assemblies) and chains (open assemblies) exist in equilibrium and the concentration at which the rings and chains are equal is termed the critical concentration, C_{cr} (crossover concentration, overlap concentration, equal-fraction concentration, transition from "free oligomers dominated" state to "chain dominated" state, etc.). Below this concentration only rings and free monomers exist in solution and above this concentration the concentration of rings remains relatively the same, while the concentration of chains grows. The C_{cr}, for a system consisting of divalent monomers, is dependent upon numerous factors including dimerization affinity, linker length and flexibility.[12]

1.5.2 Carothers' Equation.

The design of reversible polymeric systems may appear straightforward on paper, but there are a number of factors that must be taken into consideration. This section is intended to explain such guiding parameters. To curb inherent challenges in supramolecular polymer formation, the system should contain pure monomeric material, exact stoichiometry of reactants, high dimerization binding affinity ($>10^4$), and a singular reactivity (no competing side reactions). To make clear the importance of these variables, we can look at the Carothers' equation (Equation I-1).

$$\overline{DP} = \frac{1}{1-p} \qquad \text{(Eq. I-1)}$$

$$p = \frac{(N_0 - N_t)}{N_0} \qquad \text{(Eq. I-2)}$$

For step-growth polymerizations of bifunctional monomers, the Carothers' equation gives the degree of polymerization (DP) for a given fractional monomer conversion, *p*. [Carothers, W.H. Trans. Faraday Soc. 1936, 32, 39-49.] A measure of the extent of a reaction is given by *p* (Equation I-2) which is equal to the difference in the number of monomers at time *t* from the number of monomers originally present (N_0-N_t) divided by the number of initial monomers (N_0). The *p* value can be substituted into Equation I-1. For example, a *p* value of 98% is required for DP = 50 and a *p* value of 99% is required for a DP = 100. The following example illustrates the importance of exact stoichiometry of the monomers undergoing polymerization. If there are 100 moles of monomer A and 98 moles of monomer B, the polymerization stops at *p* = 0.98, yielding a DP = 50. This means that a high monomer conversion is required to achieve a high DP. In turn, a high monomer conversion is achieved with high monomer association constants, pure starting materials, and exact stoichiometry of monomers.

1.6 Mechanism of Formation.

Supramolecular polymerization is the process of assembling repeat units that give rise to a polymer. The growth of a supramolecular polymer may operate through a multistage open association mechanism (*MSOA*). This is a reversible step-growth process that can be represented by the following equation:

$$M_1 + M_1 \rightleftharpoons M_2 \qquad C_2 = K\,(C_1)^2$$

$$M_2 + M_1 \rightleftharpoons M_3 \qquad C_3 = K^2(C_1)^3$$

$$M_{s-1} + M_1 \rightleftharpoons M_s \qquad C_s = K^{-1}(KC_1)^s \qquad \text{(Eq. I-3)}$$

Where C_s is the concentration of the *s*-mer and identical equilibrium constants K for each step are assumed.[14] In this situation, the binding constant is independent of the molecular weight (no cooperation). Assuming no ring formation, the degree of polymerization (DP) will be approximately proportional to $(K_a[M])^{1/2}$, where K_a is the association constant and [M] is the total monomer concentration. [Sivakova, S.; Bohnsack, D.A.; Mackay, M.E.; Suwanmala, P.; Rowan, S.J. *J. Am. Chem. Soc.* **2005**, *127*, 18202-18211.] Below the C_{cr}, the degree of ring formation is highly dependent upon the K_a and not the concentration of monomer. Growth of a supramolecular polymer operating by a *MSOA* mechanism can be characterized by the lack of side-reaction products and are common for systems containing monomers with high dimerization constants. Other growth mechanisms that govern polymer processes but will not be discussed here are: helical or tubular growth, engineered growth, and growth coupled with liquid crystalline orientation.

1.7 Properties and Characterization Techniques.

The reversibility of the association between monomeric units of supramolecular polymers imparts both unique materials properties while also presenting challenges in their characterization. Multiple techniques are typically required to provide evidence for the formation of supramolecular polymers, some of

which interfere with the non-covalent interactions, thus disrupting the overall polymeric structure. In this section, some common techniques for the characterization of supramolecular polymers will be presented. Size exclusion chromatography (SEC) is a common technique for obtaining molecular weights and size distribution of covalent polymers. The constant redistribution of products on the column is an inherent limitation of the technique. This is because non-covalent polymers exist in dynamic equilibrium with rings or smaller aggregates and this equilibrium is concentration-dependent. Therefore, obtaining accurate values of molecular weights from SEC requires low product dispersity and high dimerization constants. Vapor pressure osmometry (VPO) has been traditionally employed for molecular weight analysis and does not involve separation techniques. This can be advantageous for organic systems containing polymeric species up to 10^5 molecular weight and up to 10^4 molecular weight for aqueous systems.[11,16] Pulsed-field-gradient NMR techniques (DOSY) can provide a non-invasive means to study polymer assembly in solution. Ideally, the rates of diffusion of different species can be determined and their sizes extrapolated according to the Stokes-Einstein equation.[17] The validity of this technique is contingent upon slow exchange rates and separated resonances for distinct species. Viscometry can be an informative technique but cannot provide absolute degrees of polymerization. If the monomer concentration is plotted against the viscosity on double-logarithmic axes and a linear relationship is observed, this behavior is indicative of linear polymer formation.[18] As the solution concentration changes, not only does the viscosity change but the DP is effected as well. Therefore, obtaining accurate values of the size of a polymer is a

challenging aspect of this technique. A direct method of probing the size of supramolecular assemblies is microscopic imaging, such as atomic force (AFM), scanning electron (SEM), or tunneling electron (TEM). In employing these methods, the challenge lies within the sample preparation, but the analysis is telling and can provide valuable size and topology information. Collectively, these techniques can complement one another and provide convincing evidence for the formation of a supramolecular polymer and its approximate size.

1.8 Literature Examples of Supramolecular Polymers.

1.8.1 Non-covalent Interactions leading to Supramolecular Polymer Formation.

Despite the challenges inherent in characterizing supramolecular polymers, their occurrence in the literature has grown increasingly prevalent. Hydrogen-bonding, metal coordination, aromatic stacking, and host-guest interactions have allowed for construction of supramolecular polymers. The geometry of the monomeric units dictate the two- and three-dimensional topology of the polymer.

1.8.2 Supramolecular Polymer Based on Hydrogen-bonding Interactions.

Hydrogen bonds are an often desired functionality in the design of monomeric units for assemblage into larger complexes. This is due to the well defined geometrical features of the hydrogen-bonding interactions which impart a distinct spatial relationship between the two interacting monomers. The first chemical

description of a macromolecule termed a supramolecular polymer appeared in 1990 from the lab of Jean-Marie Lehn.[8] The formation of triple hydrogen-bonds assembled the 2,6-diacylaminopyridine, **I-2**, and uracil, **I-3**, containing monomers together (Scheme I-1).

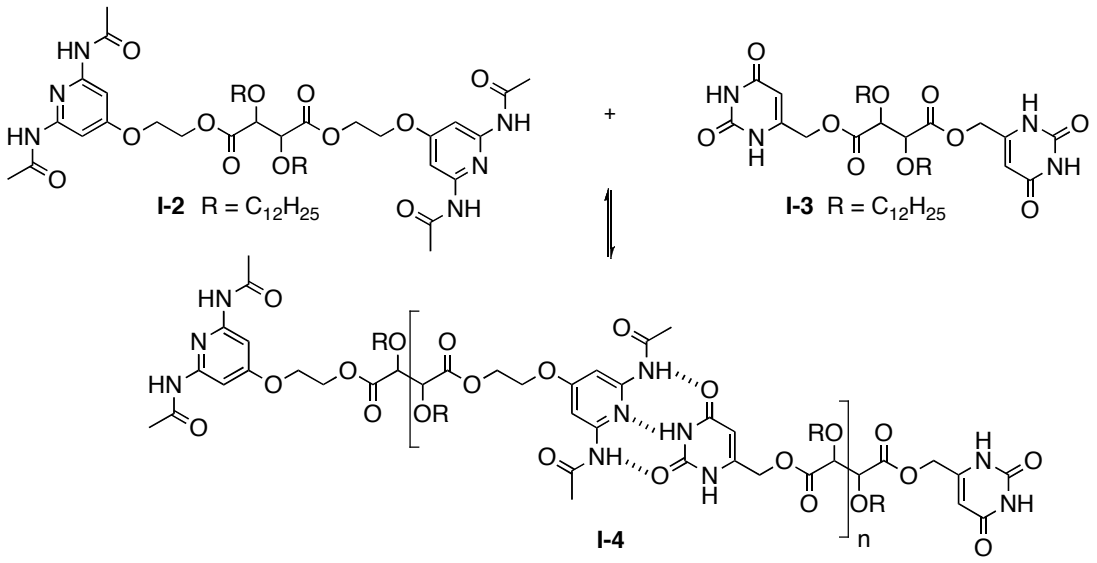

Scheme I-1. Equilibrium between 2,6-diacylaminopyridine-functionalized, **I-2**, and uracil-functionalized, **I-3**, monomeric units and resulting supramolecular polymer, **I-4**, synthesized by Lehn.

According to polarizing microscopy images, the resulting liquid crystalline polymer appeared as stretched and helically wound fibers and from X-ray diffraction data formed hexagonal columnar superstructures. One of the most well studied and potentially applicable supramolecular polymers containing hydrogen-bonding interactions was created in E.W. Meijer's lab. Figure I-5 depicts the ditopic 2-ureido-4-pyrimidone units employed.

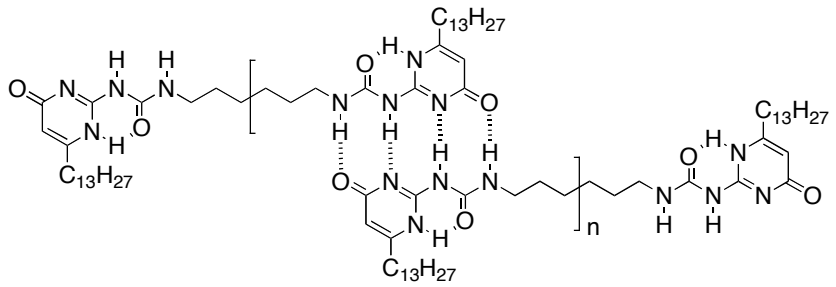

I-5

Figure I-5. Supramolecular polymer introduced by E.W. Meijer based on quadruple hydrogen-bonding interactions.

These monomeric units dimerize with a $K_{dim} > 10^6$ M^{-1} in $CHCl_3$. The DDAA arrangement of four hydrogen bonds on either end of the repeat unit allows for construction of a linear, main chain supramolecular polymer. An increase in viscosity was observed in $CHCl_3$ as the monomer concentration was increased, evidence for formation of an oligo- or polymeric assembly in solution. [Sijbesma, R.P.; Beijer, F.H.; Brunsveld, L.; Folmer, B.J.B.; Hirschberg, J.H.K.K.; Lange, R.F.M.; lowe, J.K.L.; Meijer, E.W. *Science*, **1997**, *278*, 1601-1604.] The viscosity is highly concentration-dependent and shows a linear relationship on a double-logarithmic plot (Figure I-6).

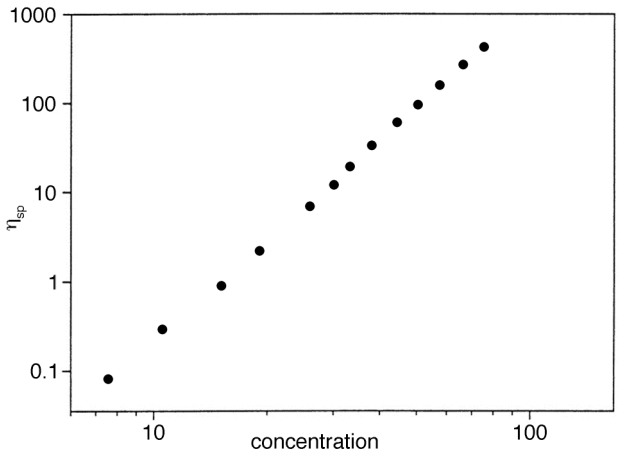

Figure I-6. Specific viscosity of $CHCl_3$ solutions containing **I-5** versus concentration (grams per liter) at 20 ˚C.

These results indicate that the measurements were taken of solutions that are above the C_{cr} and the change in viscosity corresponds to a change in the DP of the supramolecular polymer. The above examples used hydrogen-bonding as a force to polymerize repeat units. The strength of interaction between two monomers can be tuned by varying the number and pattern of hydrogen-bonds. This tunability makes these systems advantageous toward the production of stimuli-responsive or "smart" materials.

1.8.3 Supramolecular Polymer Based on Metal-ligand Coordination and Hydrogen-bonding Interactions.

Metal-ligand coordination, on the other hand, can provide for stronger interactions than hydrogen-bonds, which may limit the extent of polymer

reversibility. Schubert *et al.* employed a combination of hydrogen-bonds and metal-ligand coordination in the construction of a supramolecular polymer (Figure I-7).[20]

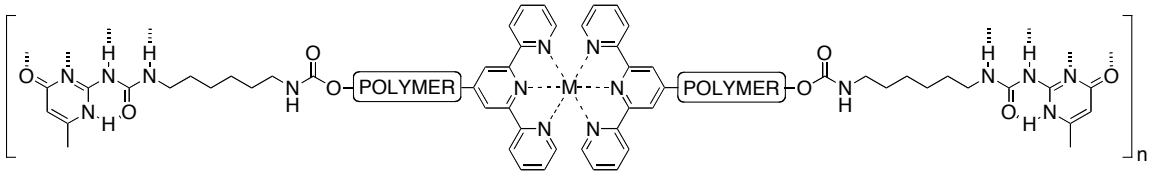

I-6

Figure I-7. Supramolecular polymer by Ulrich, comprising metal coordination and quadruple hydrogen-bonding interactions.

A poly(ε-caprolactone) polymer was end-functionalized with both a terpyridine and ureidopyrimidone moiety. In the absence of any metal ions, hydrogen-bonded dimers were present in solution. Upon addition of Fe(II) ions, the relative viscosity increased and continued to increase with an increase in monomer concentration, supplying evidence for the formation of high molecular weight polymers. This example was the first report of an extended supramolecular polymer containing alternating metal-ligand coordination and quadruple hydrogen-bonding interactions. To affirm the reversible nature of this supramolecular polymer, HEEDTA (hydroxyethyl ethylenediaminetriacetic acid) was added to the polymer solution. Accordingly, the dissociation of the supramolecular polymer was realized by free terpyridine bands in the UV-Vis spectra.

1.8.4 Supramolecular Polymer Based on Host-Guest Interactions.

Host-guest interactions have also been used to effect polymerization. Harada has employed cinnamamidoyl-functionalized α-cyclodextrin as an A—B type repeat unit as shown in Figure I-8.[21]

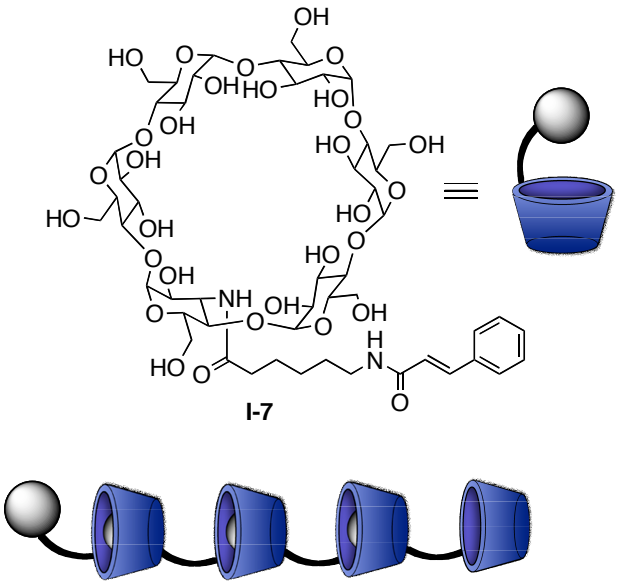

Figure I-8. Structure of A—B type monomeric unit, **I-7**, and schematic representation of resulting supramolecular polymer prepared by Harada.

The appended guest portion can be encapsulated by another α-cyclodextrin, thus extending this non-covalent system. ^{1}H NMR spectroscopy confirmed the formation of an inclusion complex between α-cyclodextrin of one monomer and the cinnamamide moiety of another. ESI-TOF mass spectrometry was performed on a solution containing the A—B type monomers and revealed the presence of a pentameric species, indicating at the very least, oligomers are formed. Viscosity measurements were performed and showed a moderate increase in viscosity with an increase in monomer concentration, corresponding to an increase in the DP.

In a similar fashion, Scherman employed cucurbit[8]uril (CB[8]) as a host molecule for bringing together two polymers, thus extending the overall polymeric species (Scheme I-2).[22]

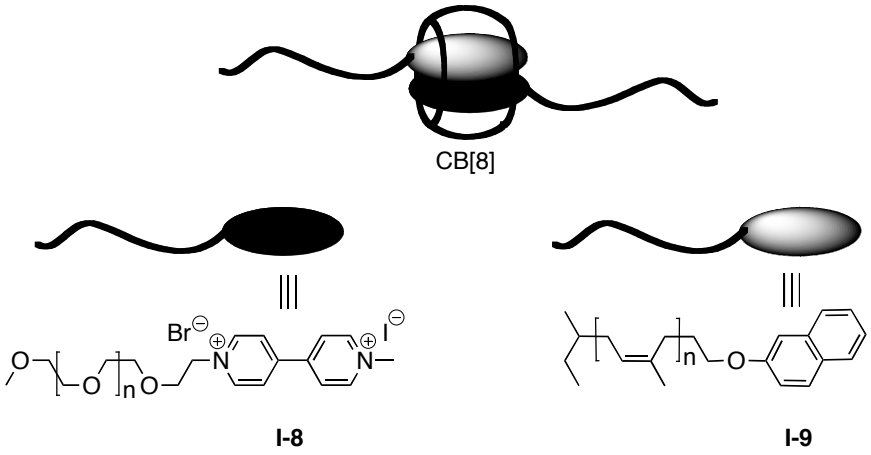

I-8 I-9

Scheme I-2. Schematic representation of ternary complex prepared by Scherman, comprising CB[8] and an AB diblock copolymer.

It is well documented that CB[8] can form a ternary complex with viologen derivatives and hydroxynapthalene in water, due to the stability of the resulting charge-transfer (CT) complex. Poly(ethylene glycol) (PEG) and *cis*-1,4-poly(isoprene) (PI) were end-functionalized with viologen and hydroxynapthalene, respectively. Acting as a supramolecular handcuff, CB[8] was able to recognize the binding regions of the polymer units and form a ternary complex. Evidence for the formation of a CT complex within CB[8] was realized through UV-Vis and ^{1}H NMR spectroscopy.

Another example involving host-guest chemistry in the fabrication of a supramolecular polymer is given by Rebek on the synthesis of polycaps. In this system, an A—A type monomer was constructed from two calix[4]arenes that

undergo hydrogen-bond driven dimerization to self-assemble to form a polymer (Scheme I-3).[23]

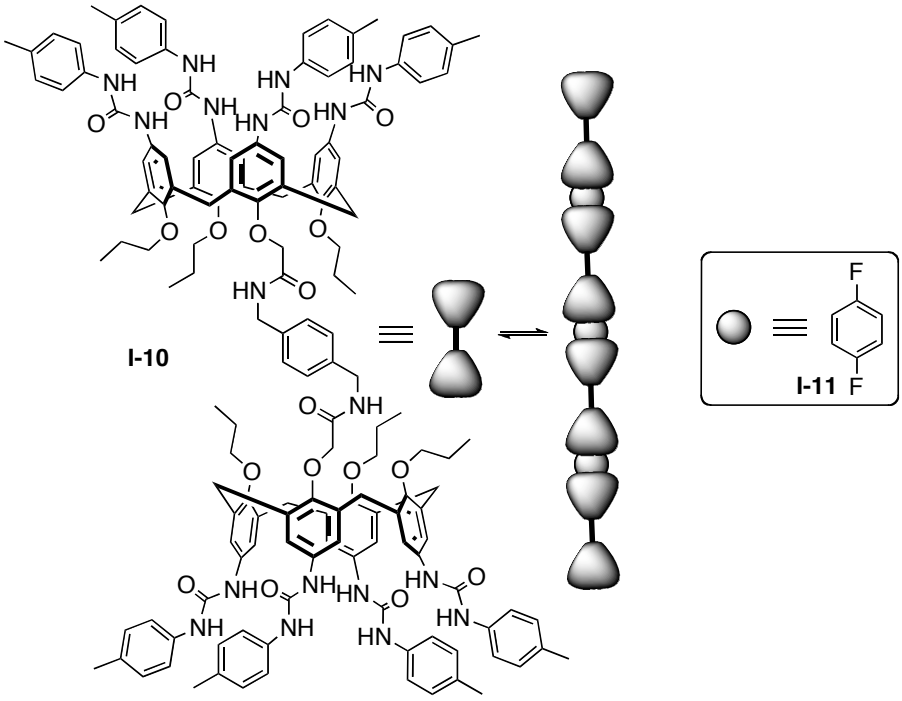

Scheme I-3. Chemical structure of A—A type monomeric unit resulting in formation of polycaps, introduced by Rebek.

The upper rims of the calix[4]arenes are functionalized with ureidyl groups, allowing for hydrogen-bonding between two calix[4]arenes, and the lower rim is monofunctionalized to a linker through covalent bonds. The ureidyl hydrogens appear downfield-shifted in the ^{1}H NMR spectrum of a solution containing the polycaps in $CDCl_3$, evidence for the hydrogen-bonding between two monomeric units. *P*-difluorobenzene, was added to a solution containing the supramolecular polymer and a new aromatic resonance appeared indicating the inclusion of *p*-difluorobenzene within a capsule comprising two calix[4]arene units. From the ^{1}H

NMR data, the guest addition drives the equilibrium further toward the assembly of polycaps, as evidenced by an increase in the integration of resonances for the polymeric species compared to the ^{1}H NMR spectra recorded for a solution containing the polycaps without *p*-difluorobenzene.

Highlights from a collection of the most noted papers on the topic of supramolecular polymers have been presented above. Following is a more particular introduction to the class of compounds used in studies described in this dissertation.

1.9 Overview of the Cucurbit[*n*]uril Family of Macrocycles.

In 1981 Mock and co-workers reinvestigated the work by Behrend, who in 1905 explained that the condensation reaction of glycoluril with formaldehyde in concentrated HCl produced an insoluble polymer.[24,25] What had formed, as Mock later illustrated, was a macrocycle he termed cucurbituril due to its shape which resembled that of a pumpkin (family *cucurbitaceae*). This later became known as cucurbit[6]uril, abbreviated CB[6], where the numeral denotes the number of monomers comprising the macrocycle (Figure I-9).

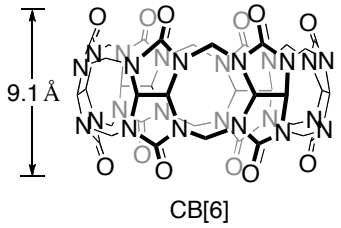

Figure I-9. Chemical structure of CB[6]. Width accounts for the van der Waals radius of the O-atoms.

The work presented in the following chapters is based upon macrocyclic host bis-*nor-seco*-CB[10] (bis-*ns*-CB[10]), one of a growing number of members of the cucurbit[*n*]uril (CB[*n*]) class of molecular containers.

The formation of CB[*n*] occurs through the condensation of glycoluril (**I-12**) with paraformaldehyde under acidic conditions (Scheme I-4).[26-28] To exert control over product outcome within this complex reaction mixture, reaction conditions can be tuned by altering the temperature, time, equivalents, and solvent system.

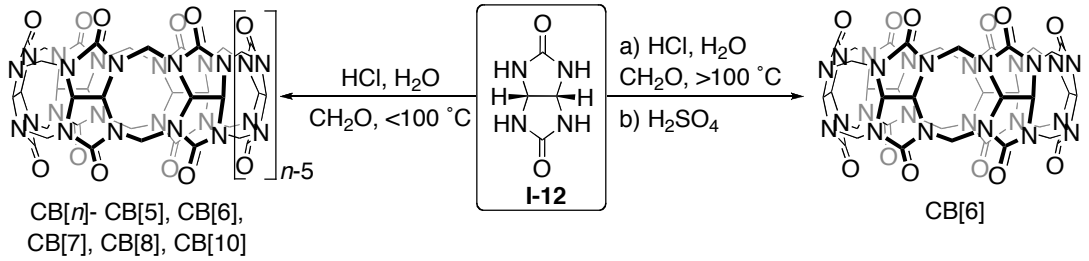

Scheme I-4. Synthesis of CB[6] and CB[*n*] homologues.

1.10 Structure and Properties of CB[*n*].

1.10.1 Structural Diversity of CB[*n*].

Since the structural elucidation of CB[6], the interest in CB chemistry has grown and as such, resulted in the isolation and characterization of CB[5], CB[6], inverted CB[6] (*i*CB[6]), *i*CB[7], CB[8], CB[10], *ns*-CB[6], (±)-bis-*ns*-CB[6], and bis-*ns*-CB[10] by the research groups of Kim, Day, and Isaacs.[26-33] The different sizes of the macrocycles exhibit binding selectivity among a number of suitable guests. The host-guest complexes have been implemented in the construction of self-assembled monolayers (SAMs)[34], self-sorting systems, molecular machines, oligomer

folding and unfolding processes,[35-38] supramolecular polymers,[22,39-41] and sensors.[42,43] The X-ray crystal structures of homologues, CB[5] – CB[8], are depicted in Figure I-10 and their dimensions listed in Table I-1.

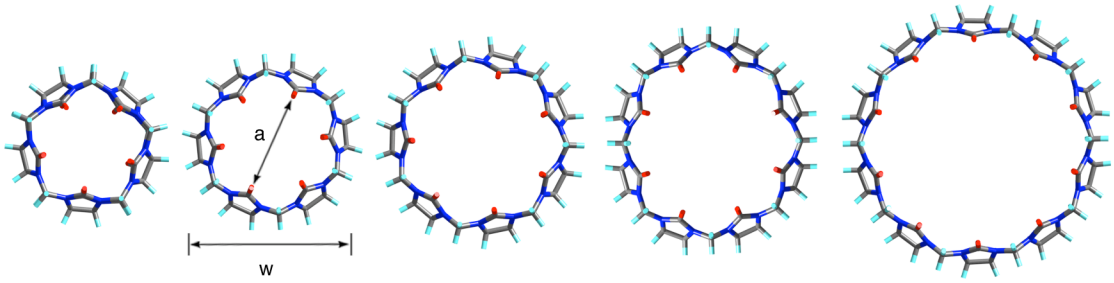

Figure I-10. CrystalMaker representations of the X-ray crystal structures for CB[*n*] (*n* = 5, 6, 7, 8, 10, left to right).

Table I-1. Structural parameters of CB[*n*][a].

	h/Å	*w*/Å	*a*/Å	*V*/Å
CB[5]	9.1	4.4	2.4	82
CB[6]	9.1	5.8	3.9	164
CB[7]	9.1	7.3	5.4	279
CB[8]	9.1	8.8	6.9	479
CB[10]	9.1	11.3–12.4	9.5–10.6	870

[a]Values of *h, w, a,* and *V* account for the van der Waals radii of the various atoms.

1.10.2 Guest Binding Affinities Toward CB[*n*].

The macrocycles are composed of glycoluril (**I-1**) units connected through methylene bridges. The "top" and "bottom" of each structure is faceted with ureido carbonyls that can undergo hydrogen-bonding with protonated species, ammonium ions in particular. The interior of the cavity is hydrophobic and facilitates the binding to non-polar regions of guest molecules. The top to bottom depth of the CB[*n*] series is

dictated by the length of glycoluril monomer and is therefore the same for this series- 9.1 Å. The diameter of the portals for guest entry are more narrow than the diameter of the cavity, which influences the rate of guest exchange. CB[*n*] have been reported to bind to alcohols, diamides, nitriles, amines, and diazonium compounds, as well as metal ions and gases.[44] The most encouraging results in terms of exhibiting high binding association constants and selectivity stem from amine-functionalized guests. Chart I-1 shows a series of guests, some of whose binding affinities toward CB[6], CB[7], and CB[8] were measured.[45]

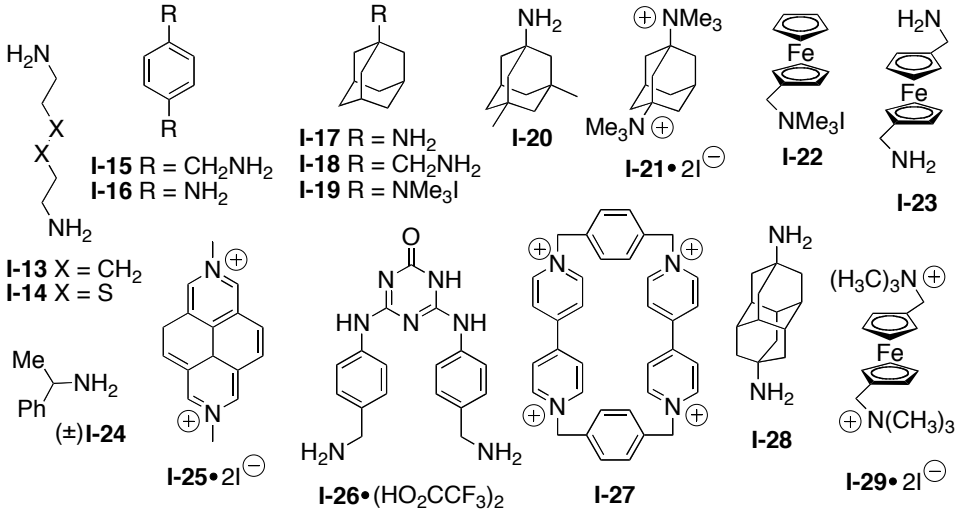

Chart I-1. Chemical structures of guests used to bind to CB[*n*].

The breadth of binding capabilities of CB homologues is apparent from the results of this work, shown in Table I-2.

Table I-2. Values of K_a (M^{-1}) for the interaction of various guests with CB[6], CB[7], and CB[8], measure in 50 mM NaO_2CCD_3-buffered D_2O (pD 4.74).

	CB[6] (M^{-1})	CB[7] (M^{-1})	CB[8] (M^{-1})
I-13	$(4.49 \pm 0.84) \times 10^8$	$(8.97 \pm 1.43) \times 10^7$	nd
I-17	nd	$(4.23 \pm 1.00) \times 10^{12}$	$(8.19 \pm 1.75) \times 10^8$
I-19	nd	$(1.71 \pm 0.40) \times 10^{12}$	$(9.70 \pm 2.48) \times 10^{10}$
I-20	nd	$(2.50 \pm 0.39) \times 10^4$	$(4.33 \pm 1.11) \times 10^{11}$
I-21	nd	$(6.42 \pm 1.02) \times 10^4$	$(1.11 \pm 0.28) \times 10^{11}$
I-22	nd	$(3.31 \pm 0.62) \times 10^{11}$	$(3.12 \pm 0.80) \times 10^9$
I-25	nd	$(3.81 \pm 0.61) \times 10^7$	$(6.37 \pm 1.20) \times 10^8$
I-26	nd	$(1.78 \pm 0.34) \times 10^7$	$(5.78 \pm 1.36) \times 10^{10}$

Among the K_a values listed, the complexes exhibiting the strongest interaction are CB[6]•**I-13** ($K_a = 4.5 \times 10^8$ M^{-1}), CB[7]•**I-17** ($K_a = 4.2 \times 10^{12}$ M^{-1}), and CB[8]•**I-20** ($K_a = 4.3 \times 10^{11}$ M^{-1}). The highest association constant to be reported thus far for a CB inclusion complex is that of CB[7]•**I-29** with $K_a = 3.0 \times 10^{15}$ M^{-1}.[46] The strength of binding interaction between CB[*n*] and ammonium-functionalized guests allows them to be used in the construction of complex supramolecular architectures in dilute aqueous solution.

1.11 Detection of CB[*n*] Inclusion Complexes.

The most routinely employed technique performed for monitoring CB inclusion of guests is ^{1}H NMR spectroscopy. For example, an ^{1}H NMR spectrum containing CB[7] and excess adamantaneamine (**I-17**) will show upfield-shifted resonances for the hydrogens on adamantaneamine bound within the cavity of CB[7] (Figure I-11).

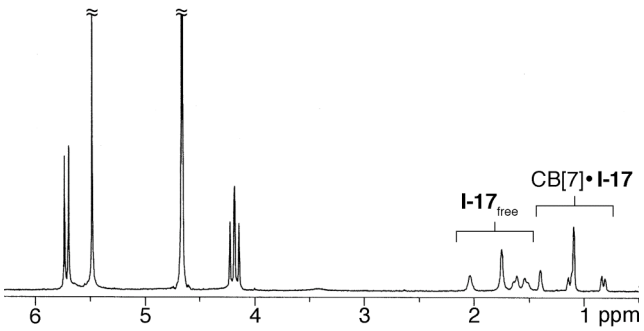

Figure I-11. ^{1}H NMR spectrum recorded (400 MHz, D_2O) for a solution containing CB[7]•**I-17** and free **I-17**.

Solubility can provide a simple physical indication of formation of a CB inclusion complex, provided initially the empty CB is insoluble in aqueous media. UV-Vis spectroscopy is especially helpful in determining the formation of a charge-transfer complex within CB[8] and a routine technique for monitoring CB inclusion complexes in the realm of sensing.

1.12 Inverted CB[*n*] and *Nor-Seco*-Cucurbit[*n*]urils.

1.12.1 Inverted CB[*n*].

More recent investigations into the isolation of new CB[*n*] from complex mixtures have resulted in the isolation, and characterization of inverted cucurbiturils *i*-CB[6] and *i*-CB[7] as shown in Figure I-12.

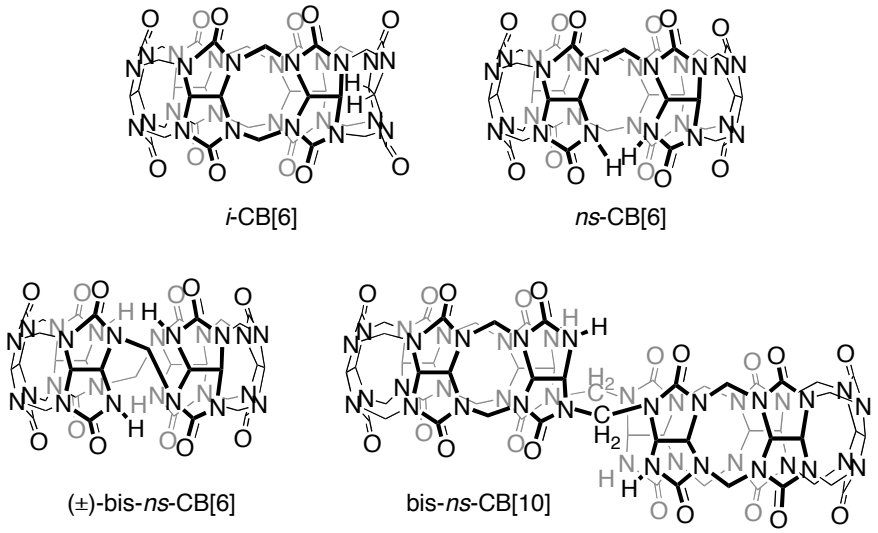

Figure I-12. Chemical structures of inverted CB[6] and *nor-seco*-CB[*n*] macrocyclic receptors.

The structure of *i*CB[6] and *i*CB[7] contain one glycoluril unit whose methylene hydrogens are pointing into the cavity.[29,30] They are able to bind guests **I-15** and **I-13**, though the binding affinities are a few orders of magnitude lower than their CB[*n*] counterparts. Resubmission experiments produced different mixtures of CB[*n*] which established that *i*-CB[*n*] are kinetic products of the CB[*n*] forming reaction. The isolation of *i*-CB[*n*] contributed to the understanding of the mechanism of CB[*n*] formation.

1.12.2 *Nor-Seco*-Cucurbit[*n*]urils.

CB[*n*] derivatives lacking methylene bridges have been isolated within the last few years. *Ns*-CB[6] is similar in structure to CB[6], lacking one methylene bridge.[33] The novelty of this macrocycle is evident from its ability to be functionalized. Functionalization of CB[*n*] has been a long-standing challenge in the area of CB

chemistry and *ns*-CB[6] allowed for the first synthetic modification to the N-atoms, other than methylene groups.

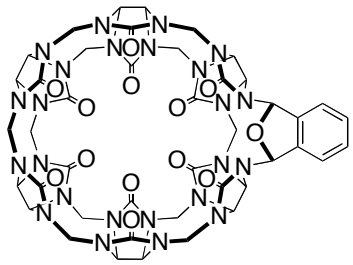

Figure I-13. Chemical structure of *ns*-CB[6].

The insertion of *o*-pthalaldehyde into *ns*-CB[6] causes a difference between the sizes of the upper and lower rims (Figure I-13). This structural modification to *ns*-CB[6] allows for diastereoselective complex formation with unsymmetrical guests.

1.12.3 Bis-*nor*-*seco*-Cucurbit[*n*]urils.

(±)-bis-*ns*-CB[6] was the first chiral CB to be isolated.[32] As such, its ability to discriminate between the enantiomers of a racemic mixture of guest **I-24** was investigated. Selective formation of one of the diastereomers upon guest complexation was observed and values of diastereomeric excess for these complexes determined.

The impetus to work on generating supramolecular polymers from a CB[*n*] derivative was fueled by the isolation of a double cavity CB, namely bis-*ns*-CB[10]. Bis-*ns*-CB[10] was isolated from a reaction mixture initially containing 1 equivalent of glycoluril and 1.67 equivalents of paraformaldehyde, heated to 50 ˚C in

concentrated HCl for 3 days.[31] The isolated yield can be as high as 25%, which for CB chemistry is very good.

1.13 Structure and Properties of Bis-*ns*-CB[10].

1.13.1 Structure of Bis-*ns*-CB[10].

Bis-*ns*-CB[10] is composed of two pentameric glycoluril oligomers that are joined by two methylene bridges, connecting the bottom rim of one oligomer to the upper rim of another. The absence of two methylene bridges when compared to its CB[10] counterpart confers the flexibility in the shape assumed by the cavities. This is important in the study of guest complexation. Computational results indicate the distance between bridging methylene units can vary depending on the guest, from approximately 5.5 – 9.3 Å, corresponding to an overall cavity volume range between 450 – 740 $Å^3$. The structures of termolecular complexes bis-*ns*-CB[10]•**I-28**$_2$ and bis-*ns*-CB[10]•**I-13**$_2$ are shown for comparison in Figure I-14.

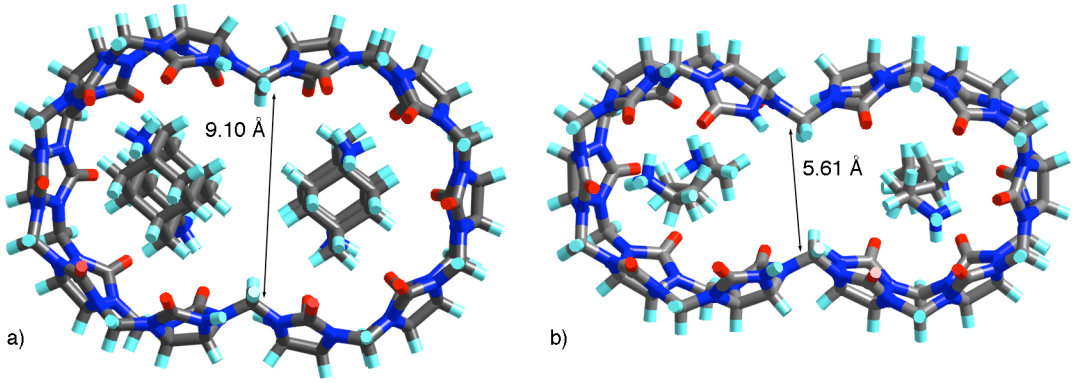

Figure I-14. MMFF minimized models (Spartan) of ternary complexes of bis-*ns*-CB[10] rendered with CrystalMaker. The diameter values given refer to the non-bonded $H_2C{\bullet\bullet\bullet}CH_2$ distance. a) bis-*ns*-CB[10]•**I-28**$_2$: d = 9.10 Å, b) bis-*ns*-CB[10]•**I-13**$_2$: d = 5.61 Å.

1.13.2 Bis-*ns*-CB[10] Exhibits Homotropic Allostery.

The most interesting feature of bis-*ns*-CB[10] is its ability to perform homotropic allostery among different sized guests. This event begins with the binding of a guest to one of the two cavities of bis-*ns*-CB[10], which induces a conformational change, preorganizing the second cavity to preferentially bind a second identical guest. This behavior can be illustrated by using different sized guests, for example, **I-15** and **I-23**. When presented to bis-*ns*-CB[10], only homomeric complexes, bis-*ns*-CB[10]•**I-15**$_2$ and bis-*ns*-CB[10]•**I-23**$_2$, were observed by ^{1}H NMR spectroscopy. The orientation of the two guests comprising a homomeric ternary complex can be described as a mixture of diastereomers (Scheme I-5), where the guest orientation relative to its neighbor can be termed top-top, center-center, or top-center.

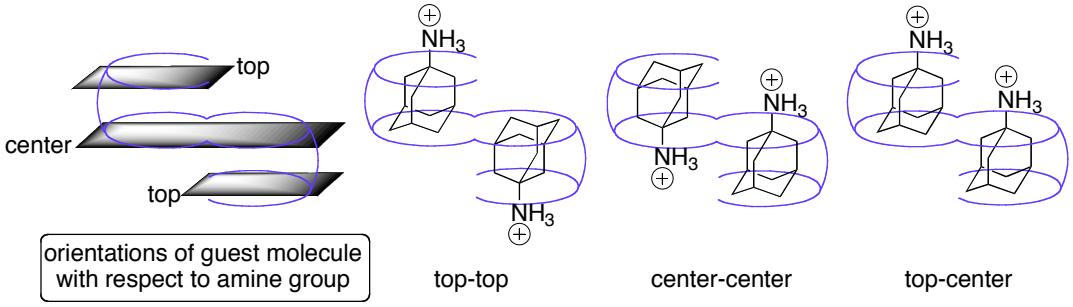

Scheme I-5. Three potential diastereomers of bis-*ns*-CB[10]•**I-17**$_2$.

1.13.3 Suitable Guests for Bis-*ns*-CB[10].

Chart I-1 lists various compounds that formed inclusions complexes with bis-*ns*-CB[10]. Guests **I-13** — **I-19**, **I-23**, and **I-28** form ternary complexes with bis-*ns*-CB[10]. As evident from ^{1}H NMR integration, two molecules of the aforementioned guests reside within one molecule of bis-*ns*-CB[10]. Guests **I-26** and **I-27** form 1:1 guest inclusion complexes with bis-*ns*-CB[10], and are otherwise too large to be accommodated within the cavities of CB[6] or CB[7].

1.13.4 Solubility.

Bis-*ns*-CB[10] is not soluble in neutral water by itself, but its inclusion complexes are nicely soluble. Acidic water can bring bis-*ns*-CB[10] readily into solution. Though insolubility can pose problems, this property was actually advantageous for controlling the stoichiometry between bis-*ns*-CB[10] and water-soluble guests.

1.14 Bis-*ns*-CB[10] as Host for Construction of Supramolecular Polymers.

Bis-*ns*-CB[10] is the first isolated CB to contain two identical binding domains and is therefore a prime candidate for the construction of higher order architectures, including supramolecular polymers. In theory, the generation of a linear polymer comprising A—A and B—B type monomers seems reasonable (Figure I-15).

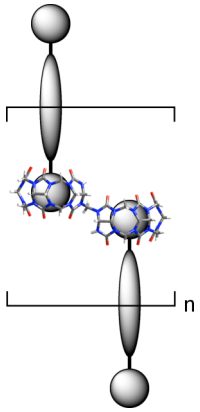

Figure I-15. Hypothetical linear polymer comprising bis-*ns*-CB[10] and divalent guest.

However, efforts to achieve this type of structure brought valuable lessons to the forefront of our minds. If we consider a ditopic guest molecule that contains two identical binding domains on either end, connected through a linker as shown in Figure I-15, formation of closed complexes (2:2, 3:3) are also plausible. The following variables taught us about the sensitivity of this supramolecular system and the requirements necessary to generate a supramolecular polymer: 1) the size of the guest, 2) the length of the linker, 3) the rigidity of the linker, and 4) the host:guest ratio. Concentration undoubtedly effects the equilibrium of host-guest systems. Fortunately, due to the high K_a values between CB[*n*] and guests, concentration was

not a challenging aspect in the formation of the higher order complexes contained herein.

1.15 Literature Examples of CB[*n*] and Higher Order Structures.\

1.15.1 Self-Assembled Monolayers.

A few pertinent examples from the literature that report on CB encapsulation of guests to promote macromolecular assemblies will be described. The research group of Kimoon Kim has investigated supramolecular architectures at great length. A self-assembled monolayer (SAM) was fabricated on a gold surface, exploiting the ability of CB[8] to stabilize a charge-transfer (CT) complex within its cavity.[47] One component that enabled formation of a SAM was synthesis of a ditopic guest molecule containing both a 4,4'-bipyridinium unit and a 2-hydroxynapthalene unit, **I-30**, (Scheme I-6).

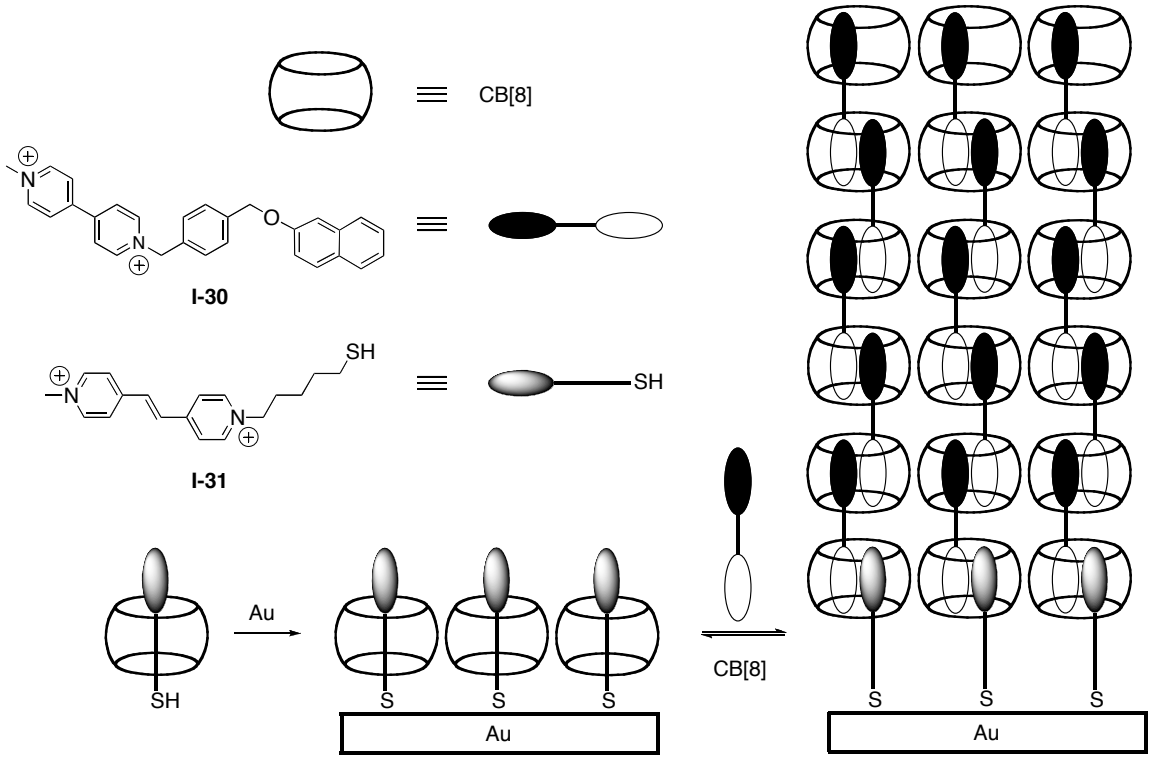

Scheme I-6. Schematic representation of growth of poly(pseudorotaxane) on gold using host-stabilized charge-transfer interactions, prepared by Kim.

The rigidity and length of the linker is a critical aspect in the design strategy of this system. If the linker is long and flexible opposite ends of the ditopic guest molecule can fold back on itself and form a 1:1 inclusion complex with CB[8].[48] In this case, the *p*-xylylene linker of the hydroxynapthol guest is rigid and short to promote extension of a polymer. A dipyridiniumethylene binding unit is attached to the gold surface through thiol linkages. This binding unit is a stronger electron-acceptor than the 4,4'-bipyridinium unit and acts as an anchor to keep the CB chain intact rather than equilibrating in solution, possibly leading to formation of discrete 2:2 host-guest complexes rather than oligomer or polymer. The polymer growth could be controlled by monomer concentration and immersion time; the degree of polymerization

increases with increasing concentration of monomer. The change in thickness of the monolayer with subsequent immersion into a colution containing CB[8] and ditopic guest was determined by AFM. Surface plasmon resonance (SPR), FT-IR, and extensive 2D NMR studies also confirmed the growth of a supramolecular polymer attached to a gold surface.

1.15.2 Construction of Molecular Necklaces.

The formation of higher order discrete complexes are simple to design, but challenging to carry out experimentally. Efficient syntheses of mechanically interlocked structures are appealing for their potential applications as molecular machines and switches. The construction of molecular necklaces mediated by transition metal directed self-assembly was carried out by Kimoon Kim *et al*.[49,50] These were the first molecular necklaces to be obtained as thermodynamically favored products.

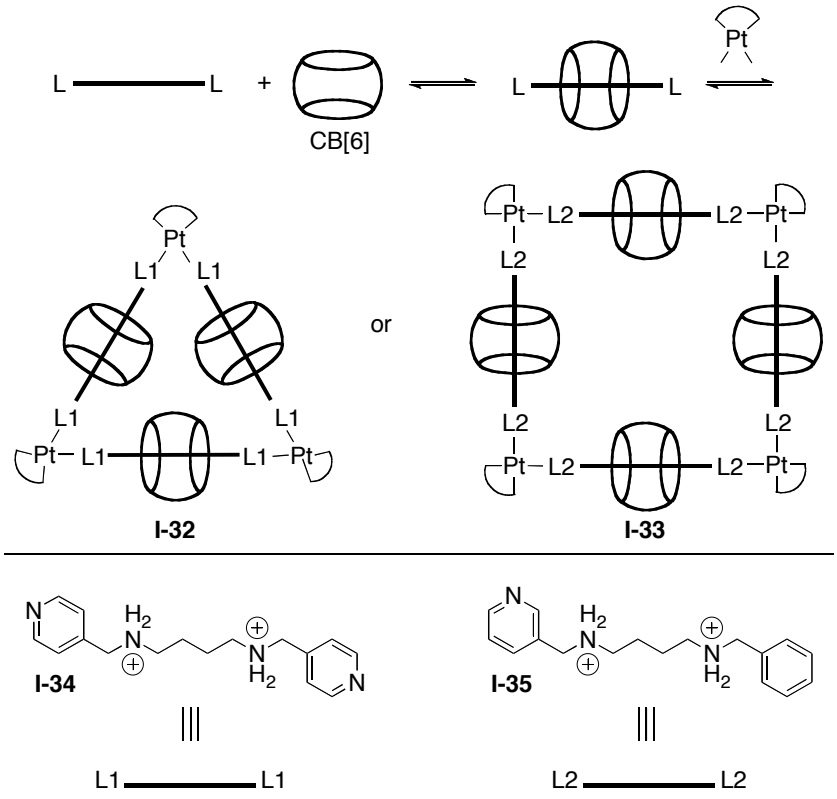

Scheme I-7. Cartoon depiction of molecular necklaces comprising metal coordination and host-guest interactions, prepared by Kim.

The threads, **I-32** and **I-33**, contain a central butanediammonium ion flanked by two pyridylmethyl groups to coordinate to the Pt(en) (en = ethylenediamine) metal. The molecular necklaces in Scheme I-7 were prepared in the following manner. First, a peudorotaxane between CB[6] and the appropriate thread was formed. Then the metal was added to the solution containing the preformed pseudorotaxane. The tetra-coordinate geometry of the Pt metal and the use of a *cis* en ligand enables formation of cyclic products. The attachment position of the pyridylmethyl group to the CB binding unit dictated the size of the ring structure. More specifically, attachment at

the 4-pyridyl position to the CB binding unit generated a triangular structure whereas attachment at the 3-pyridyl position generated a square complex. The formation of these structures could be monitored by ^{1}H NMR spectroscopy, eventually producing a spectrum containing a highly symmetric structure which is evident from simplification of the resonances. ESI-MS and X-ray diffraction also confirmed adequate structure designation.

1.15.3 [10]pseudorotaxane Dendrimer.

A second-generation rotaxane dendrimer was prepared from 13 molecular components in a step-wise manner.[51] A trivalent core molecule, appended with three *trans*-1,2-bis(1-methyl-4-pyridino)ethylene units formed a [4]rotaxane with CB[8] as depicted in Scheme I-8.

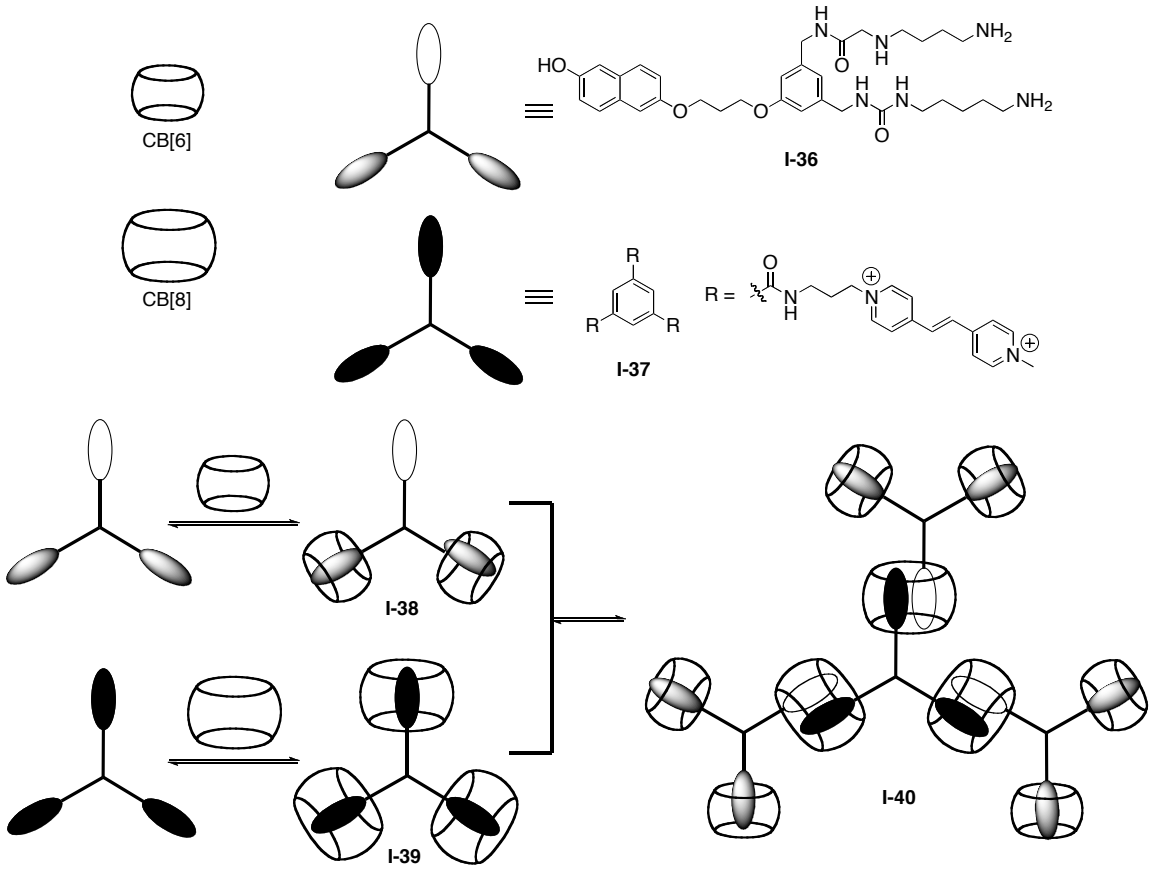

Scheme I-8. Schematic representation of dendritic [10]pseudorotaxane prepared by Kim.

Again, making use of a ternary complex formed from encapsulation of a CT complex by CB[8] another triply branched guest was synthesized, containing a 2-hydroxynapthalene moiety and two diaminobutane arms. In this way, the 2-hydroxynapthalene portion of the guest can slip inside the preformed CB[8]$_3$•**I-37**. What remains is six diaminobutane binding sites that are then allowed to be encapsulated by three molecules of CB[6]. ^{1}H NMR confirmed the binding of guests within their respective CB cavities, along with UV-Vis spectral data to confirm formation of a CT complex within CB[8]. DOSY NMR confirmed the relative trend

of dendrimer growth correlating to a decrease in rates of diffusion. Fortunately, as crystals become increasingly difficult to grow with expansion of supramolecular assemblies, cold-spray ionization mass spectrometry revealed a molecular ion peak corresponding to multiply charged ions of the [10]pseudorotaxane. Construction of large supramolecular architectures benefits from the rational design using simple geometry and established host-guest chemistry.

1.16 Conclusion.

An introduction to the field of supramolecular polymers has been presented. The importance of their development, factors controlling their formation, examples of supramolecular polymers from the literature, and the role of CB[*n*] in their construction have been addressed and serve as a platform for the information contained in subsequent chapters. The inherent selectivity and high affinity host properties of CB[*n*] render them prime components for the growth of supramolecular polymers.

In the following chapter, the chemistry of bis-*ns*-CB[10] will be illuminated through a multitude of binding experiments with a series of guests. The synthesis of guests that led to interesting solution behavior will be presented alongside discussion of the parameters that govern the behavior of the system. Lastly, experiments providing evidence for the formation of a supramolecular polymer between bis-*ns*-CB[10] and a polymeric guest will be presented.

II. Chapter 2: Toward Supramolecular Polymers Incorporating Double Cavity Cucurbituril Hosts.[52]

2.1 Introduction.

The synthetic and supramolecular chemistry of the cucurbit[n]uril family (CB[n]) of macrocycles has undergone extensive development since the pioneering work of Mock on CB[6] during the 1980's.[22,44,53-56] For example, the large values of K_a and high selectivities based on guest size, shape, and functional group preferences of CB[6] have been shown to transfer to the larger homologues CB[7] and CB[8].[45] In turn these large values of K_a, the associated free energy ($\Delta\Delta G$), and the inherent stimuli responsiveness of CB[n]•guest complexes (e.g. pH, photochemical, electrochemical, chemical) has led to their use in the development of a variety of molecular machines and biomimetic systems.[57-61] Our research group has been involved in studies of the mechanism of CB[n] formation which has resulted in the preparation of new CB[n] type molecular containers (bis-*ns*-CB[10], (±)-bis-*ns*-CB[6], and *ns*-CB[6]) with exciting properties (homotropic allosterism, chiral recognition, and folding).[31-33]

The use of supramolecular chemistry as a means to create and modify the properties of polymers has been the subject of active investigation over the past decade.[9,62-68] For example, a number of groups have demonstrated the oligo- and polymerization of suitable dimeric systems based on reversible hydrogen bonding and

metal-ligand interactions.[19,23,69-73] Most relevant to the work described in this paper is the work of Harada who has investigated the use of cyclodextrin molecular containers as building blocks for supramolecular polymers by hydrophobically driven host-guest complexation in water.[74-76] In supramolecular polymeric systems, the degree of polymerization is controlled by the strength of the non-covalent interactions between monomers with higher values of K_a leading to longer polymers. As such, the use of members of the CB[n] family – with their exceedingly large values of K_a (up to 10^{15} M^{-1})[45,46,77] – in the preparation or modification of polymeric and macromolecular species holds great promise. Accordingly, several groups have decorated the main-chain or side-chains of linear polymers[78-87] or dendrimers[88] with CB[n] binding groups and were therefore able to modify the properties of the polymer by addition of CB[n]. Kim's group even used a CB[6] derivative as the monomer to form covalent polymeric nanocapsules.[89] Lastly, the groups of Kim, Kaifer, and Scherman have used the ability of CB[8] to form homo-ternary or hetero-ternary complexes[57] to drive the formation of self-assembly dendrimers and a self-assembled diblock copolymer.[22,51,61]

In 2006, we reported the isolation and recognition capacity of bis-*ns*-CB[10].[31] Bis-*ns*-CB[10] contains two cavities that are able to bind to two guests simultaneously to form ternary complexes. In this process, the binding of the first guest preorganizes the second binding site for binding of the second guest which is known as allostery. Even more interesting was the ability of bis-*ns*-CB[10] to distinguish between small and large guests within a mixture and form ternary complexes with two identical guests. This latter process is known as *homotropic*

allostery. This ability is due to the flexibility of the central CH_2-bridges which adjust their non-bonded CH_2•••CH_2 distance to accommodate the size of the guest. We envisioned that bis-*ns*-CB[10] with its ability to form tight ternary complexes under positive homotropic allosteric control would render bis-*ns*-CB[10] as an ideal component of supramolecular polymers in combination with suitable guests containing two binding epitopes. Figure II-1 depicts the mode of polymerization that might result from the combination of bis-*ns*-CB[10] and suitable guests. Given the fact that such supramolecular polymers would be composed of two components we expected the behavior of the system to be sensitively dependent on host-guest stoichiometry. In addition, we expected the system to be responsive to the addition of exogenous host or guest by the formation of competitive host•guest complexes. This chapter reports our initial studies in this research direction.

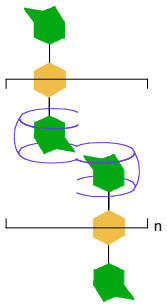

Figure II-1. Hypothetical linear polymer comprising bis-*ns*-CB[10] and **II-1**.

2.2 Results and Discussion.

This results and discussion section is subdivided into several parts. We start with a discussion of the design of the guests (**II-1** – **II-8**, Chart II-1) and their synthesis. Next, we discuss the characterization of the supramolecular species formed in the presence of bis-*ns*-CB[10] with a particular emphasis on absolute host:guest stoichiometry. Finally, we discuss the application of stimuli in the form of additional CB[n] hosts to control absolute binding stoichiometry in this system.

Chart II-1. Compounds Used in this Study.

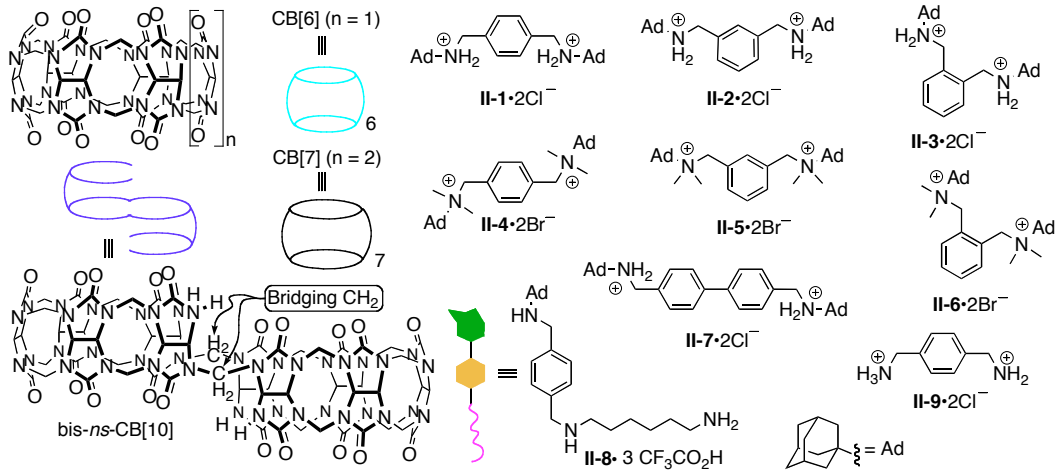

2.2.1 Design of Guests **II-1 – II-6**.

Chart II-1 shows the structures of hosts CB[6], CB[7], and bis-*ns*-CB[10] and guests **II-1** – **II-9** used in this study. We were attracted to the possibility of preparing supramolecular polymers using the double cavity host bis-*ns*-CB[10] in combination with suitable guests (e.g. **II-1** – **II-8**) containing two binding domains (e.g. bis-*ns*-$CB[10]_n$•$guest_n$). Figure II-1 depicts the desired n:n interaction between bis-*ns*-CB[10] and divalent guests. Although this proposed supramolecular polymerization appears straightforward, in reality the situation is more complex. For example, although linear supramolecular polymers can be formed from solutions comprising n hosts and n guests, the formation of discrete (cyclic) 1:1, 2:2, 3:3, or n:n aggregates can also be readily envisioned.[90] Compounding the situation is the reality that smaller discrete assemblies are likely to be favored on entropic grounds. Therefore, we decided to start simple and targeted guests **II-1** – **II-6** (Chart II-1) which contain two adamantylammonium binding domains linked together by *o*-, *m*-, and *p*-xylylene units for several reasons. First, we envisioned that **II-1** – **II-6** would be straightforward to synthesize by substitution reactions. Second, we hoped that the different substitution patterns of **II-1** – **II-6** would result in the formation of different discrete or polymeric assemblies. Lastly, we hoped that the xylylene spacer between the adamantylammonium binding domains would be rigid enough to prevent the formation of a 1:1 host:guest inclusion complex. Upon closer inspection *post facto*, we realized that guests **II-1**, **II-2**, and **II-4** – **II-6** are more complex than we anticipated and actually contain one xylenediamine and two adamantylammonium

binding domains (Figure II-2). In the discussion below we abbreviate these domains as PXDA and Ad respectively.

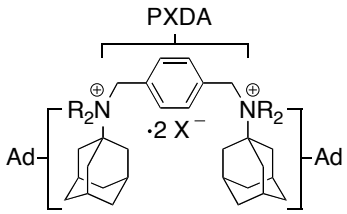

Figure II-2. Depiction of the two different binding domains of the xylylene derived guests (**II-1**, **II-2**, and **II-4** – **II-6**) along with their abbreviations used in this paper.

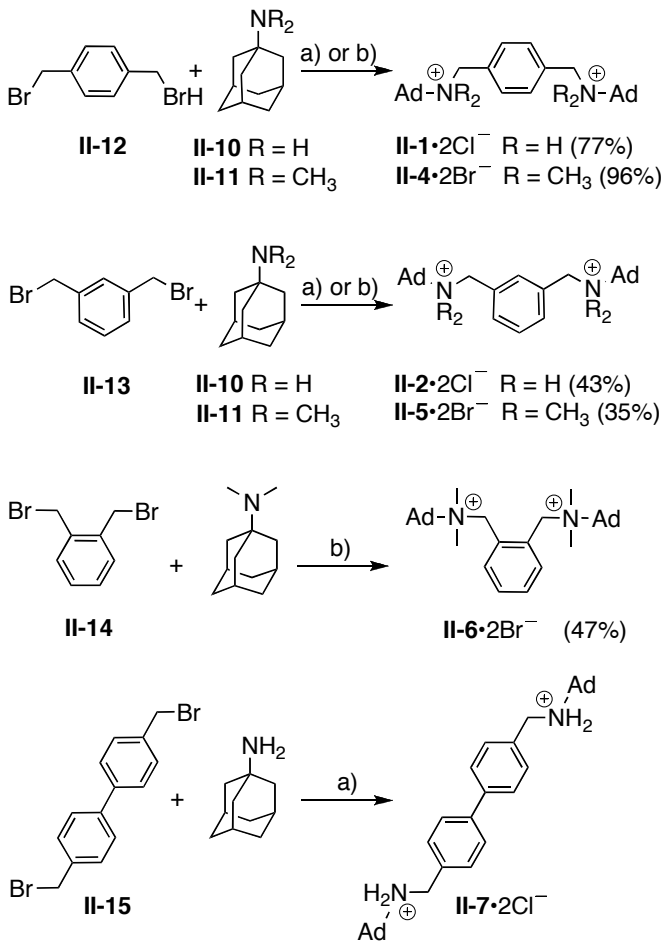

Scheme II-1. Synthesis of guest compounds **II-1**, **II-2**, **II-4** – **II-7**. Conditions: a) Ag_2O, THF, b) CH_3CN, reflux.

2.2.2 Synthesis of Guests **II-1**, **II-2**, and **II-4 – II-6**.

The synthesis of **II-1** and **II-2** was achieved by two-fold S_N2 reaction of the corresponding bis-(bromomethyl)benzenes (**II-12** and **II-13**) with adamantylamine (**II-10**) using Ag_2O in THF (Scheme II-1). The free base amines were then converted to the hydrochloride salts (**II-1** and **II-2**) by treatment with anhydrous HCl. All attempts to synthesize *ortho*-substituted **II-3** were unsuccessful due to competing intramolecular five-membered ring formation. Accordingly, we decided to prepare

the tetramethylated series (**II-4 – II-6**) of compounds to complete the substitution pattern series. Compounds **II-4 – II-6** were prepared by reacting bis-(bromomethyl)benzenes (**II-12 – II-14**) with N,N-dimethyladamantylamine **II-11** in refluxing CH_3CN.

2.2.3 Characterization of Bis-*ns*-CB[10] Complexes with Guests **II-1**, **II-2**, and **II-4 – II-6**.

After we had synthesized guests **II-1**, **II-2**, and **II-4 – II-6** we decided to investigate their use in the preparation of supramolecular polymers. Figure II-3 shows the ^{1}H NMR spectra recorded for guests **II-1**, **II-2**, and **II-4 – II-6** alone and in the presence of bis-*ns*-CB[10]. The ^{1}H NMR spectra for the complexes between *p*-xylylenediamine derivatives **II-1** and **II-4** and bis-*ns*-CB[10] (Figure II-3b and 3f) are sharp and dispersed which is indicative of a single well-defined geometry. In contrast, the spectra obtained for the bis-*ns*-CB[10] complexes of *m*-xylylene diamine derivatives **II-2** and **II-5** (Figures II-3d and 3h) and *o*-xylylene diamine derivative **II-6** are broader and less well defined which suggested the possibility of oligomeric or polymeric assemblies. Comparision of the ^{1}H NMR spectra for *para*-substituted **II-1** before (Figure II-3a) and after the addition of bis-*ns*-CB[10] (Figure II-3b) reveals that the protons corresponding to the Ad binding domain are shifted upfield whereas those of the PXDA binding domain are shifted downfield. It is well known that the cavity region of CB[n] compounds constitutes an NMR shielding region whereas the regions just outside the C=O lined portals are deshielding.[56] Accordingly, within the bis-*ns*-CB[10]•**II-1** complex, both Ad binding domains are inside the cavities of bis-

ns-CB[10] whereas the PXDA group is outside the portal. Similar observations were made for the complex between *p*-substituted **II-4** and bis-*ns*-CB[10]. In contrast, the ^{1}H NMR spectra recorded for the complexes between bis-*ns*-CB[10] and **II-2**, **II-5**, and **II-6** show two classes of resonances for the PXDA (unshifted and downfield shifted) and Ad groups (unshifted and upfield shifted) which suggested that some of the Ad and PXDA domains are unbound and remote from the cavities of bis-*ns*-CB[10]. The integration of the resonances present in the ^{1}H NMR spectra of each of the bis-*ns*-CB[10] complexes with **II-1**, **II-2**, and **II-4** – **II-6** suggests that host and guest are present in equimolar amounts.[91] This observed relative stoichiometry is consistent with 1:1, 2:2, or the desired n:n complexes (Figure II-4).

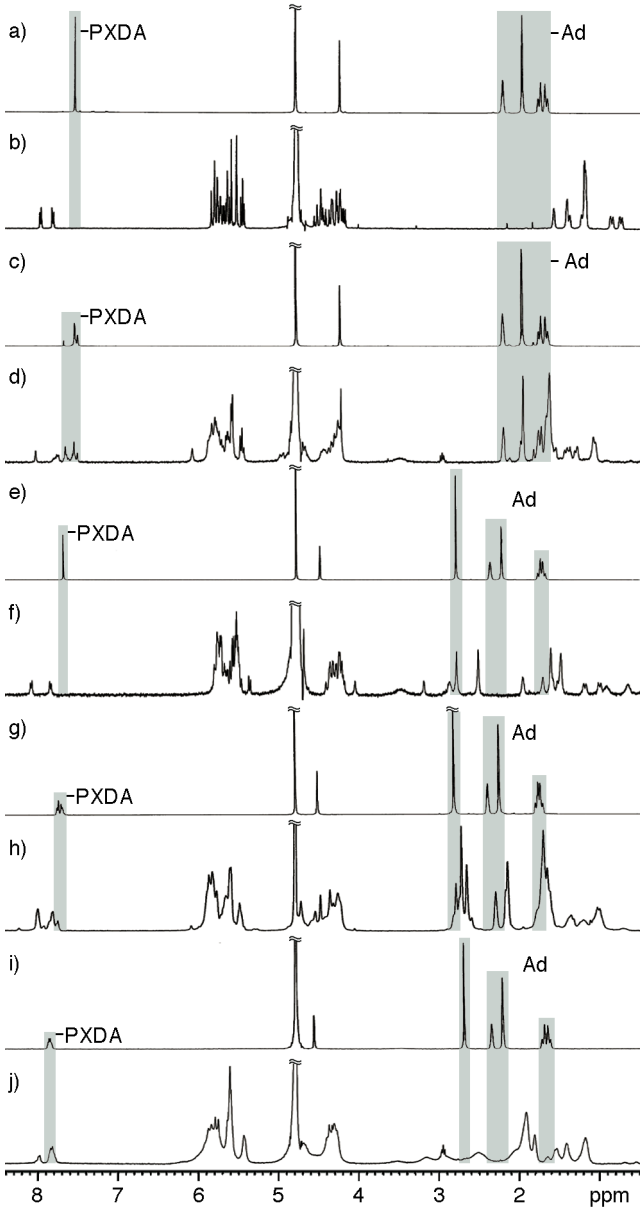

Figure II-3. ^{1}H NMR spectra (400 MHz, D_2O, RT) recorded for solutions of: a) **II-1**, b) bis-*ns*-CB[10]•**II-1**, c) **II-2**, d) a mixture of **II-2** and bis-*ns*-CB[10]•**II-2**, e) **II-4**, f) a mixture of **II-4** and bis-*ns*-CB[10]•**II-4**, g) **II-5**, h) a mixture of **II-5** and bis-*ns*-CB[10]•**II-5**, i) **II-6**, j) bis-*ns*-CB[10]•**II-6**.

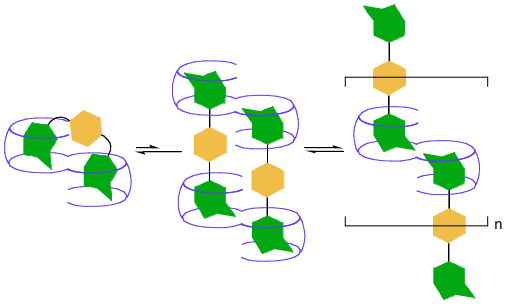

Figure II-4. Potential equilibrium between bis-*ns*-CB[10]•**II-1**, bis-*ns*-CB[10]$_2$•**II-1**$_2$, and bis-*ns*-CB[10]$_n$•**II-1**$_n$ complexes.

2.2.4 Determination of Absolute Host:Guest Stoichiometry by Diffusion Ordered Spectroscopy.

In order to determine the absolute stoichiometry of complexes between bis-*ns*-CB[10] and guests **II-1**, **II-2**, and **II-4** – **II-6** we performed diffusion ordered NMR spectroscopy (DOSY).[92] DOSY spectroscopy allows a determination of the diffusion coefficients (D_s) of a given species in solution. From this knowledge of the values of D_s it is possible to infer the size of the species and therefore the absolute stoichiometry of the supramolecular complexes. Diffusion NMR was performed on samples prepared from equimolar amounts of host and guest for compounds **II-1**, **II-2**, and **II-4** – **II-6** with bis-*ns*-CB[10]. The bis-*ns*-CB[10]•**II-9**$_2$ complex – which does not undergo exchange processes with assemblies formed from bis-*ns*-CB[10] and guests **II-1**, **II-2**, and **II-4** – **II-6** – was used as an internal standard of known molecular size.[31] The diffusion coefficients for these complexes were determined in the standard manner by fitting a plot of field strength versus intensity using equation II-1.

$$I = I_0 e^{-D\gamma^2 g^2 \delta^2 (\Delta - \delta/3)} \qquad \text{(II-1)}$$

In equation II-1, I and I_0 are signal intensities, D is the diffusion coefficient measured in $m^2\ s^{-1}$, γ is the gyromagnetic ratio measured in $s^{-1}\ T^{-1}$, g is the gradient strength measured in G cm^{-1}, δ is the length of the gradient measured in milliseconds, and Δ is the diffusion time measured in milliseconds.[17,92] Table II-1 summarizes the results of the DOSY measurements. The diffusion coefficients measured for the complex between bis-*ns*-CB[10] and *p*-xylylene diamine derivative **II-1** was nearly identical to that measured for bis-*ns*-CB[10]•**II-9**$_2$ which indicates this complex is best formulated as the 1:1 complex (bis-*ns*-CB[10]•**II-1**). Figure II-5a shows an MMFF minimized model of the bis-*ns*-CB[10]•**II-1** complex. In contrast, the diffusion coefficient measured for the complex between *p*-substituted quaternary ammonium guest **II-4** is only 61% of that of bis-*ns*-CB[10]•**II-9**$_2$. For *perfect spheres*, theory predicts that increasing the molecular weight n-fold should lead to a decreased diffusion coefficient by a factor of $n^{-1/3}$; dimers (trimers) are therefore expected to have diffusion coefficients 79% (69%) those of the corresponding monomers. For the rod-like oligomers expected for assemblies based on bis-*ns*-CB[10] we have previously shown that dimers should have diffusion coefficients roughly 67-72% those of monomers.[93] We, therefore, formulate the complex between bis-*ns*-CB[10] and **II-4** as bis-*ns*-CB[10]$_2$•**II-4**$_2$. Examination of an MMFF model of bis-*ns*-CB[10]$_2$•**II-4**$_2$ (Figure II-5b) illustrates the 2:2 stoichiometry.[94] For the complexes between **II-2**, **II-5**, **II-6** and bis-*ns*-CB[10] the diffusion coefficients are significantly smaller and clustered in the range 0.47 – 0.49. This clearly suggests an absolute

stoichiometry greater than 2:2. Unfortunately, in the absence of well defined ^{1}H NMR spectra, x-ray crystallographic results, or electrospray mass spectrometric data assignment of an absolute stoichiometry to these aggregates is speculative.[50,95] Disappointed by these results, we decided to investigate some of the structural variables that might circumvent 1:1 or 2:2 complex formation and promote the formation of higher order linear oligomers or polymers.

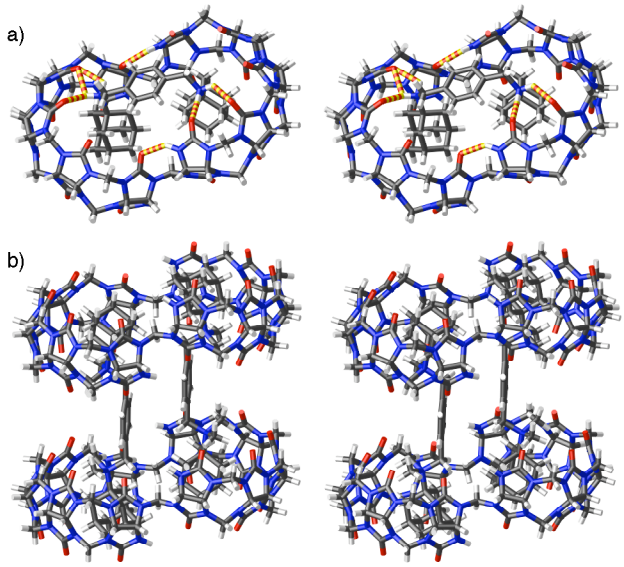

Figure II-5. Stereoviews of the MMFF minimized geometries of: a) bis-*ns*-CB[10]•**II-1** and b) bis-*ns*-CB[10]$_2$•**II-4**$_2$. Color code: C, gray; H, white; N, blue; O, red; H-bonds, red-yellow striped.

Table II-1. Diffusion coefficients (10^{-10} m^2 s^{-1}) measured for the complexes between bis-*ns*-CB[10] and guests **II-1** – **II-8** (D_2O, 400 MHz, 25˚ C) and the corresponding dimensionless ratio of diffusion coefficients relative to internal standard bis-*ns*-CB[10]•**II-9**$_2$.

Guest	D_s complex	D_s bis-*ns*-CB[10]• **II-9**$_2$	Ratio (D_s / $D_{s(\text{bis-}ns\text{-CB[10]•II-9•II-9})}$)
II-1	2.47 ± 0.03	2.45 ± 0.01	1.01
II-2	1.10 ± 0.11	2.24 ± 0.02	0.49
II-4	1.40 ± 0.04	2.27 ± 0.02	0.61
II-5	1.04 ± 0.14	2.18 ± 0.02	0.48
II-6	1.08 ± 0.12	2.31 ± 0.01	0.47
II-7	1.61 ± 0.04	2.42 ± 0.03	0.67
II-8 (10 ˚C)	1.22 ± 0.14	1.54 ± 0.06	0.79

2.2.5 Increased Linker Length Between Ad Binding Domains.

First, we decided to investigate the influence of the length of the linker between the Ad binding domains. For this purpose we targeted compound **II-7** which connects two Ad binding domains with a biphenyl linker. We surmised that the length and rigidity of the biphenyl linking group would preclude the formation of a

1:1 complex and promote the formation of n:n oligomeric or polymeric structures. The synthesis of **II-7** was achieved by treatment of **II-15** with adamantylamine in the presence of Ag_2O in THF (Scheme II-1).

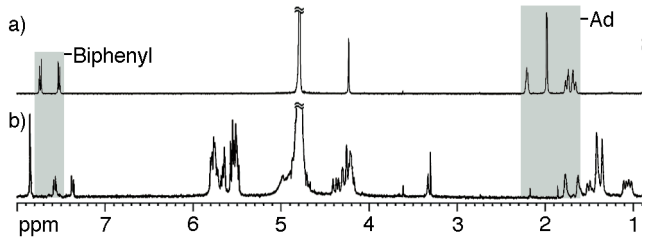

Figure II-6. ^{1}H NMR spectra (400 MHz, D_2O, RT) recorded for solutions of a) **II-7**, b) bis-*ns*-CB[10]$_2$•**II-7**$_2$.

2.2.6 Characterization of the Complex Between Bis-*ns*-CB[10] and **II-7**.

The ^{1}H NMR spectrum of a sample containing equimolar amounts of bis-*ns*-CB[10] and **II-7** shows a single set of resonances which is consistent with a single well-defined host•guest complex (Figure II-6). The bis-*ns*-CB[10]:**II-7** ratio was determined to be 1:1 based on integration of the ^{1}H NMR spectrum. The protons of the Ad domain in Figure II-6b are shifted upfield relative to the adamantyl protons of uncomplexed **II-7** in Figure II-6a which suggests that the Ad domain of **II-**is bound inside the bis-*ns*-CB[10] cavity. Also of interest were the resonances for the biphenyl group which split into one upfield and one downfield shifted set of resonances in the complex. To differentiate between the multitude of possible n:n complexes formed, we performed diffusion NMR experiments. Figure II-7 shows a plot of intensity versus field strength for an equimolar mixture of (bis-*ns*-CB[10]•**II-7**)$_n$ and bis-*ns*-

CB[10]•**II-9**$_2$ as an internal monomeric standard. Fitting these curves to the theoretical equation (eq. II-1) allowed us to extract diffusion coefficients for (bis-*ns*-CB[10]•**II-7**)$_n$ ($D_s = 1.61 \times 10^{-10}$ m^2 s^{-1}) and bis-*ns*-CB[10]•**II-9**$_2$ ($D_s = 2.42 \times 10^{-10}$ m^2 s^{-1}) as an internal standard. The ratio of the values of D_s for (bis-*ns*-CB[10]•**II-7**)$_n$ and bis-*ns*-CB[10]•**II-9**$_2$ is 0.67. This diffusion constant ratio falls in the lower end of the range expected (0.67 – 0.72) for rod-shaped dimers.[93,96] On the basis of the DOSY measurements we formulate the complex as bis-*ns*-CB[10]$_2$•**II-7**$_2$. In contrast to the 1:1 complex observed between bis-*ns*-CB[10] and guest **II-1** which contained a short *p*-xylylene linking group, guest **II-7** did form a higher order complex but with a 2:2 absolute stoichiometry. Although the longer biphenyl linker present in **II-7** did preclude 1:1 complex formation as designed, we believe that the rigidity of the linking group resulted in a preference for 2:2 complex formation (e.g. cyclization) rather than oligomerization. This result highlights one of the main challenges in the formation of supramolecular polymers from pairs of monomers containing two binding groups.

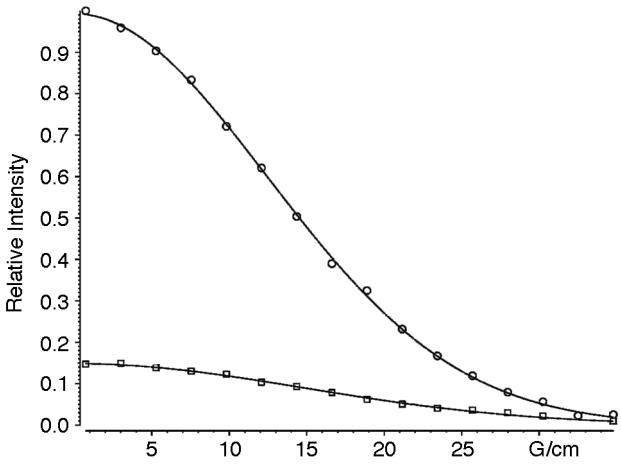

Figure II-7. Plot of signal intensity versus gradient strength and the best fit of the data to eq. II-1. Symbols: o, bis-*ns*-CB[10]$_2$•**II-7**$_2$; □, bis-*ns*-CB[10]•**II-9**$_2$.

2.2.7 Design of Heterovalent Guest **II-8**.

Although we were disappointed that guest **II-7** with a rigid linker did not result in supramolecular polymers when combined with bis-*ns*-CB[10] we hypothesized that the presence of two identical Ad binding domains was to blame. Given that bis-*ns*-CB[10] exhibits homotropic allosterism we wondered what would happen if we synthesized **II-8** which contains Ad and hexanediammonium (HDA) binding domains connected by a *p*-xylylene linker (Figure II-8). Would bis-*ns*-CB[10] choose to form the 1:1 complex bis-*ns*-CB[10]•**II-8** in which the two cavities are filled by different sized binding groups (e.g. Ad and HDA) and violate homotropic allostery? Would bis-*ns*-CB[10] choose to form the 2:2 complex bis-*ns*-CB[10]$_2$•**II-8**$_2$ (Figure II-8)? We hypothesized that homotropic allostery might destabilize the cyclic aggregate bis-*ns*-CB[10]$_2$•**II-8**$_2$ that contains two molecules of bis-*ns*-CB[10] of different non-bonded CH_2•••CH_2 distance (e.g. steric mismatch).

When both of those hypotheses are true we might expect the formation of a supramolecular polymer bis-*ns*-CB[10]$_n$•**II-8**$_n$.

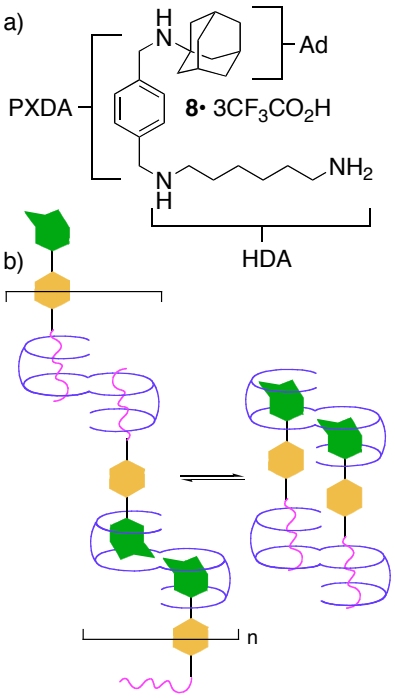

Figure II-8. a) Depiction of the three binding domains of **II-8** along with their abbreviations used in this chapter. b) Theoretical equilibrium between a linear polymer comprising bis-*ns*-CB[10] and **II-8** and bis-*ns*-CB[10]$_2$•**II-8**$_2$.

2.2.8 Synthesis of Heterovalent Guest II-8.

The synthesis of **II-8** was achieved in three steps, starting with commercially available nitrile **II-16** as depicted in Scheme II-2. Conversion of nitrile **II-16** to aldehyde **II-17** was carried out according to the literature procedure.[97] Benzyl

bromide **II-17** was alkylated with **II-10** to afford compound **II-18** in 47% yield. Subsequent reaction of **II-18** with N-(tert-butoxycarbonyl)-1,6-hexanediamine (**II-19**), afforded the corresponding diamine which was deprotected to yield **II-8** (75%) as a water-soluble trifluoroacetate salt.

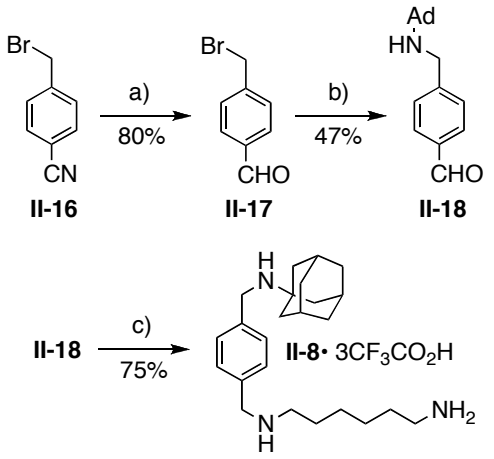

Scheme II-2. Synthesis of **II-8**. Reaction conditions: a) i. DIBAL, toluene, 0 °C, 1 h. ii. 10% HCl, 1 h, rt. b) **II-10**, Ag_2O, THF. c) i. N-(tert-butoxycarbonyl)-1,6-hexanediamine (**II-19**), toluene, reflux, 20 h. ii. $NaBH_4$, MeOH, reflux (30 min.), then stir at RT (15 h). iii. TFA/CH_2Cl_2 (1:1), RT, 8 h.

2.2.9 Characterization of the Complex Between Bis-*ns*-CB[10] and Guest **II-8**.

We first prepared the complex between equimolar amounts of bis-*ns*-CB[10] and **II-8**. The ^{1}H NMR spectra of uncomplexed guest **II-8** and its complex are shown in Figure II-9a-b. The ^{1}H NMR spectrum of the complex (Figure II-9b) is composed of a significant number of relatively sharp resonances which suggested that the

system is not polymeric. Integration of the ^{1}H NMR spectrum of the assembly confirmed that equal numbers of molecules of bis-*ns*-CB[10] and **II-8** were incorporated. The diffusion coefficient for the complex was 79% that of the monomeric standard bis-*ns*-CB[10]•**II-9**$_2$ (Table II-1) which suggests that complex is best formulated as bis-*ns*-CB[10]$_2$•**II-8**$_2$.[98] Fortunately, we also observed a peak at *m/z* = 1339 in the ESI-MS which corresponds to [bis-*ns*-CB[10]$_2$•**II-8**$_2$]$^{3+}$ which confirms the assignment of 2:2 stoichiometry.[99]

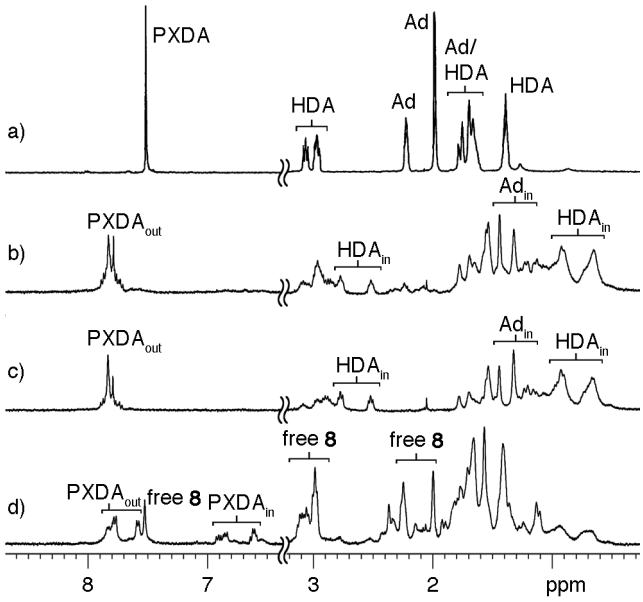

Figure II-9. ^{1}H NMR spectra (400 MHz, D_2O, RT) recorded for: a) **II-8**, and mixtures of bis-*ns*-CB[10] and **II-8** at different relative stoichiometry b) 1:1, c) 2:1, and d) 1:2.

It was possible to tease some information from the chemical shifts of the resonances for distinct regions of guest **II-8** within the bis-*ns*-CB[10]$_2$•**II-8**$_2$ complex. For example, when either the Ad or HDA portion of guest **II-8** is bound within the

interior of bis-*ns*-CB[10] the adjacent PXDA domain is positioned directly outside of the host cavity. We refer to this situation as $PXDA_{out}$. The spectroscopic fingerprint for a $PXDA_{out}$ situation is a slight deshielding of the resonances for the PXDA domain. Conversely, when a PXDA binding domain is inside the cavity of bis-*ns*-CB[10], we refer to the situation as $PXDA_{in}$. The spectroscopic fingerprint for a $PXDA_{in}$ situation is a shielding of the resonances for the PXDA domain. Figure II-9b shows spectroscopic fingerprints for $PXDA_{out}$, Ad_{in}, and HDA_{in} binding modes. Accordingly, we formulate the geometry of the bis-*ns*-$CB[10]_2$•**II-8**$_2$ complex as shown in Scheme II-3. We depict the bis-*ns*-$CB[10]_2$•**II-8**$_2$ assembly which displays homotropic allostery but we believe the alternate diastereomer where each molecule of bis-*ns*-CB[10] contains one HDA and one Ad binding domain is also formed.

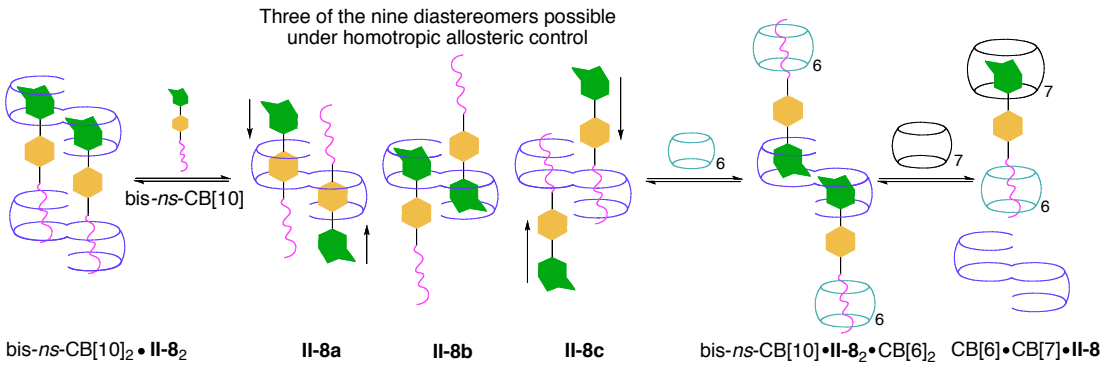

Scheme II-3. Depiction of the equilibrium structures obtained upon treatment of bis-*ns*-$CB[10]_2$•**II-8**$_2$ with **II-8** then CB[6] then CB[7].

Given the ability of bis-*ns*-CB[10] to display homotropic allosterism we wondered whether changing the relative stoichiometry of bis-*ns*-CB[10] to guest **II-8** would result in changes in the molecularity of the resulting complex or changes in the location of the host along guest **II-8** (e.g. $PXDA_{in}$ binding mode). Figure II-9c shows the ^{1}H NMR spectrum obtained from a 2:1 mixture of bis-*ns*-CB[10] and **II-8**. This spectrum is nearly identical to that shown in Figure II-9b which indicates that an excess of host bis-*ns*-CB[10] is not sufficient to change the absolute molecularity of the assembly.[100] In contrast, Figure II-9d shows the ^{1}H NMR obtained from a 1:2 mixture of bis-*ns*-CB[10] and **II-8**. At a 1:2 relative stoichiometry, the ^{1}H NMR spectrum shows a reduction in the intensity of the resonances corresponding to HDA_{in} and Ad_{in} geometries and the appearance of a new set of resonances corresponding to an $PXDA_{in}$ geometry. Scheme II-3 depicts three possible diastereomers of the bis-*ns*-CB[10]•**II-8**$_2$ complex under homotropic allosteric control. The diastereomers with two $PXDA_{in}$, Ad_{in}, and HDA_{in} binding modes are referred to as **II-8a**, **II-8b**, and **II-8c**, respectively. Because the cavity of bis-*ns*-CB[10] contains two distinct ureidyl C=O portals (e.g. top and center) there are three possible diatereomers (e.g. top-top, top-center, and center-center) for **II-8a**, **II-8b**, and **II-8c**.[101] The dominant formation of a 1:2 host:guest stoichiometry complex was further supported by the observation of a peak at *m/z* = 794 in the ESI-MS which corresponds to the [bis-*ns*-CB[10]•**II-8**$_2$]$^{3+}$ ion. We confirmed a spacing of 0.33 *m/z* units which supports our formulation of a 3^+ ion. We also observed an ion of substantial intensity for the 4^+ state. The driving force for this stoichiometry induced change from bis-*ns*-CB[10]$_2$•**II-8**$_2$ to bis-*ns*-CB[10]•**II-8**$_2$ is interesting and informative. Bis-*ns*-CB[10] contains two cavities

each of which contribute significant binding free energy upon complexation. In contrast, guest **II-8** contains three binding sites (Ad, PXDA, and HDA). Because the Ad, PXDA, and HDA binding regions are connected by common NH_2^+ groups, it is not possible for two adjacent binding regions (e.g. Ad and PXDA or PXDA and HDA) to be bound simultaneously. In contrast, the more widely spaced Ad and HDA binding domains may be complexed simultaneously. Consequently, at a 1:1 bis-*ns*-CB[10]:**II-8** stoichiometry guest **II-8** is forced to use both the Ad and HDA binding domains in order for both cavities of bis-*ns*-CB[10] to be filled. When the bis-*ns*-CB[10]:**II-8** stoichiometry is raised to 1:2 there is enough guest present so that the Ad, PXDA, and HDA binding domains compete for inclusion inside each cavity of bis-*ns*-CB[10] based on their individual binding affinities.[102-104]

2.2.10 Reversibility of Host:Guest Molecularity.

Understanding that the molecularity of the bis-*ns*-CB[10]•**II-8**$_2$ complex is responsive to host:guest stoichiometry, we wanted to demonstrate the reversibility of the switching process shown in Scheme II-3 in a stimuli-responsive manner. Figure II-10a shows the ^{1}H NMR spectrum of an initial sample containing bis-*ns*-CB[10]•**II-8**$_2$. Figure II-10b shows the ^{1}H NMR spectrum recorded after the sample of Figure II-10a was saturated with solid bis-*ns*-CB[10]. The spectrum shown in Figure II-10b – which shows only peaks for a $PXDA_{out}$ binding mode – indicates the transformation from bis-*ns*-CB[10]•**II-8**$_2$ molecularity to bis-*ns*-CB[10]$_2$•**II-8**$_2$. Figure II-10c shows the ^{1}H NMR spectrum recorded after the sample of Figure II-10b was treated with

two equivalents of **II-8**. The ^{1}H NMR spectrum shows return of the equilibrium to favor the bis-*ns*-CB[10]•**II-8**$_2$ complex in the presence of excess guest. We find this reversible change in molecularity intriguing because it results, in principle, in a change in the overall length of the aggregate which could be very useful in the construction of molecular muscles.[36,105,106]

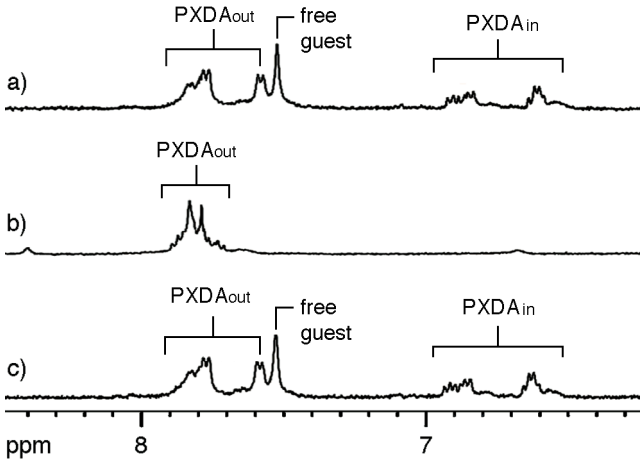

Figure II-10. Aromatic region of the ^{1}H NMR spectra (400 MHz, D_2O, RT) of a sample undergoing alternate successive additions of bis-*ns*-CB[10] and **II-8**: a) a 1:2 ratio of bis-*ns*-CB[10] to **II-8**, b) after addition of excess bis-*ns*-CB[10], and c) after addition of excess **II-8**.

2.3 Stimuli-Responsive Switching Behavior.

In the previous sections, we showed that a change in bis-*ns*-CB[10]:**II-8** stoichiometry resulted in a reversible change in the molecularity of the host•guest complex. We rationalized this behavior in terms of the binding constants of various binding domains of the guest toward bis-*ns*-CB[10]. Given the very high binding

affinity and high selectivity exhibited by various members of the CB[n] family toward ammonium ion guests (e.g. K_a (CB[6]•hexanediammonium) = 4.5×10^8 M^{-1}) and K_a (CB[7]•adamantylammonium) = 4.2×10^{12} M^{-1}) we wondered whether CB[6] and CB[7] could be used to selectively complex the HDA and Ad binding domains of **II-8** and thereby serve as an exogenous chemical stimulus to control the molecularity of the interaction of bis-*ns*-CB[10] with **II-8** and potentially reduce the number of diastereomers observed.

Figure II-11b shows the ^{1}H NMR spectrum measured after the addition of two equivalents of CB[6] to a solution containing the mixture of diastereomers of bis-*ns*-CB[10]•**II-8**$_2$ which is shown in Figure II-11a. The addition of CB[6] results in the selective complexation of the HDA binding domain by CB[6] because of its high K_a value which sterically precludes binding at the PXDA binding domain of **II-8** and leaves only the Ad binding domain open for complexation with bis-*ns*-CB[10]. There are three possible diastereomers of the pentamolecular complex bis-*ns*-CB[10]•**II-8**$_2$•CB[6]$_2$ which are shown in Figure II-12. The ^{1}H NMR spectrum of the major diastereomer of bis-*ns*-CB[10]•**II-8**$_2$•CB[6]$_2$ shows a pair of doublets for the PXDA binding domain in the $PXDA_{out}$ region along with a single set of resonances for the Ad and HDA binding domains in the Ad_{in} and HDA_{in} regions. The observation of a pair of doublets in the $PXDA_{out}$ region is consistent with the top-top and center-center diastereomers, but is inconsistent with the top-center diastereomer based on symmetry considerations.[107] Most interesting to us is the observation that bis-*ns*-CB[10]•**II-8**$_2$•CB[6]$_2$ is on average longer than the precursor mixture of diastereomers

of bis-*ns*-CB[10]•**II-8**$_2$. The free energy associated with the complexation of the HDA binding region of **II-8** by CB[6] performs work and stretches the CB[10]•**II-8**$_2$ complex. The reversible control of the extension and contraction of such supramolecular (polymeric) systems would be very interesting in the creation of molecular machines.

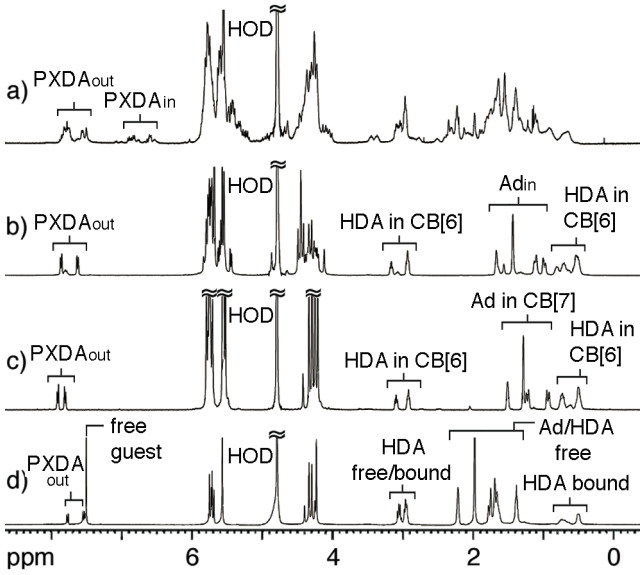

Figure II-11. ^{1}H NMR spectra (400MHz, D_2O, RT) recorded for solutions of: a) bis-*ns*-CB[10]•**II-8**$_2$, b) after addition of 2 equiv. CB[6] to obtain CB[6]$_2$•**II-8**$_2$•bis-*ns*-CB[10], and c) after addition of 2 equiv. CB[7] to obtain CB[7]•**II-8**•CB[6] and solid bis-*ns*-CB[10]. d) Control spectrum for a mixture of CB[6]•**II-8** and excess **II-8**.

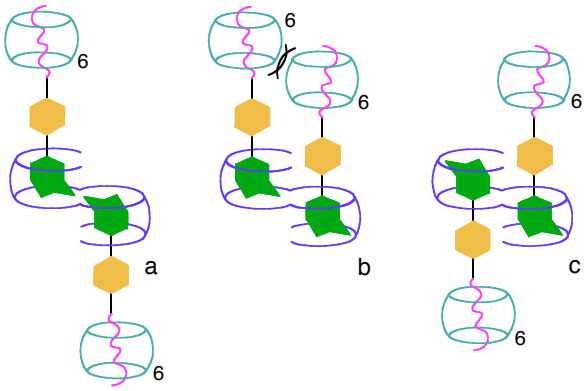

Figure II-12. Three different diastereomers of the bis-*ns*-CB[10]•**II-8**$_2$•CB[6]$_2$ complex.

To control the subsequent contraction of the bis-*ns*-CB[10]•**II-8**$_2$•CB[6]$_2$ complex we decided to take advantage of the remarkably high binding affinity of CB[7] toward adamantylammonium ions. Figure II-11c shows the ^{1}H NMR spectrum recorded for a solution containing bis-*ns*-CB[10]•**II-8**$_2$•CB[6]$_2$ that was treated with two equivalents of CB[7]. The resonances for the PXDA and Ad domains exhibit new patterns but remain in the PXDA$_{out}$ and Ad$_{in}$ regions indicative of the formation of CB[7]•**II-8**•CB[6]. Free bis-ns-CB[10] precipitates. In this process, the binding free energy of CB[7] toward the Ad domain of **II-8** and the precipitation of bis-*ns*-CB[10] provide the driving force for the reduction in the overall dimensions of the supramolecular complex.

2.4 Conclusions.

In summary, we have studied the complexation between double cavity host bis-*ns*-CB[10] and divalent guests **II-1** – **II-8** with the goal of forming stimuli

responsive supramolecular polymeric systems of n:n absolute stoichiometry. In practice, we found that guests **II-1**, **II-2**, and **II-4** – **II-6** which contain two adamantylammonium ion binding domains separated by *p*-, *m*-, and *o*-xylylene groups preferentially form 1:1 (bis-*ns*-CB[10]•**II-1**), 2:2 (bis-*ns*-CB[10]$_2$•**II-4**$_2$), and short potentially cyclic oligomeric complexes (with **II-2**, **II-5**, and **II-6**). We found that a longer spacer between the adamantyl binding groups (e.g. biphenyl spacer in **II-7**) successfully prevents 1:1 complex formation but promotes 2:2 complex formation (bis-*ns*-CB[10]$_2$•**7**$_2$) at the expense of supramolecular polymers. Finally, we investigated the interaction between bis-*ns*-CB[10] and guest **II-8** which contains Ad, PXDA, and HDA binding domains with a particular emphasis on bis-*ns*-CB[10]:**II-8** stoichiometry. At 1:1 bis-*ns*-CB[10]:**II-8** stoichiometry the Ad and HDA binding domains are complexed to satisfy the ability of bis-*ns*-CB[10] to complex two binding groups simultaneously. At 1:2 stoichiometry all three binding domains become complexed during formation of a mixture of diastereomers of bis-*ns*-CB[10]•**II-8**$_2$. Lastly, we showed that the addition of CB[6] and CB[7] molecular containers substantially simplifies the composition of this mixture by selective complexation of the HDA and Ad binding domains of **II-8**, respectively.

In conclusion, this work highlights some of the challenges that need to be overcome in the formation of supramolecular polymers from divalent hosts and divalent guests, namely the preferential formation of lower molecularity (cyclic) complexes (e.g. 1:1, 2:2) which are favored from an entropic viewpoint in the absence of enthalpic penalties for formation of 1:1 and 2:2 complex formation. In ongoing work we are targeting the preparation of trivalent guests that contain a central CB[7]

binding region and terminal adamantylammonium binding groups that will prevent 1:1 and 2:2 complex formation by steric interaction between CB[7] groups. An aspect of the work with potentially broad impact is the recognition of the special behavior of guests (e.g. **II-8**) that contain multiple *overlapping binding regions*. In such systems, binding at one domain sterically prevents binding at an adjacent domain. The addition of CB[n] molecular containers that selectively complex a given portion of guest **II-8** (e.g. CB[6] and CB[7]) can control the reversible extension and contraction of this system which is of potential use in the formation of stimuli responsive molecular machines (e.g. molecular muscles). Lastly, we would like to highlight the successful formation of the *penta*-molecular complex bis-*ns*-CB[10]•**II-8**$_2$•CB[6]$_2$ which is enabled by the extremely high affinity of CB[n] hosts for their ammonium ion targets (K_a up to 10^{15} M^{-1}) in water.[46] The formation of high molecularity complexes where multiple different components occupy a predetermined location on the basis of simple binding affinities[108] in water suggests methods for the construction of even higher molecularity functional systems.

2.5 Experimental.

2.5.1 General Experimental.

Starting materials were purchased from commercial suppliers and used without further purification. Compound **II-17** was prepared according to a literature procedure.[97] THF and toluene were distilled from sodium benzophenone ketyl before use. TLC analysis was performed using precoated plates from EMD Chemicals Inc. Column chromatography was performed using silica gel (230 – 400 mesh, 0.040 –

0.063 μm) from Sorbent Technologies using eluents in the indicated v:v ratio. Melting points were measured on a Meltemp apparatus in open capillary tubes and are uncorrected. IR spectra were recorded on a JASCO FT/IR-4100 spectrophotometer and are reported in cm^{-1}. NMR spectra were measured on Bruker AM-400, DRX-400, and DRX-500 instruments operating at 400 MHz or 500 MHz for ^{1}H and 100 MHz or 125 MHz for ^{13}C. The chemical shift for 1,4-dioxane in the ^{13}C NMR spectra was referenced at 67.19 ppm. Mass spectrometry was performed using a VG Autospec instrument by fast atom bombardment (FAB) using the indicated matrix or a JEOL AccuTOF instrument by electrospray ionization (ESI) using solutions of the complexes in 50:50 MeOH:H_2O (v:v). Diffusion experiments were carried out on a Bruker AM-400 spectrometer, using the Stimulated Echo Pulse Gradient sequence. All samples for the DOSY experiments were prepared in Shigemi tubes (Shigemi, Inc., Allison Park, PA) and the temperature was calibrated using MeOH and actively controlled. Diffusion coefficients were derived using integration of the desired peaks to an exponential decay with the "Simfit (Bruker XWINNMR)" software.

2.5.2 Synthetic Procedures and Characterization.

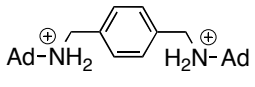

II-1•2Cl$^-$

Compound II-1: To a solution of **II-12** (117 mg, 0.442 mmol) in anh. THF (10 mL) was added Ag_2O (205 mg, 0.884 mmol). After 5 min., **II-10** (200 mg, 1.32 mmol) was added and the reaction was sonicated for 8 h. The silver salts were removed by filtration and the filtrate was concentrated by rotary evaporation. The residue was chromatographed (SiO_2, $CHCl_3$/MeOH 40:1

+ 2% NH_4OH) giving **II-1** as a white solid. The free-base was dissolved in $CHCl_3$ (25 mL) and HCl gas was bubbled through the solution to deliver **II-1**•$(HCl)_2$ (162 mg, 0.339 mmol) in 77% yield. M.p. > 300 ˚C (dec.). TLC ($CHCl_3$/MeOH 20:1 + 1% NH_4OH) R_f 0.25. IR (cm^{-1}): 3415m, 2913s, 2852m, 1616w, 1454m, 1080m, 836m. ^1H NMR (400 MHz, D_2O): 7.52 (s, 4H), 4.25 (s, 4H), 2.24 (br. s, 6H), 2.00 (br. s, 12H), 1.78 (d, J = 12.6, 6H), 1.70 (d, J = 12.2, 6H). ^{13}C NMR (100 MHz, D_2O, 1,4-dioxane as external reference): 133.3, 131.0, 59.0, 43.5, 38.6, 35.5, 29.5. MS (FAB, glycerol): m/z 405 (100, $[M + H]^+$). HR-MS (FAB, glycerol): m/z 405.3269 ($[M + H]^+$, $C_{28}H_{41}N_2$, calcd 405.3270).

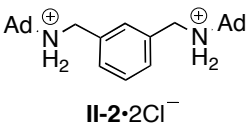

II-2•$2Cl^-$

Compound II-2: To a solution of **II-13** (175 mg, 0.662 mmol) in anh. THF (12 mL) was added Ag_2O (307 mg, 1.32 mmol). After 5 min., **II-10** was added (300 mg, 1.987 mmol) and the reaction was sonicated for 8 h. The silver salts were removed by filtration and the filtrate was concentrated by rotary evaporation. The residue was chromatographed (SiO_2, $CHCl_3$/MeOH 35:1 + 1% NH_4OH) giving **II-2** as a white solid. The free-base was dissolved in $CHCl_3$ (25 mL) and HCl gas was bubbled through the solution to deliver **II-2**•$(HCl)_2$ (136 mg, 0.284 mmol) in 43% yield. M.p. > 300 ˚C (dec.). TLC ($CHCl_3$/MeOH 30:1 + 1% NH_4OH) R_f 0.20. IR (cm^{-1}): 3419w, 2906s, 2761s, 1571m, 1452m, 1366m, 1078s, 803m, 699s. ^1H NMR (400 MHz, D_2O): 7.67 (s, 1H), 7.60-7.45 (m, 3H), 4.25 (s, 4H), 2.24 (br. s, 6H), 2.00 (br. s, 12H), 1.78 (d, J = 12.6, 6H), 1.70 (d, J = 12.4, 6H). ^{13}C NMR (125 MHz, D_2O, 1,4-dioxane as external reference): 132.6, 130.9,

130.7, 130.2, 58.5, 43.1, 38.1, 35.0, 29.0. MS (FAB, glycerol): *m/z* 405 (100, $[M + H]^+$). HR-MS (FAB, glycerol): *m/z* 405.3285 ($[M + H]^+$, $C_{28}H_{41}N_2$, calcd 405.3270).

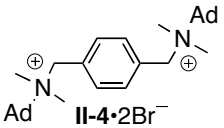

Compound II-4: A solution of **II-12** (100 mg, 0.379 mmol) and **II-11** (204 mg, 1.14 mmol) in CH_3CN (5 mL) was heated to reflux for 12 h and then cooled to RT. The resulting precipitate was filtered and washed with CH_3CN (3 mL). The white solid was dried under high vacuum to afford **II-4** (110 mg, 0.177 mmol) in 96% yield. M.p. 273-277°C. IR (cm^{-1}): 2914s, 2854m, 1475m, 1387m, 1306m, 1034m, 854s, 748m. ^1H NMR (400 MHz, D_2O): 7.55 (s, 4H), 4.37 (s, 4H), 2.68 (s, 12H), 2.26 (br. s, 6H), 2.12 (br. s, 12H), 1.65 (d, J = 12.4, 6H), 1.59 (d, J = 12.4, 6H). ^{13}C NMR (125 MHz, D_2O, 1,4-dioxane as external reference): 134.8, 131.1, 76.9, 60.6, 43.7, 35.4, 31.2 (only 7 of the 8 expected resonances were observed). MS (FAB, glycerol): *m/z* 541 (100, $[M - Br]^+$). HR-MS (FAB, glycerol): *m/z* 541.3160 ($[M - Br]^+$ $C_{32}H_{50}N_2Br$, calcd 541.3157).

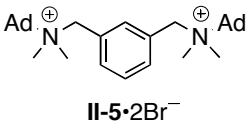

Compound II-5: A solution of **II-13** (100 mg, 0.379 mmol) and **II-11** (204 mg, 1.14 mmol) in CH_3CN (5 mL) was heated to reflux for 12 h and then cooled to RT. The resulting precipitate was filtered and washed with CH_3CN (3 mL). The white solid was dried under high vacuum to afford **II-5** (83 mg, 0.134 mmol) in 35% yield. M.p. 206-210 °C. IR (cm^{-1}): 2907s, 2851m, 1470s, 1378m, 1305m, 1035s, 817s, 756s. ^1H NMR (400 MHz, D_2O): 7.65-7.50 (m, 4H), 4.38 (s, 4H), 2.69 (s, 12H), 2.27 (br. s, 6H), 2.13 (br. s, 12H), 1.66 (d, J = 12.6, 6H), 1.60 (d, J = 12.6, 6H). ^{13}C NMR (125 MHz, D_2O, 1,4-dioxane as

external reference): 139.0, 136.3, 130.5, 129.8, 76.9, 60.8, 43.6, 35.4, 35.4, 31.3. MS (FAB, glycerol): *m/z* 541 (100, $[M - Br]^+$). HR-MS (FAB, glycerol): *m/z* 541.3168 ($[M - Br]^+$, $C_{32}H_{50}N_2Br$, calcd 541.3157).

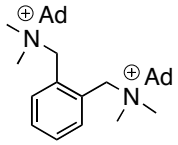

II-6•2Br$^-$

Compound II-6: A solution of **II-14** (100 mg, 0.379 mmol) and **II-11** (204 mg, 1.14 mmol) in CH_3CN (5 mL) was heated to reflux for 12 h and then cooled to RT. The resulting precipitate was filtered and washed with CH_3CN (3 mL). The white solid was dried under high vacuum to afford **II-6** (110 mg, 0.177 mmol) in 47% yield. M.p. 155-158˚C. IR (cm^{-1}): 3477m, 3380, 3044w, 2915s, 2880s, 2853m, 1478s, 1372m, 1303m, 1033s, 827m, 752s. ^{1}H NMR (400 MHz, D_2O): 7.70-7.60 (m, 4H), 4.44 (s, 4H), 2.63 (s, 12H), 2.30 (br. s, 6H), 2.17 (br. s, 12H), 1.68 (d, J = 12.6, 6H), 1.61 (d, J = 12.6, 6H). ^{13}C NMR (100 MHz, D_2O, 1,4-dioxane as external reference): 136.5, 132.0, 130.0, 78.1, 57.0, 43.4, 35.3, 35.1, 31.2. MS (FAB, glycerol): *m/z* 541 (100, $[M - Br]^+$). HR-MS (FAB, glycerol): *m/z* 541.3184 ($[M - Br]^+$, $C_{32}H_{50}N_2Br$, calcd 541.3157).

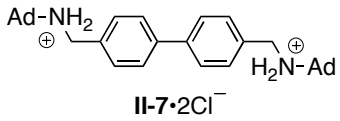

II-7•2Cl$^-$

Compound II-7: To a solution of **II-15** (225 mg, 0.662 mmol) in anh. THF (12 mL) was added Ag_2O (307 mg, 1.33 mmol). After 5 min., **II-10** (300 mg, 1.99 mmol) was added and the reaction was sonicated for 8 h. The silver salts were removed by filtration and the filtrate was concentrated by rotary evaporation. The residue was chromatographed (SiO_2, $CHCl_3$/MeOH 35:1 + 1% NH_4OH) giving **II-7** as a white solid. The free-base was dissolved in $CHCl_3$ (25 mL) and HCl gas was bubbled through the solution to deliver

II-7•$(HCl)_2$ (153 mg, 0.318 mmol) in 48% yield. M.p. > 330 ˚C (dec.). TLC ($CHCl_3$/MeOH 30:1 + 1% NH_4OH) R_f 0.10. IR (cm^{-1}): 2918s, 2851w, 2757w, 1456m, 1309m, 1099m, 794s. ^1H NMR (400 MHz, D_2O): 7.68 (d, J = 7.8, 4H), 7.47 (d, J = 7.8, 4H), 4.17 (s, 4H), 2.14 (br. s, 6H), 1.92 (br. s, 12H), 1.69 (d, J = 12.5, 6H), 1.60 (d, J = 12.5, 6H). ^{13}C NMR (100 MHz, D_2O, 1,4-dioxane as external reference): 141.3, 131.8, 131.0, 128.3, 58.9, 43.7, 38.7, 35.5, 29.6. MS (FAB, 3-NBA): *m/z* 481 (100, $[M + H]^+$). HR-MS (FAB, 3-NBA): *m/z* 481.3583 ($[M + H]^+$, $C_{34}H_{45}N_2$, calcd 481.3583).

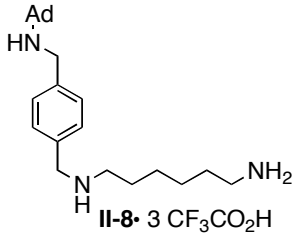

II-8• 3 CF_3CO_2H

Compound II-8: A 10 mL flask containing a solution of **II-17** (103 mg, 382 mmol) **II-19** (99 mg, 458 mmol) in anh. $PhCH_3$ (6 mL) was fitted with a Dean-Stark trap and reflux condenser. The reaction was refluxed for 16 h, then cooled to rt. The solvent was removed by rotary evaporation and the residue dried at high vacuum. The residue was dissolved in MeOH (5 mL) and cooled to 0 ˚C. A solution of $NaBH_4$ (87 mg, 2.292 mmol) in MeOH (1 mL) was added dropwise and then the mixture was heated at reflux for 30 min. before stirring at RT for 15 h. The solvent was concentrated by rotary evaporation and the residue dissolved in EtOAc (25 mL) and washed with brine (2 × 25 mL). The organic layer was dried over $MgSO_4$, filtered, and concentrated by rotary evaporation. The resulting residue was taken up in a mixture of TFA (3 mL) and CH_2Cl_2 (3 mL) and stirred at RT overnight. Upon removal of the solvent under reduced pressure and high vacuum, pure **II-8** (135 mg, 287 mmol) was afforded in 75% yield. M.p. 175-178 ˚C. IR (cm^{-1}): 2921w, 2855w,

1655s, 1459w, 1174s, 1129s, 830m, 798m, 720s. ^{1}H NMR (400 MHz, D_2O): 7.39 (s, 4H), 4.12 (s, 4H), 2.94 (t, J = 7.9, 2H), 2.85 (t, J = 7.4, 2H), 2.10 (br. s, 3H), 1.87 (br. s, 6H), 1.70-1.50 (m, 10H), 1.27 (br. m, 4H). ^{13}C NMR (100 MHz, $CDCl_3$): 133.7, 132.7, 131.2, 59.2, 51.2, 47.9, 43.7, 40.1, 38.8, 35.7, 29.7, 27.3, 26.0, 25.9. MS (FAB, 3-NBA): *m/z* 370 (100, $[M + H]^+$). HR-MS (FAB, 3-NBA): *m/z* 370.3218 ($[M + H]^+$, $C_{24}H_{40}N_3$, calcd 370.3222).

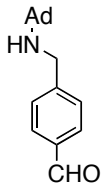

II-18

Compound II-18: To a solution of **II-17** (209 mg, 1.05 mmol) in anh. THF (10 mL) was added Ag_2O (236 mg, 1.05 mmol). After 5 min., **II-10** (159 mg, 1.05 mmol) was added and the reaction was sonicated for 8 h. The silver salts were removed by filtration and the filtrate was concentrated by rotary evaporation. The residue was chromatographed (SiO_2, $CHCl_3$/MeOH 20:1 + 1% NH_4OH) giving pure **II-18** (103 mg, 382 mmol) as a white solid in 47% yield. M.p. 75-78 ˚C. IR (cm^{-1}): 2899m, 2845m, 1686s, 1606m, 1578m, 1141m, 1096m, 820s, 776s. ^{1}H NMR (400 MHz, $CDCl_3$): 9.95 (s, 1H), 7.79 (d, J = 8.0, 2H), 7.49 (d, J = 8.0, 2H), 3.82 (s, 2H), 2.07 (br. s, 3H), 1.60-1.20 (m, 12H). ^{13}C NMR (100 MHz, $CDCl_3$): 192.1, 149.3, 135.1, 129.9, 128.7, 51.0, 44.9, 42.9, 36.7, 29.6. MS (FAB, 3-NBA): *m/z* 270 (100, $[M + H]^+$). HR-MS (FAB, 3-NBA): *m/z* 270.1861 ($[M + H]^+$, $C_{18}H_{24}NO$, calcd.

2.5.3 ^{1}H NMR and ^{13}C NMR Spectra of Guests **II-1**, **II-2**, **II-4** – **II-8**, and **II-18**.

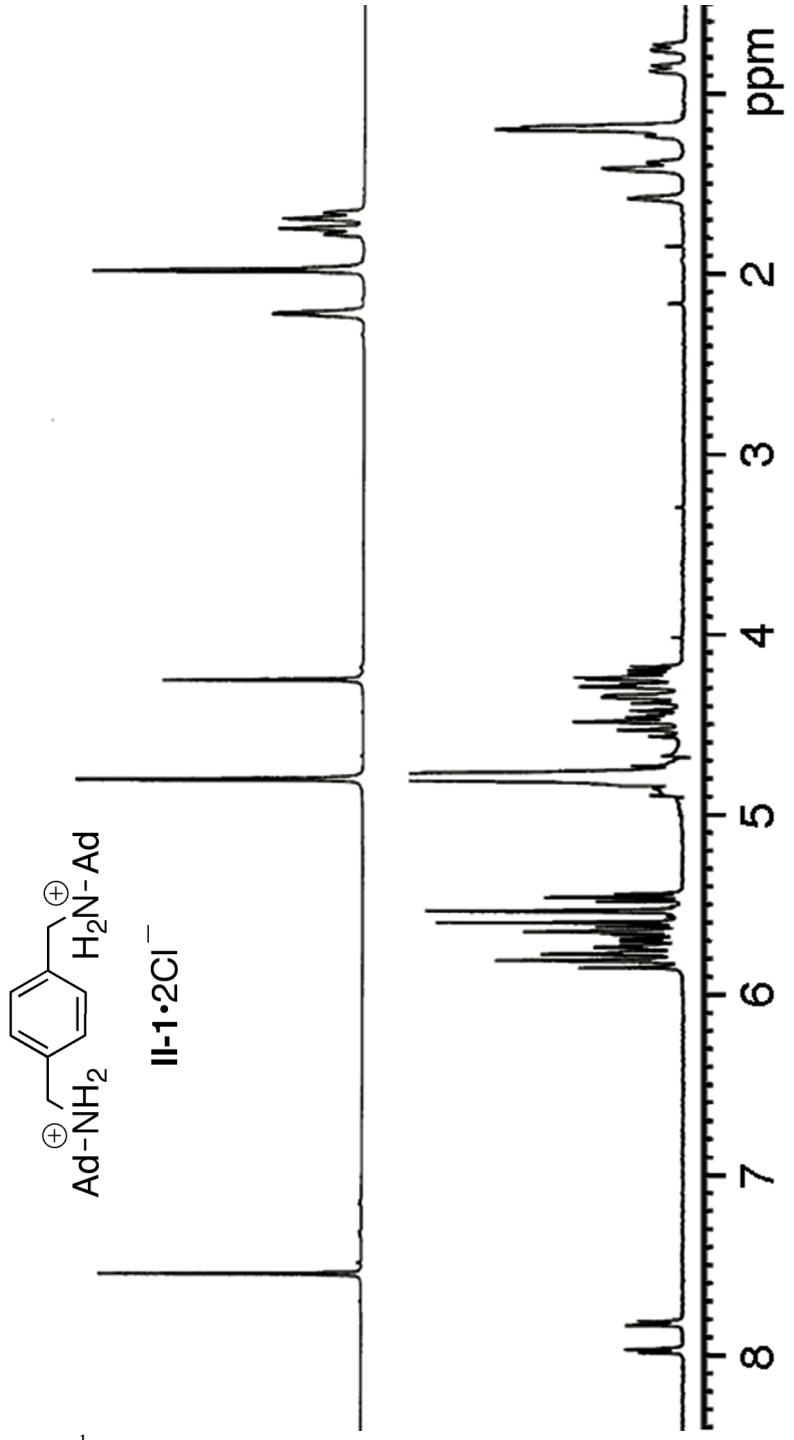

Figure II-13. ^{1}H NMR spectrum recorded for **II-1**•2Cl^{-} and its complex with bis-*ns*-CB[10] (400 MHz, D_2O, RT).

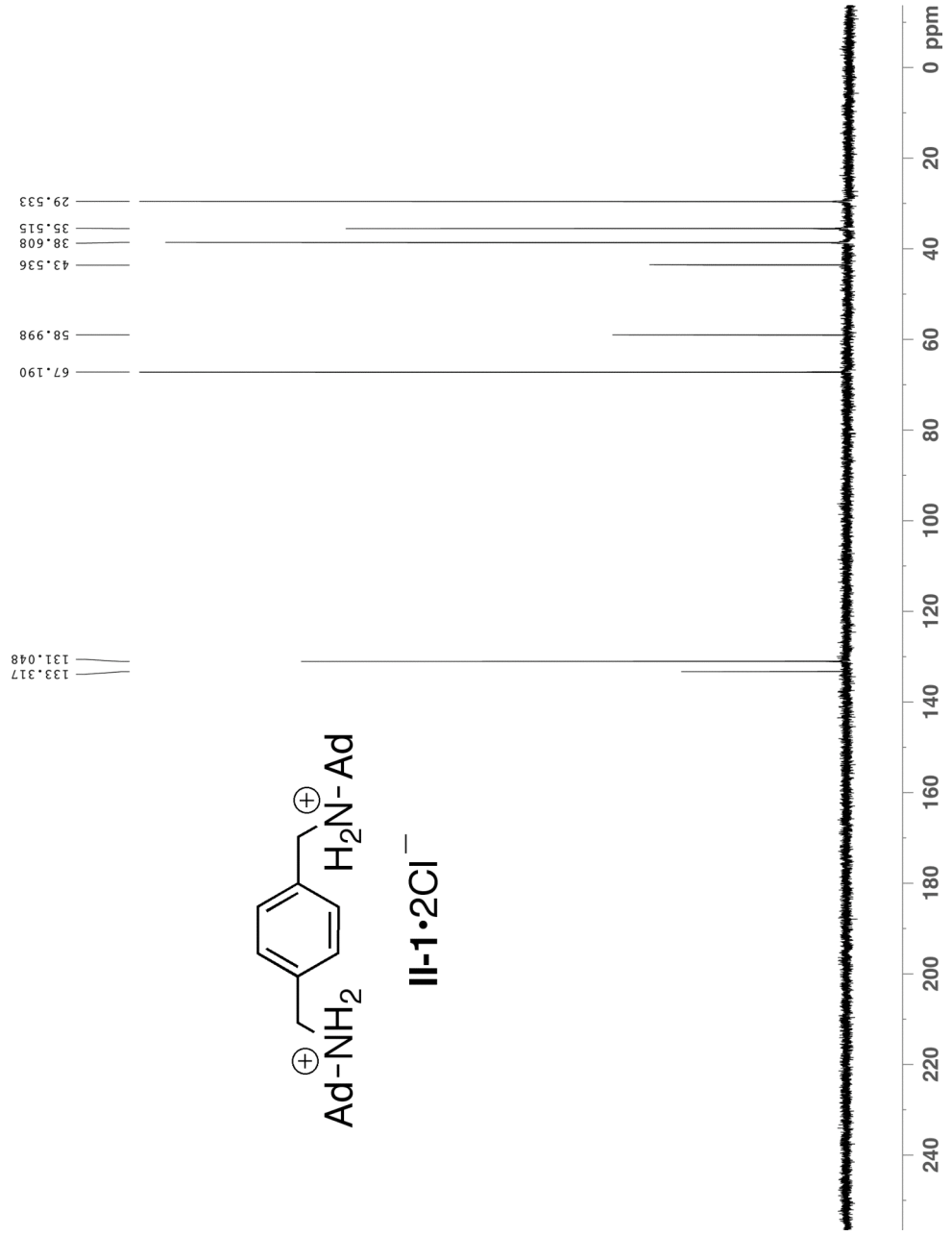

Figure II-14. ^{13}C NMR spectrum recorded for **II-1**•$2Cl^-$ (100 MHz, D_2O, RT).

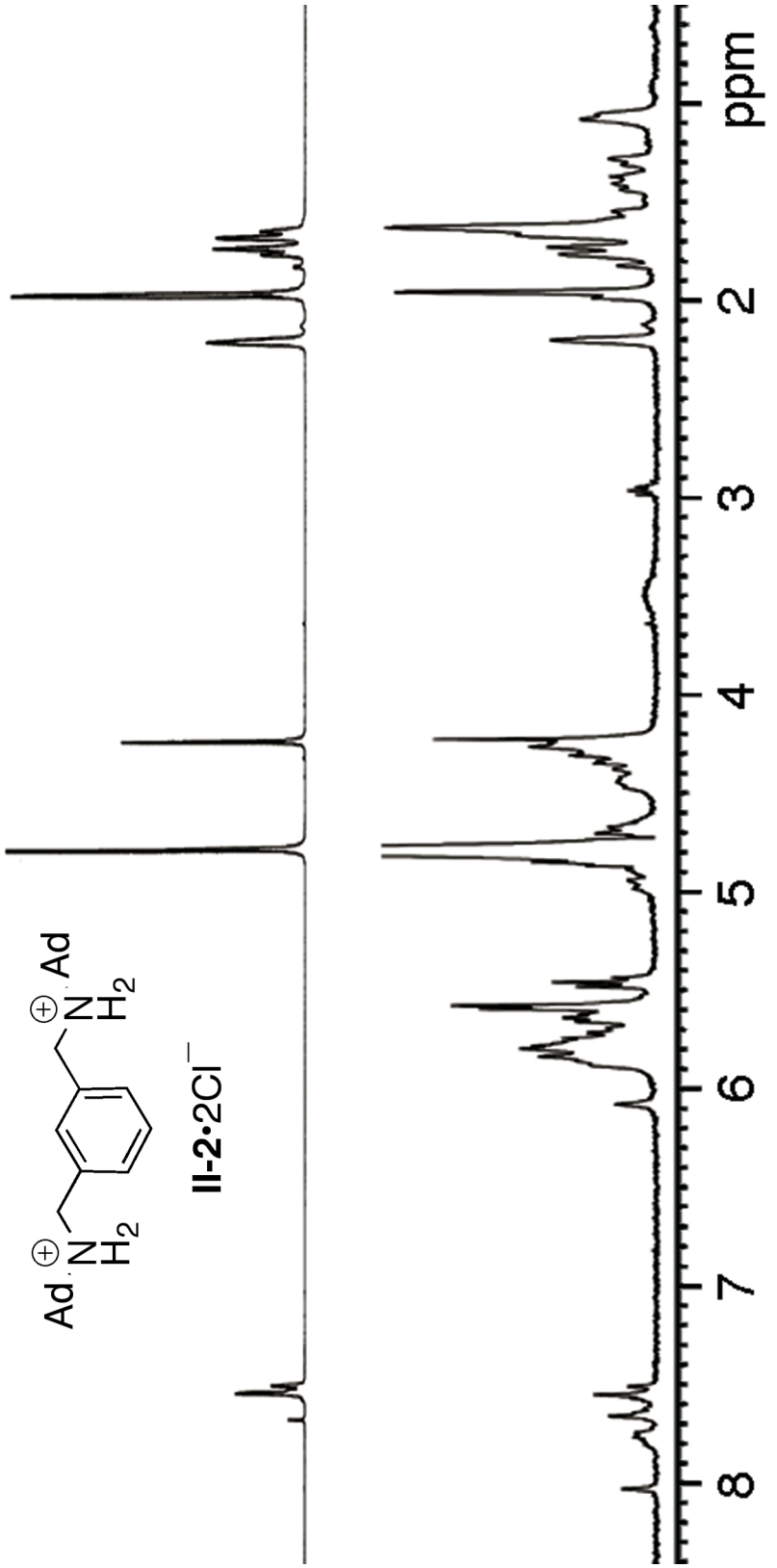

Figure II-15. ^{1}H NMR spectrum recorded for **11-2**•2Cl^{-} and its complex with bis-*ns*-CB[10] (400, D_2O, RT).

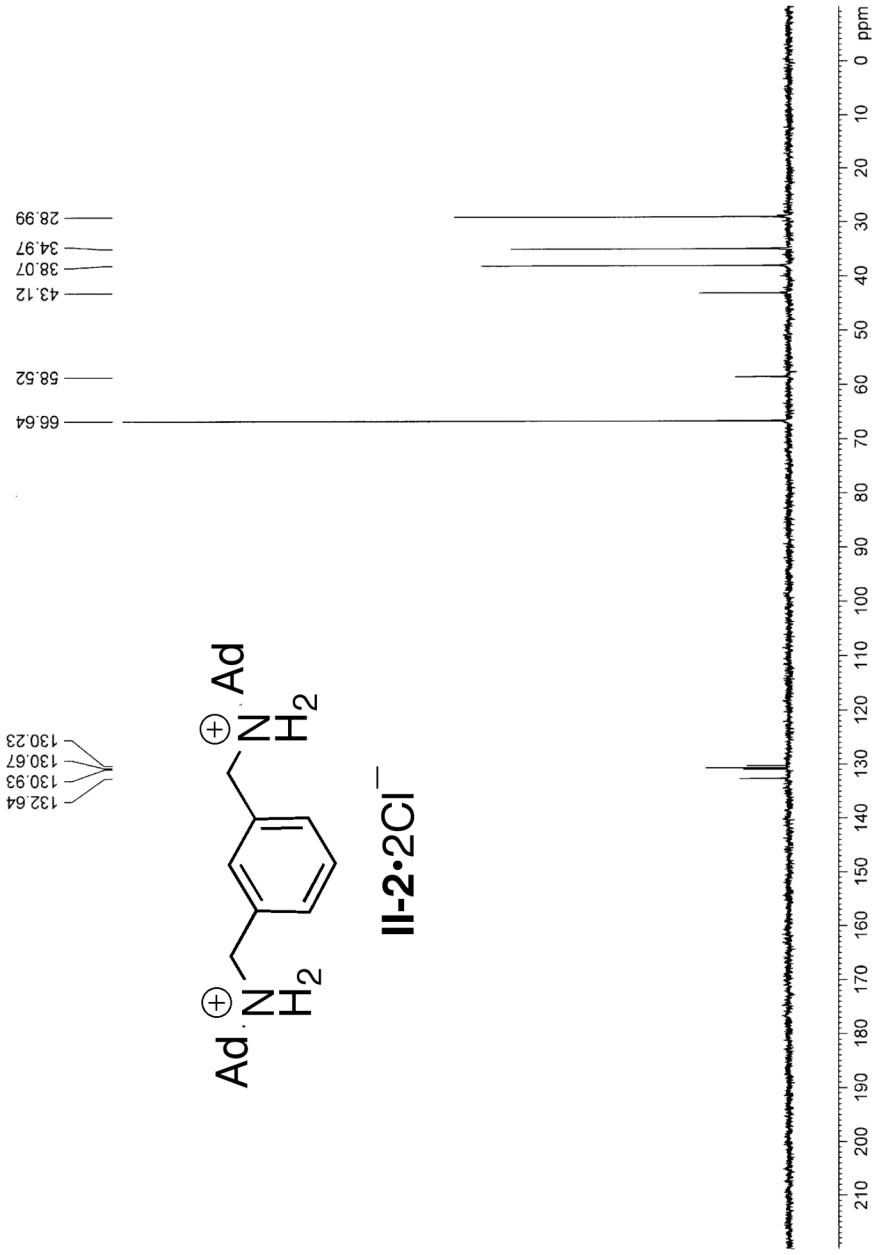

Figure II-16. ^{13}C NMR spectrum recorded for **II-2**•$2Cl^-$ (125 MHz, D_2O, RT).

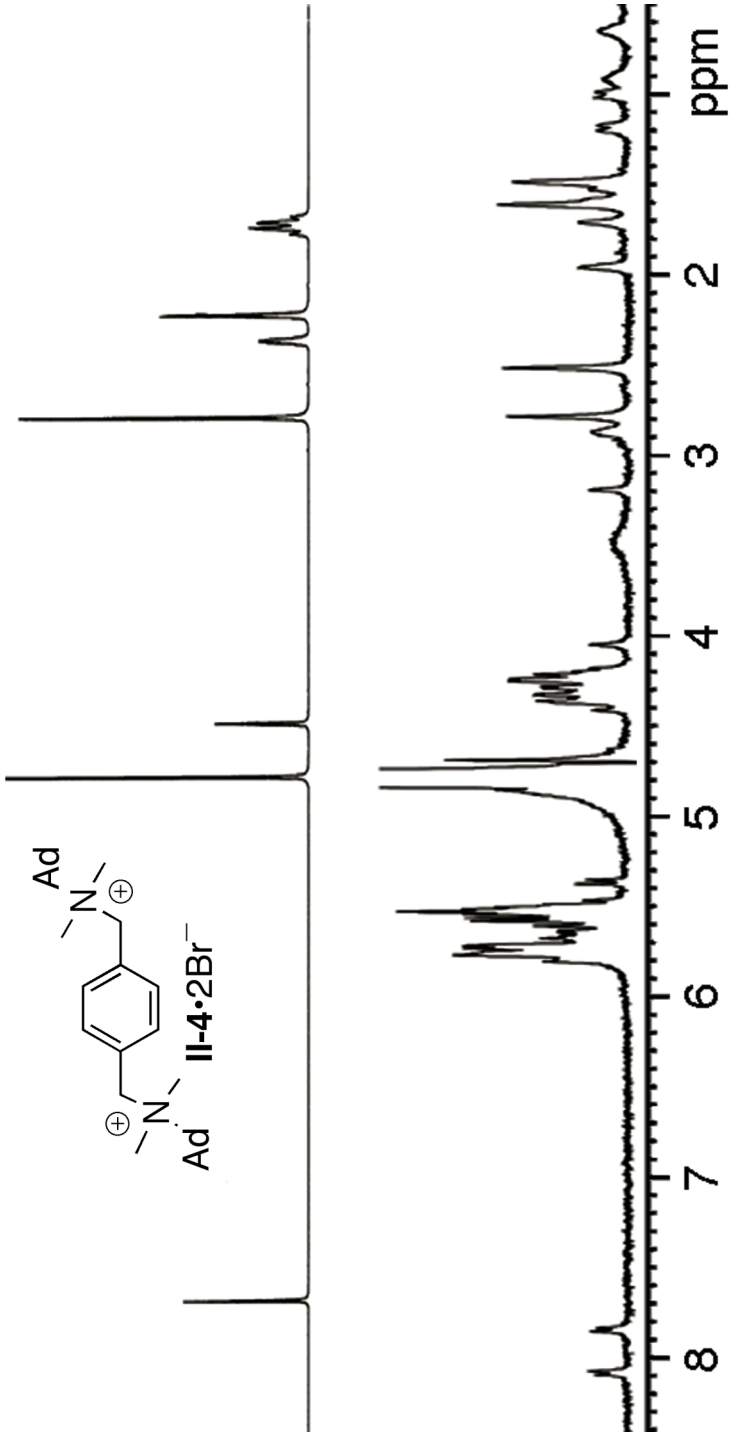

Figure II-17. ^{1}H NMR spectrum recorded for **II-4**•2Br^{-} and its complex with bis-*ns*-CB[10] (400 MHz, D_2O, RT).

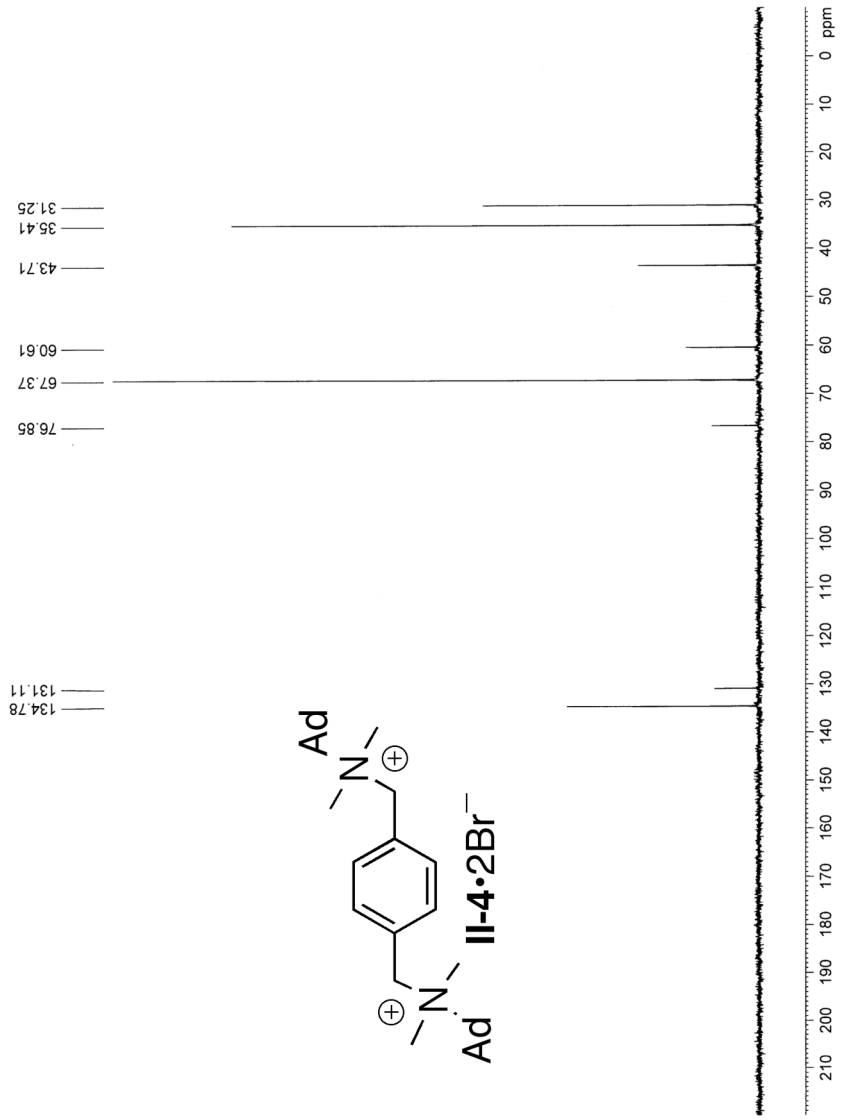

Figure II-18. ^{13}C NMR spectrum recorded for **II-4**•$2Br^-$ (125 MHz, D_2O, RT).

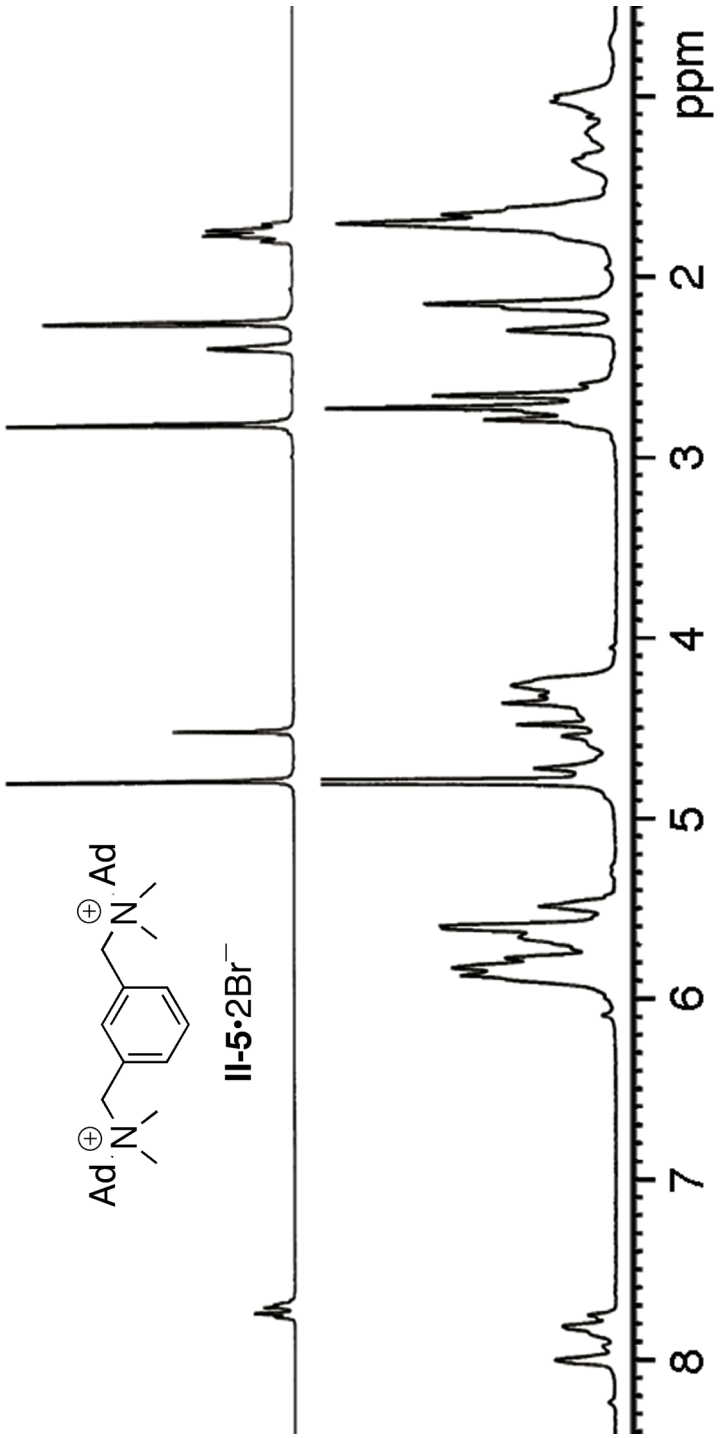

Figure II-19. ^{1}H NMR spectrum recorded for **II-5**•2Br^{-} and its complex with bis-*ns*-CB[10] (400 MHz, D_2O, RT).

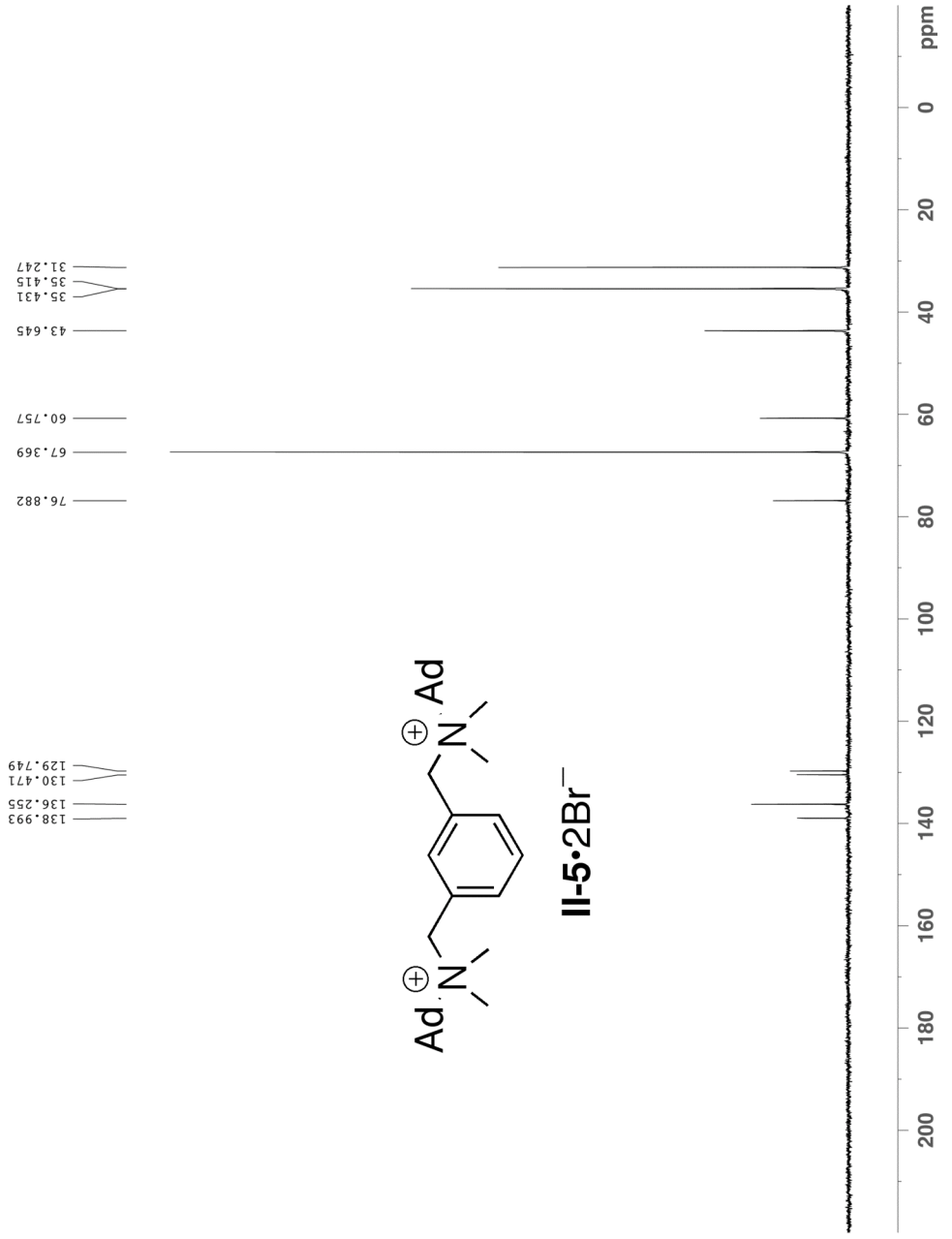

Figure II-20. ^{13}C NMR spectrum recorded for **II-5**•$2Br^-$ (125 MHz, D_2O, RT).

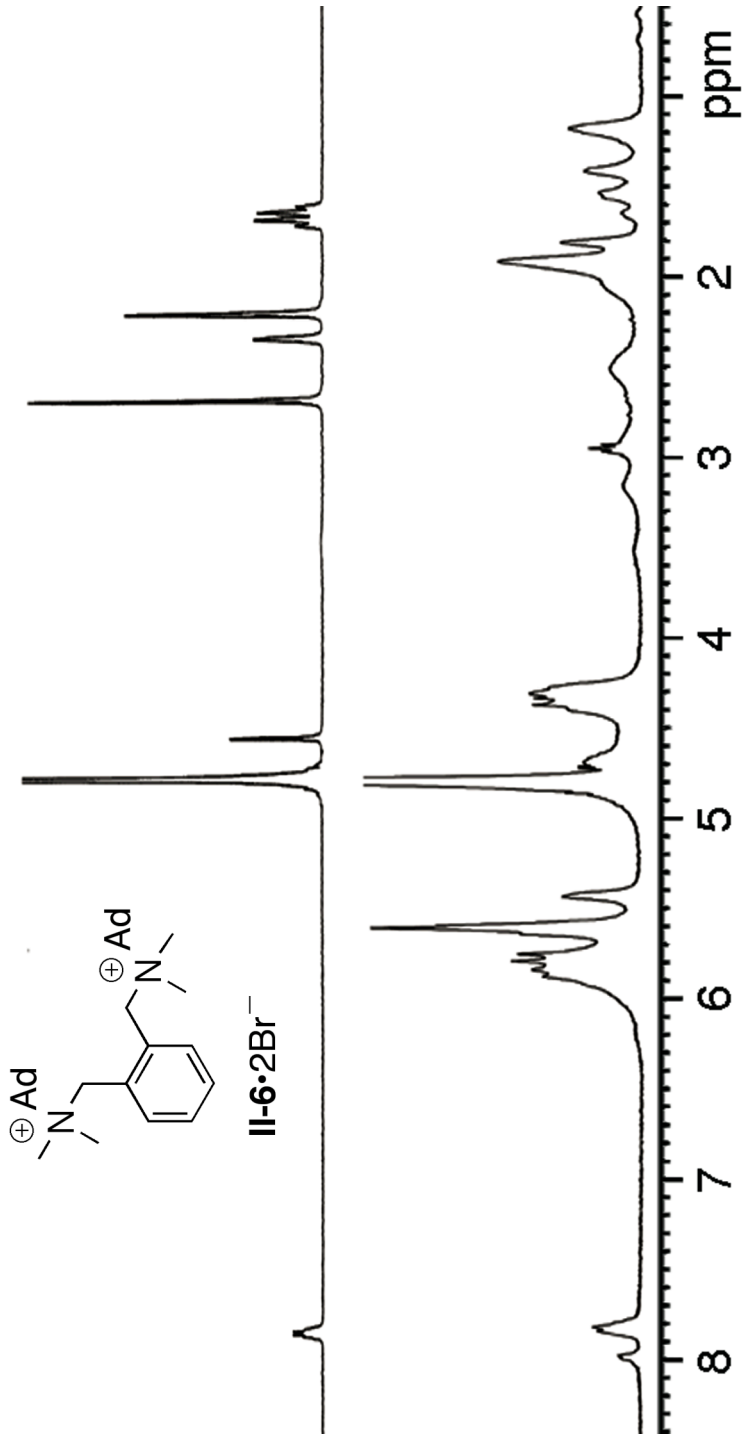

Figure II-21. ^{1}H NMR spectrum recorded for **II-6**•2Br^{-} and its complex with bis-*ns*-CB[10] (400 MHz, D_2O, RT).

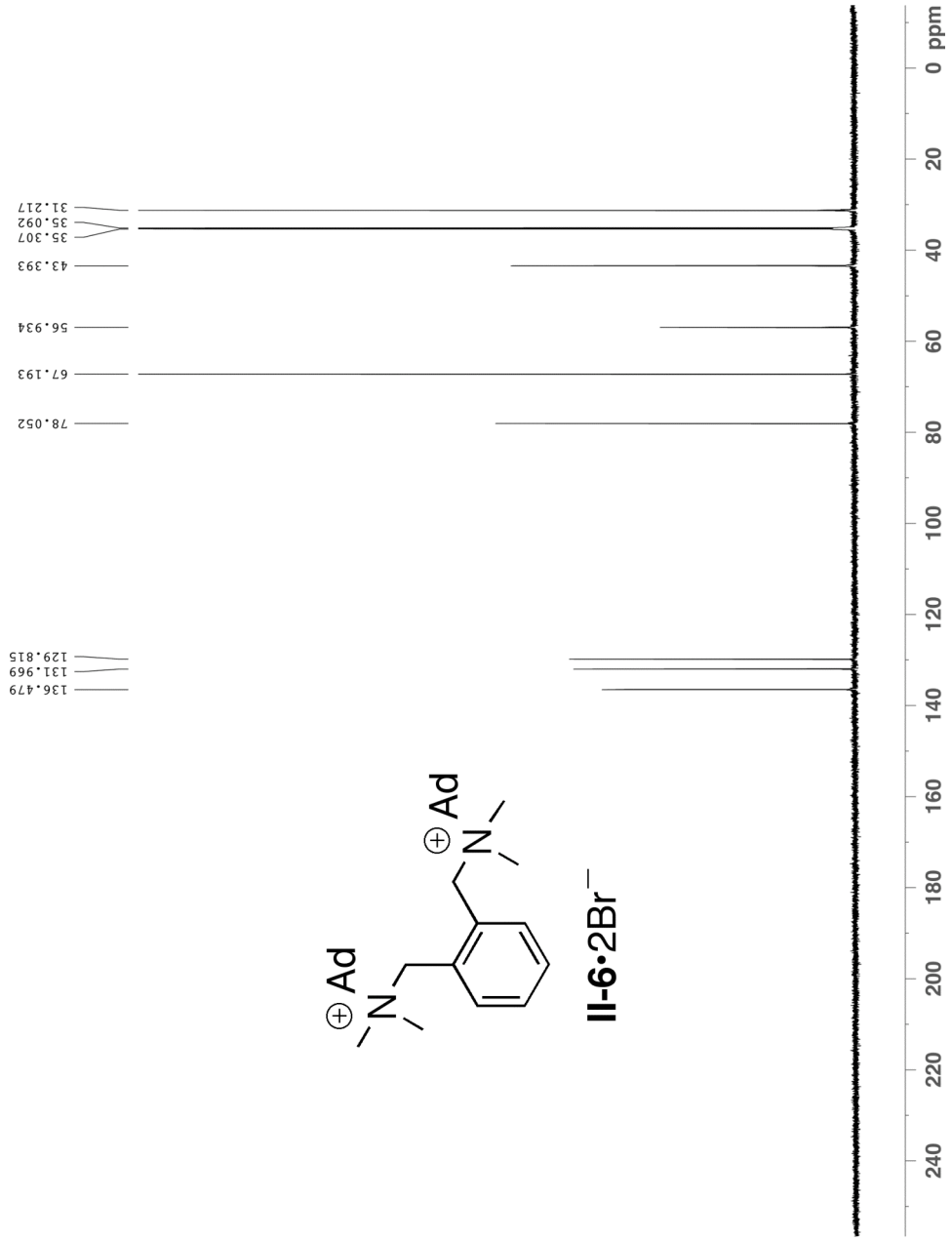

Figure II-22. ^{13}C NMR spectrum recorded for **II-6**•$2Br^-$ (100 MHz, D_2O, RT).

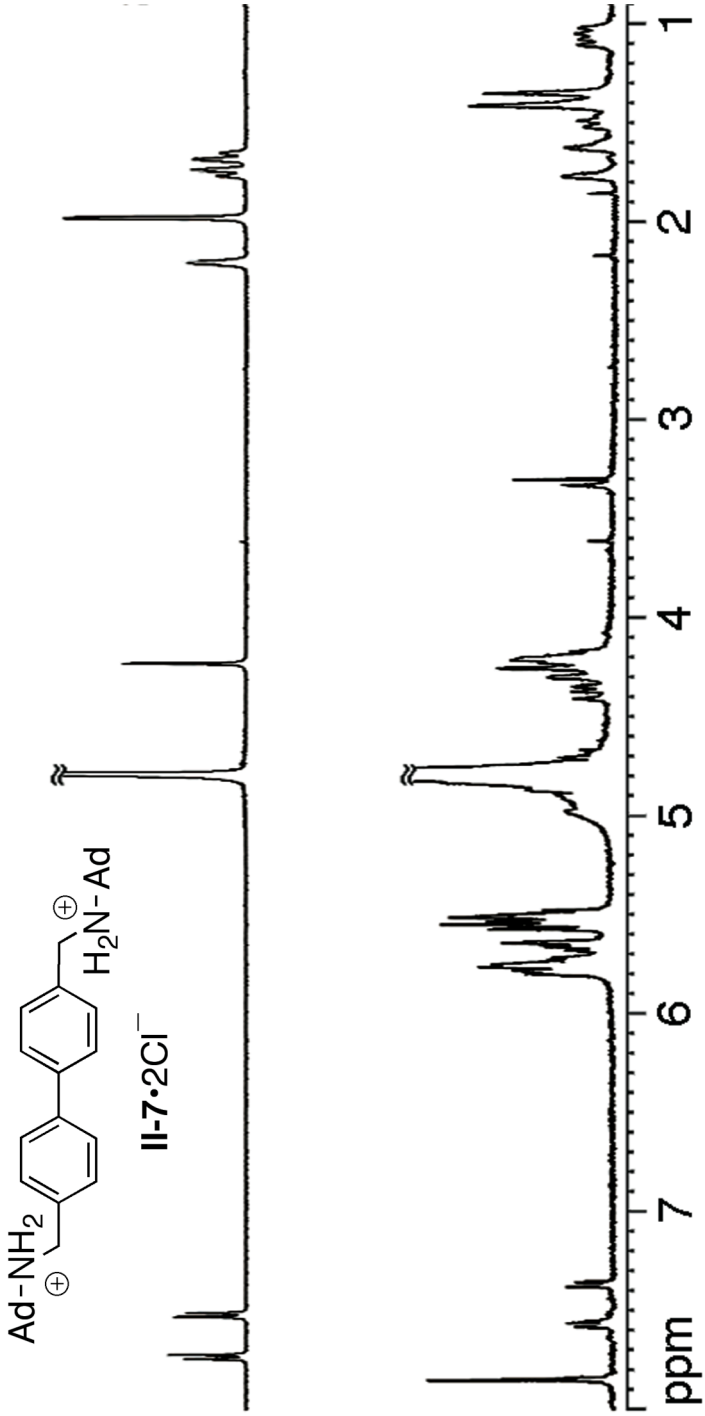

Figure II-23. ^{1}H NMR spectrum recorded for **II-7**•2Cl^{-} and its bis-*ns*-CB[10] (400 MHz, D_2O, RT).

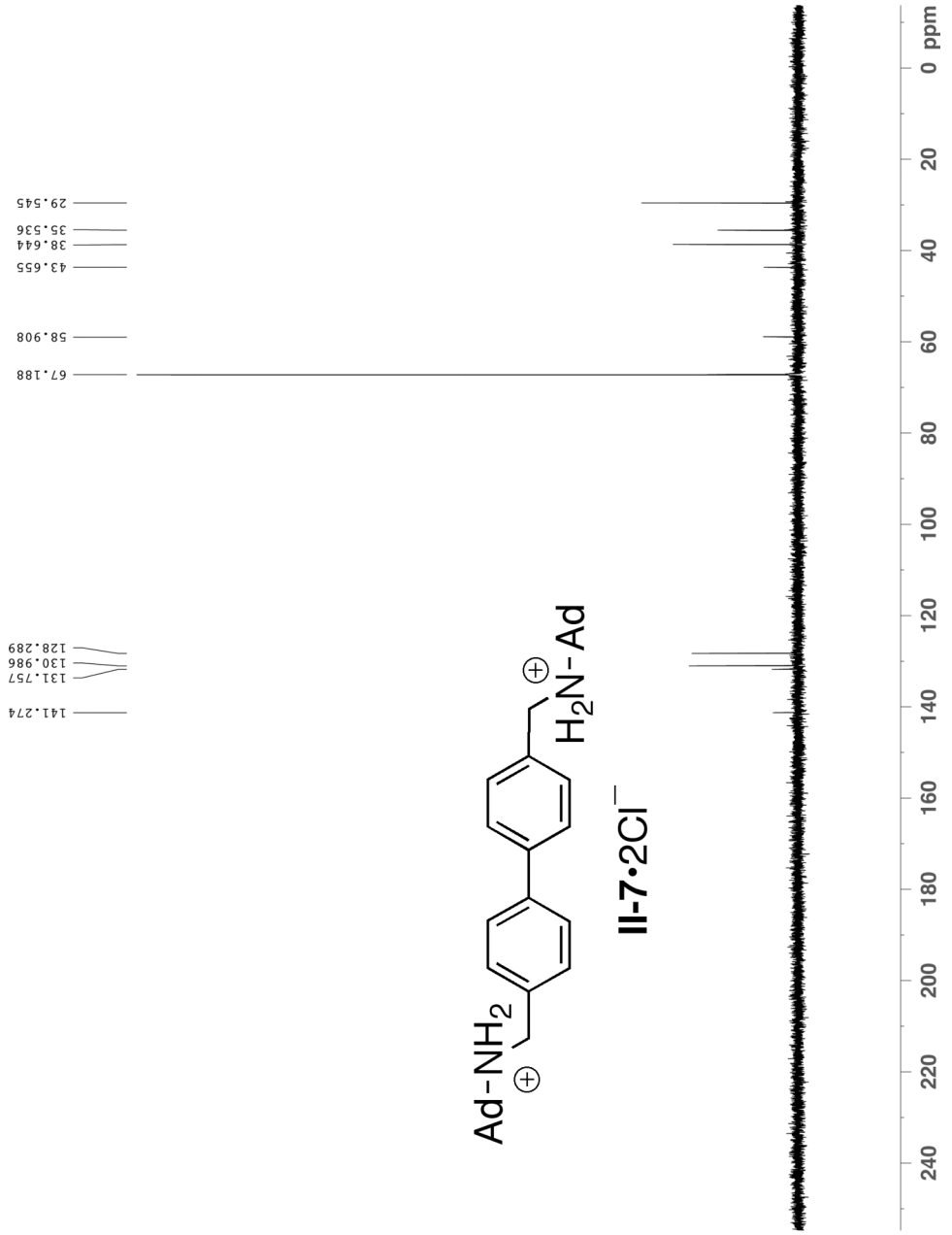

Figure II-24. ^{13}C NMR spectrum recorded for **II-7**•$2Cl^-$ (100 MHz, D_2O, RT).

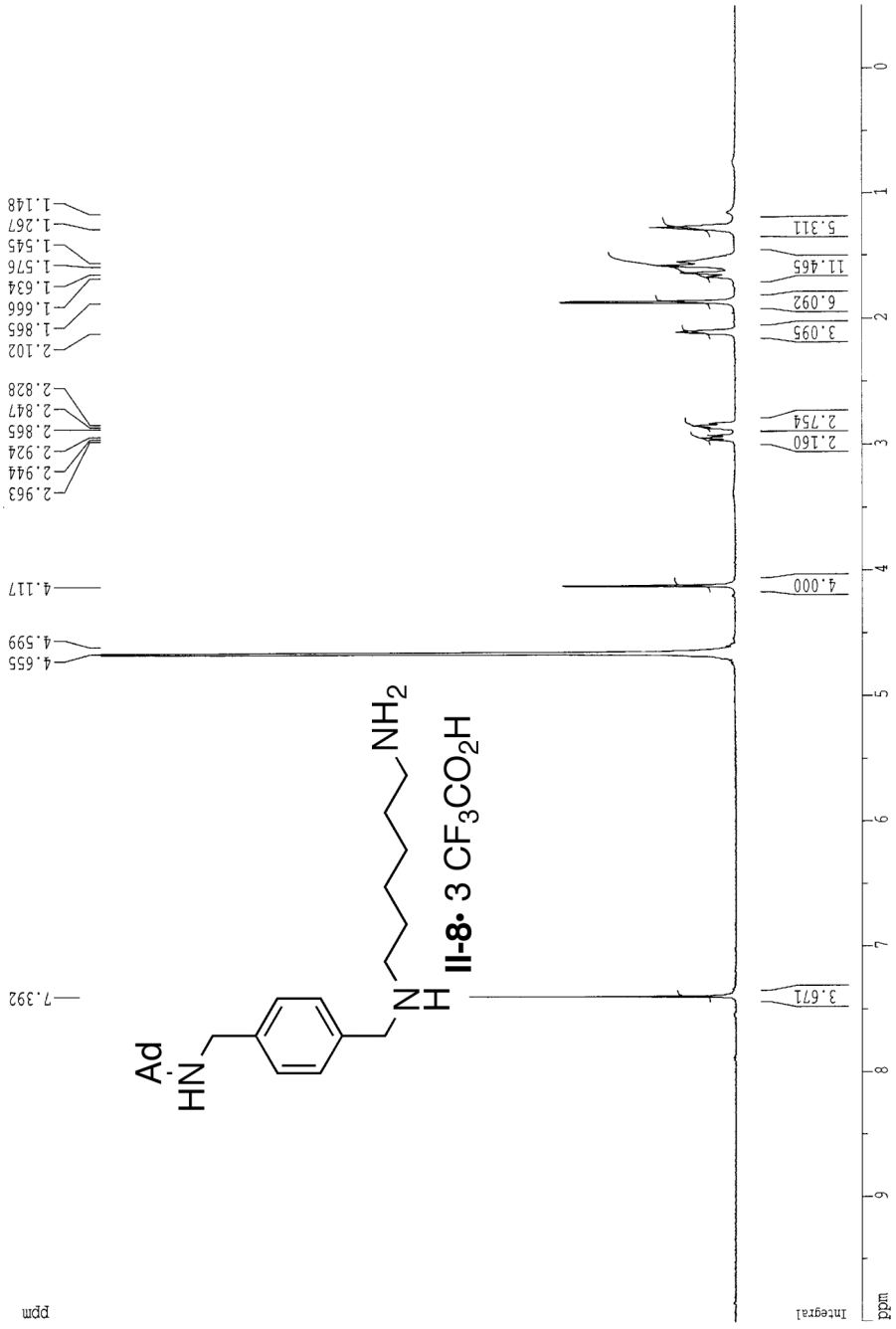

Figure II-25. ^{1}H NMR spectrum recorded for **II-8•**3 TFA (400 MHz, D_2O, RT).

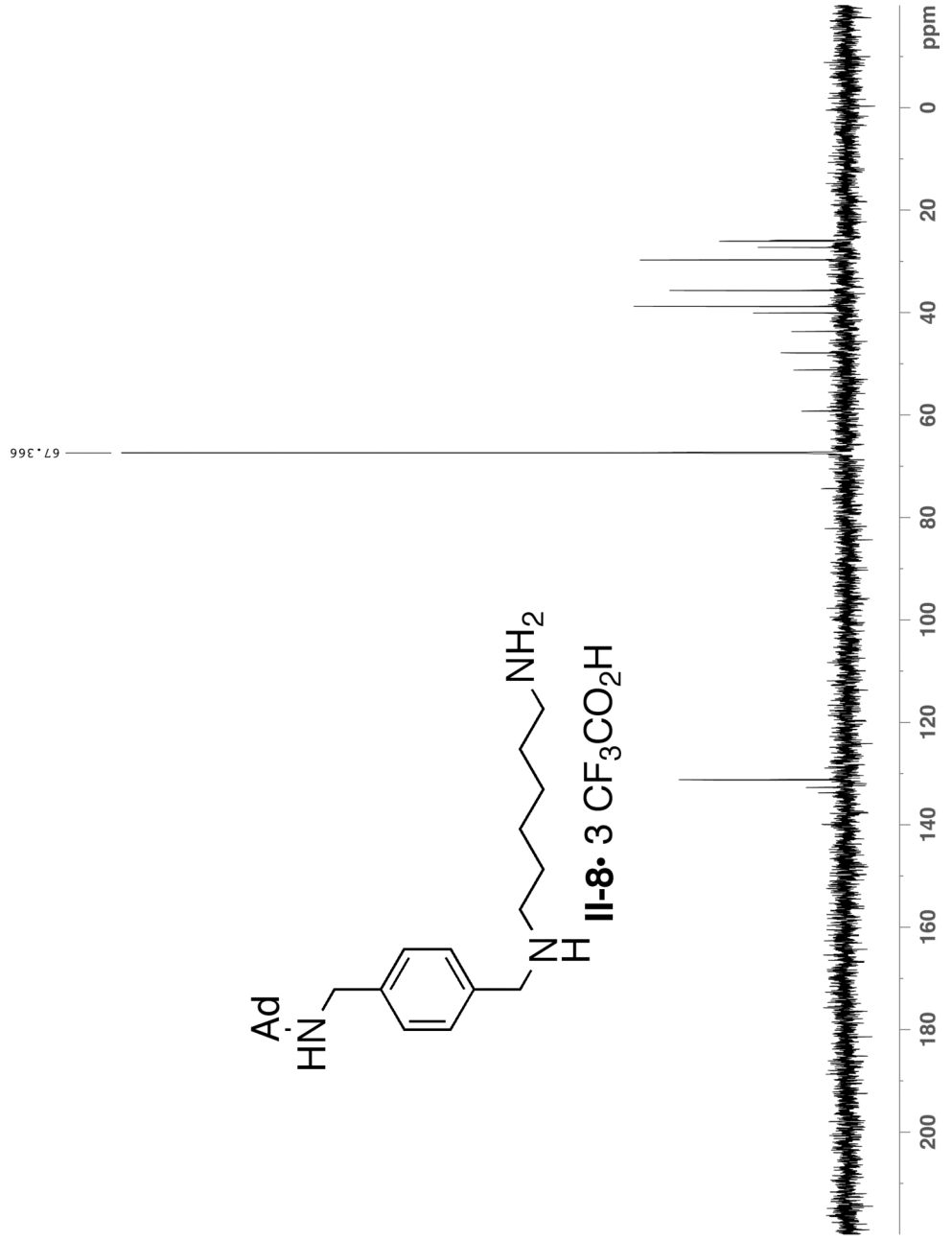

Figure II-26. ^{13}C NMR spectrum recorded for **II-8•**3 TFA (125 MHz, D_2O, RT).

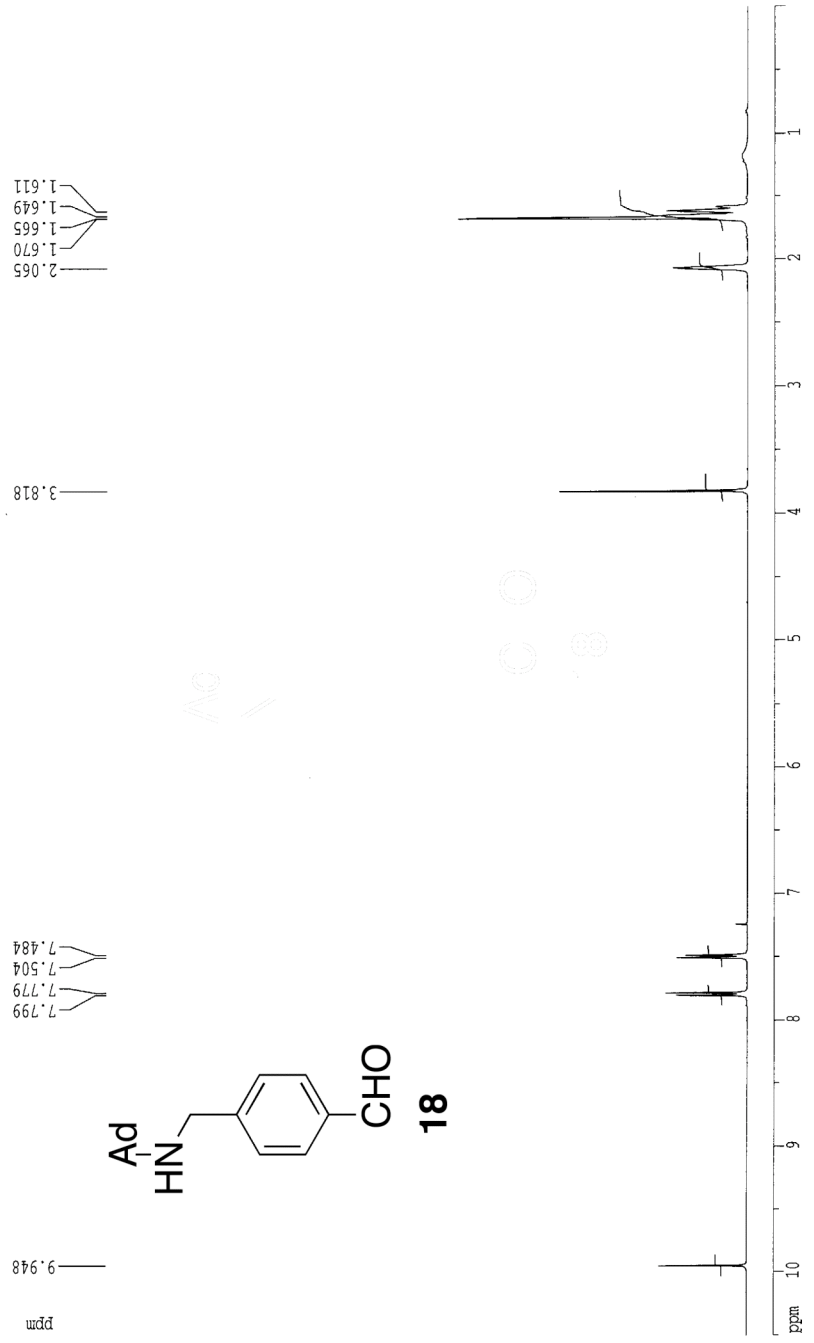

Figure II-27. ^{1}H NMR spectrum recorded for **II-18** (400 MHz, $CDCl_3$, RT).

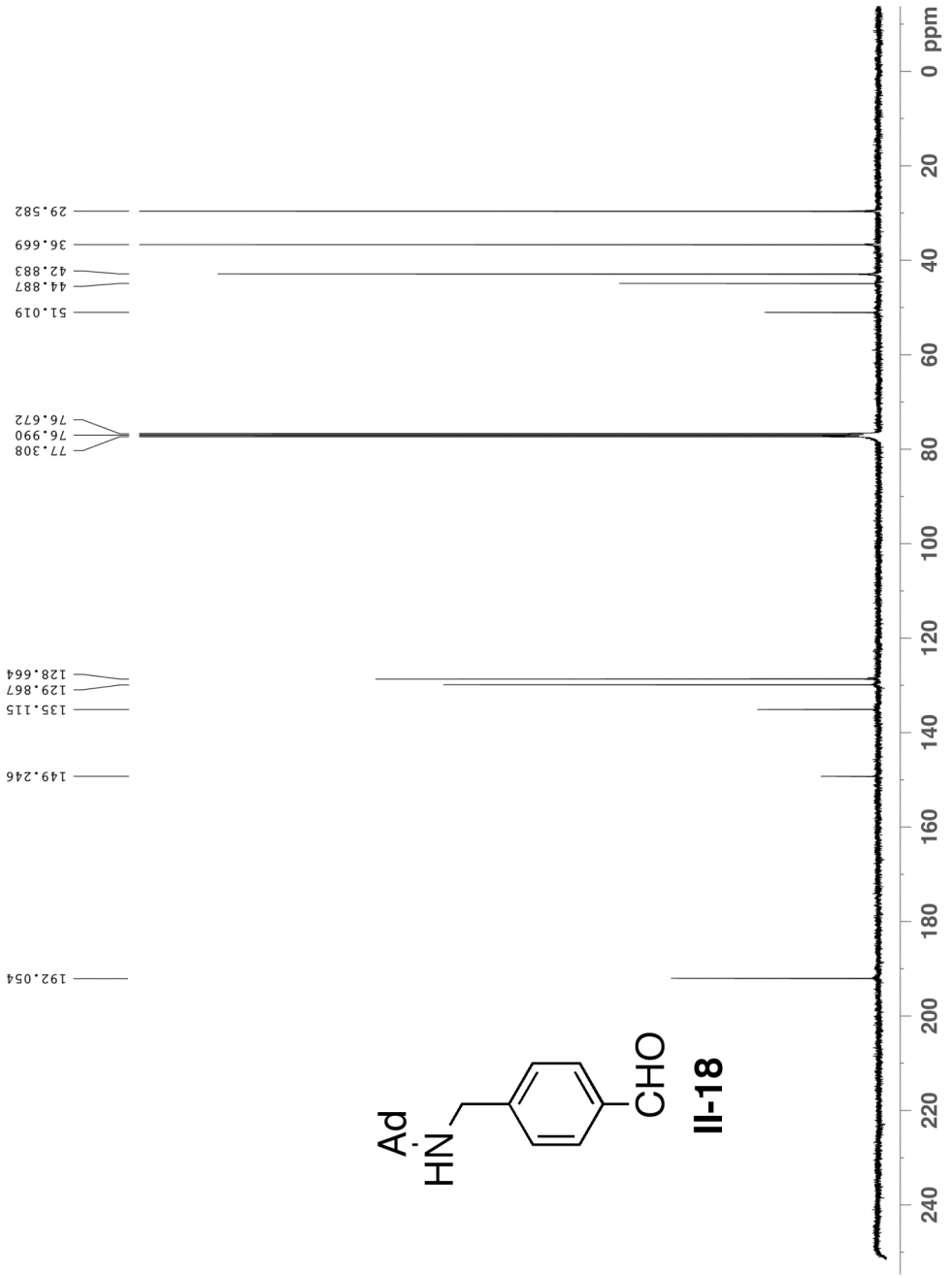

Figure II-28. ^{13}C NMR spectrum recorded for **II-18** (100 MHz, $CDCl_3$, RT).

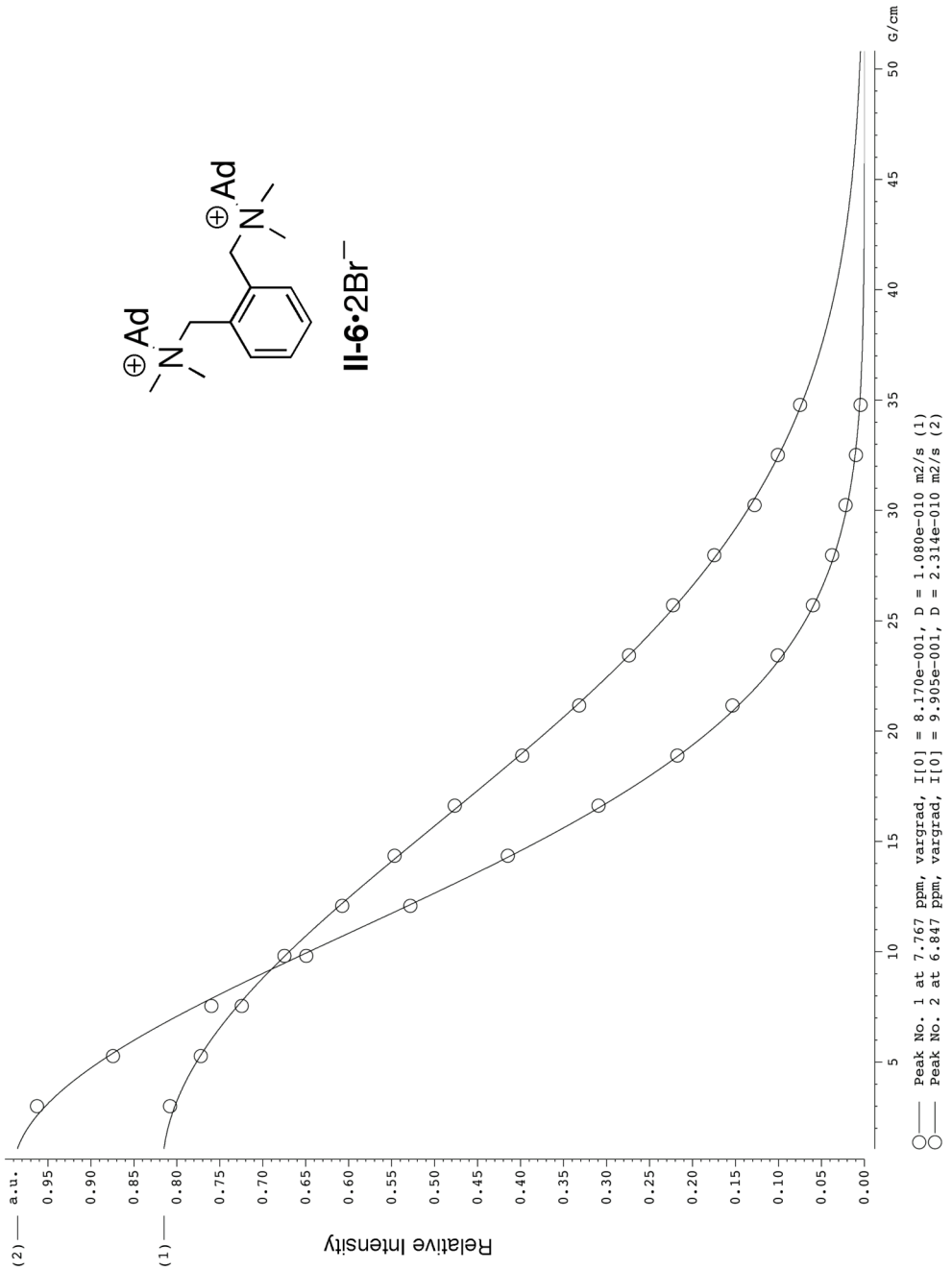

Figure II-29. Plot of signal intensity versus gradient strength and the best fit of the data to Eq. II-1 for a solution containing 1:1 *bis*-ns-CB[10]:**II-6•**$2Br^-$ (curve 1) and 1:2 *bis*-ns-CB[10]:**II-9•**$2Cl^-$ (curve 2).

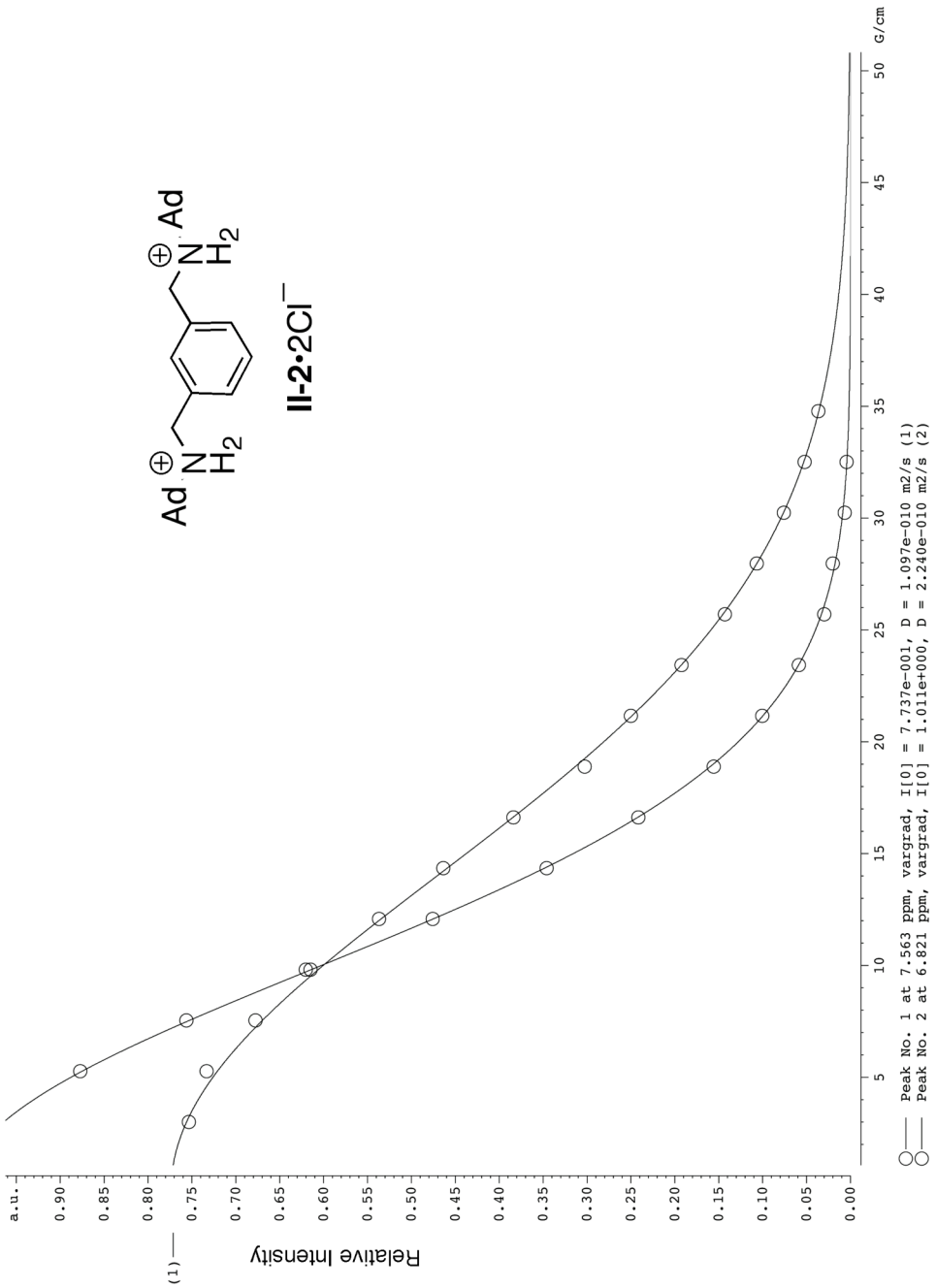

Figure II-30. Plot of signal intensity versus gradient strength and the best fit of the data to Eq. II-1 for a solution containing 1:1 *bis*-ns-CB[10]:**II-2•**2Cl$^-$ (curve 1) and 1:2 *bis*-ns-CB[10]:**II-9•**2Cl$^-$ (curve 2).

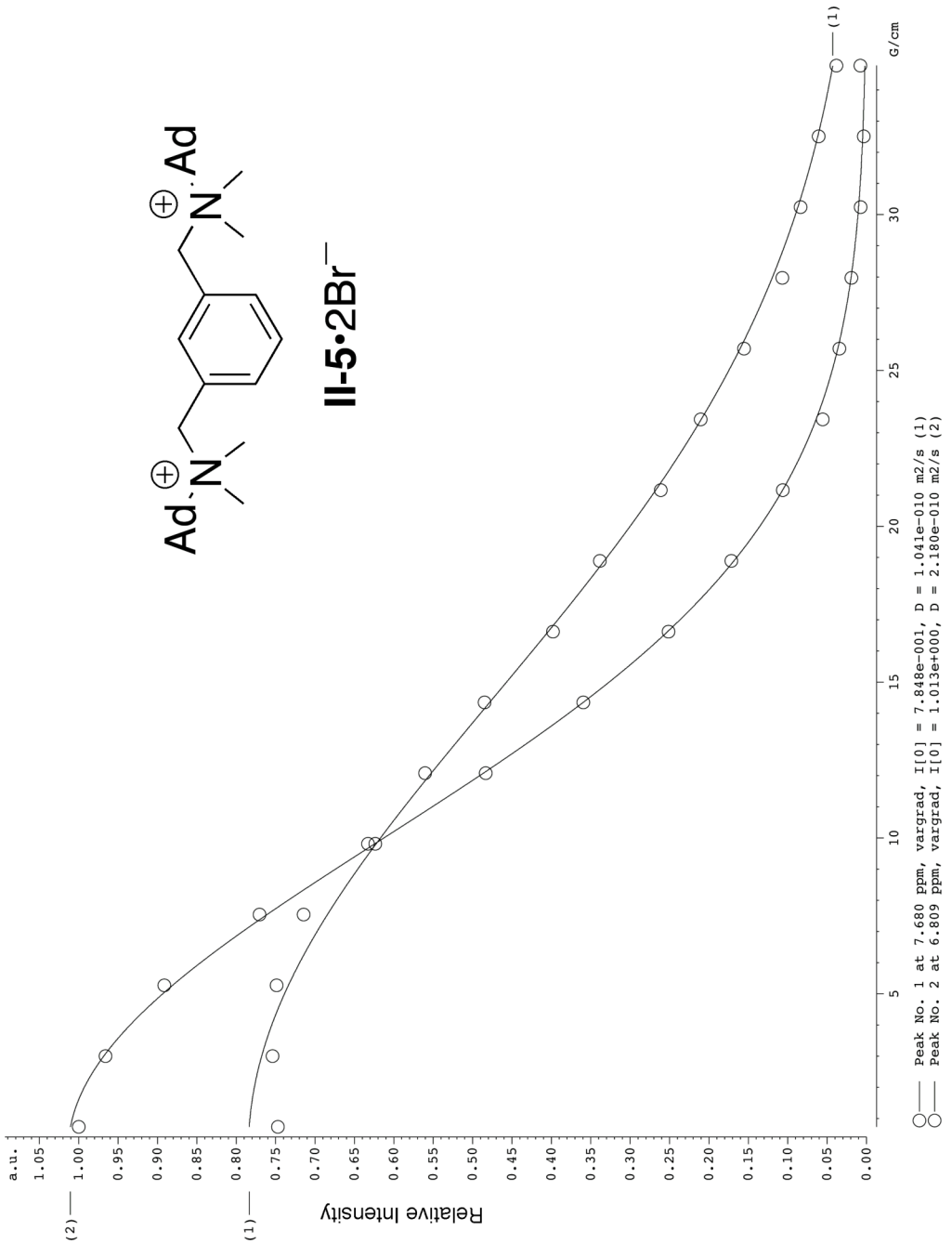

Figure II-31. Plot of signal intensity versus gradient strength and the best fit of the data to Eq. II-1 for a solution containing 1:1 *bis*-ns-CB[10]:**II-5•**$2Br^-$ (curve 1) and 1:2 *bis*-ns-CB[10]:**II-9•**$2Cl^-$ (curve 2).

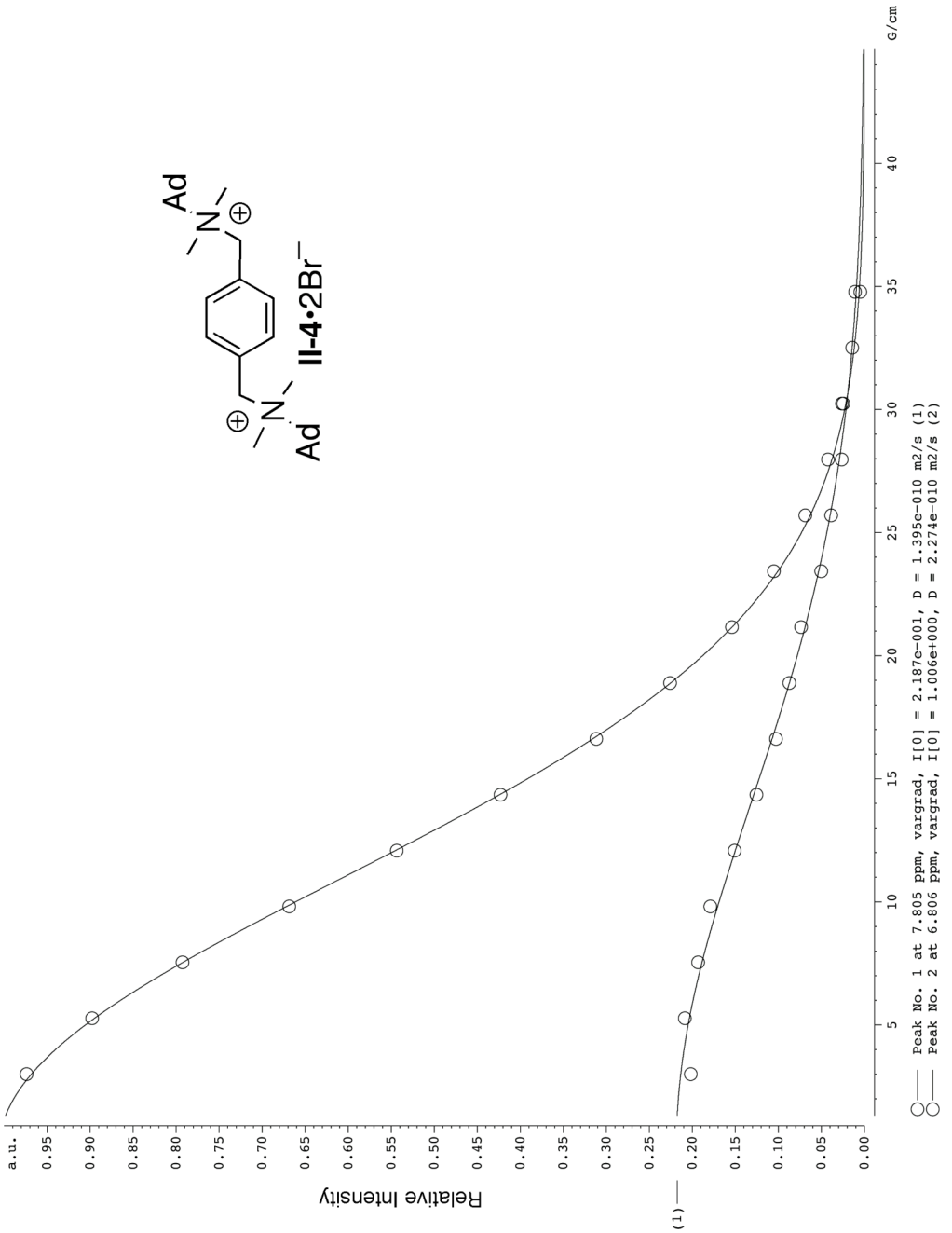

Figure II-32. Plot of signal intensity versus gradient strength and the best fit of the data to Eq. II-1 for a solution containing 1:1 *bis*-ns-CB[10]:**II-4**•2Br$^-$ (curve 1) and 1:2 *bis*-ns-CB[10]:**II-9**•2Cl$^-$ (curve 2).

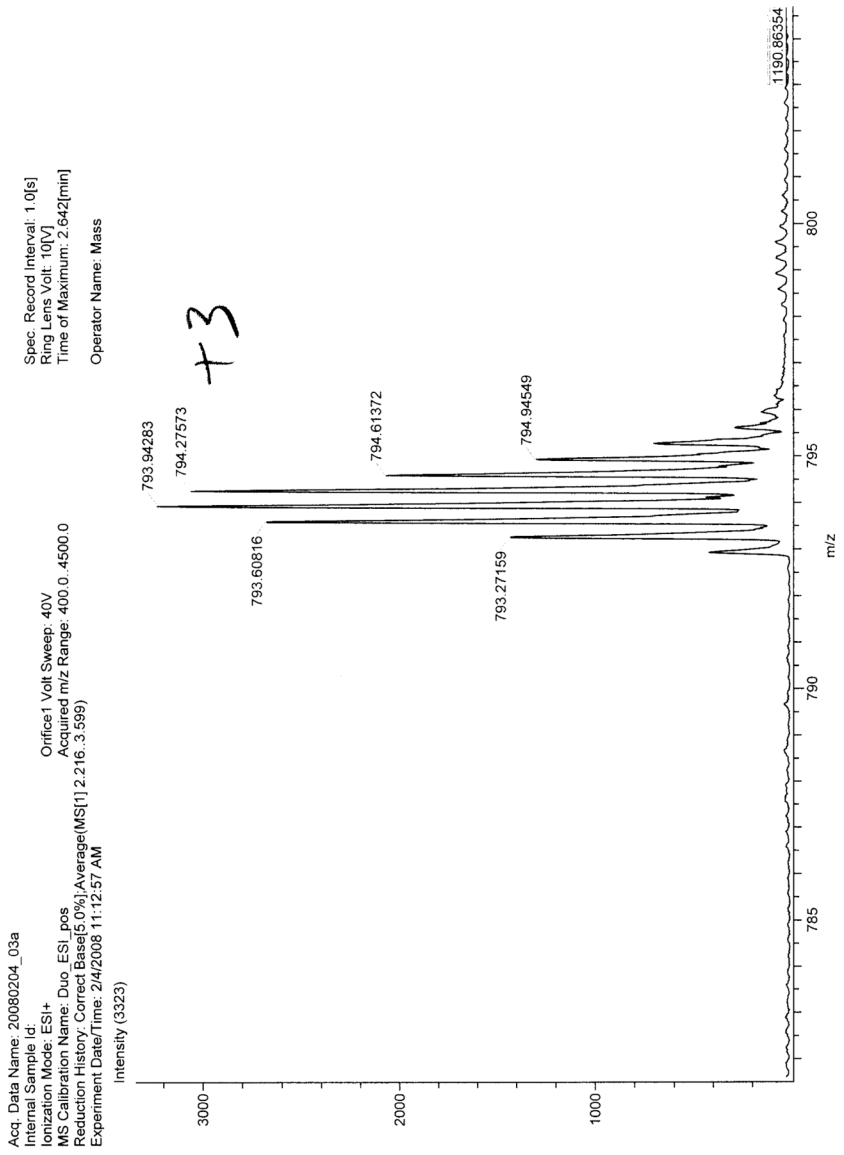

Figure II-32. ESI mass spectrum showing peak at *m/z* = 794, representing [bis-*ns*-CB[10]•**II-8**$_2$]$^{3+}$ complex.

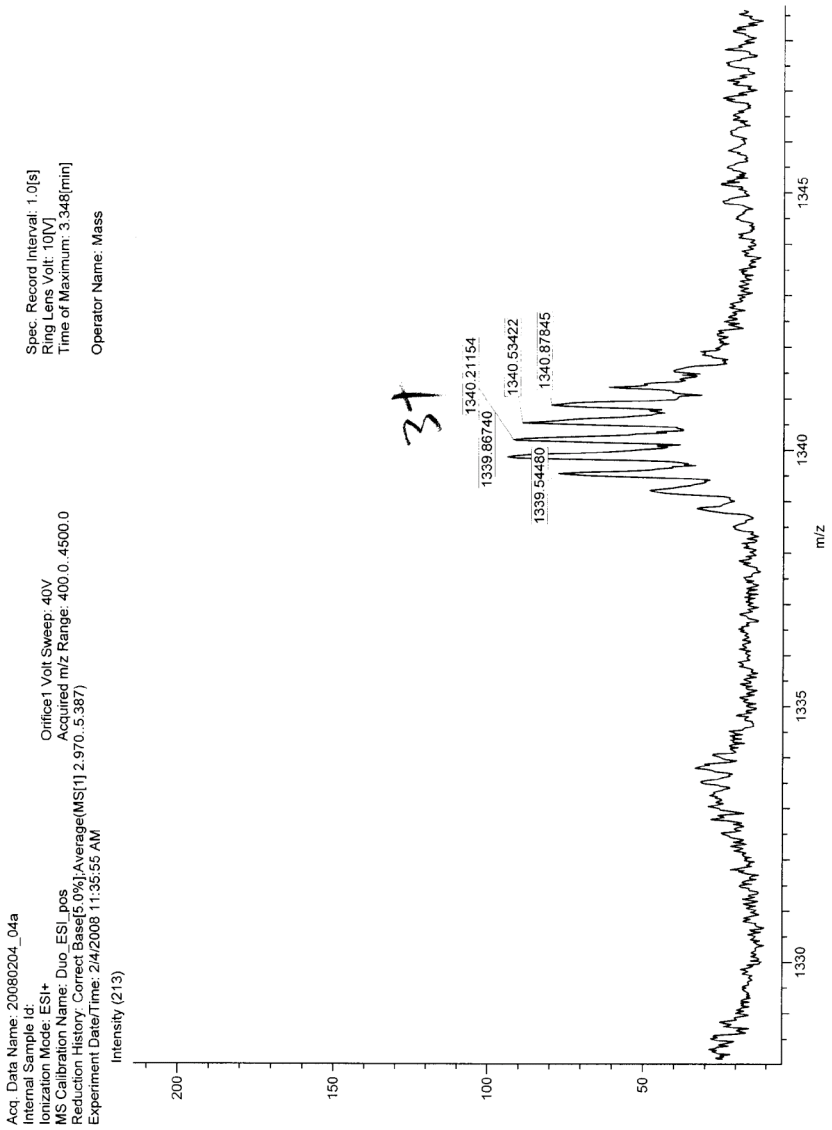

Figure II-33. ESI mass spectrum showing peak at *m/z* = 1339, representing [bis-*ns*-CB[10]$_2$•**II-8**$_2$]$^{3+}$ complex.

III. Chapter 3: Polymer Deaggregation and Assembly Controlled by a Double Cavity Cucurbituril.

3.1 Introduction.

Polymers give rise to a diversity of materials that have enabled them to improve our daily lives: from beverage containers, automotive parts, and textiles, to prosthetics and extreme weather materials.[109] While the contributions made from covalent polymers to the development of industries are substantial, there are always improvements to be made. An ongoing challenge in the realm of polymer chemistry is to be able to control the properties of polymers, through incremental changes in their structures or the altering of external variables (pH, temperature, concentration, etc.). An alternative approach to controlling polymer properties involves their assembly by non-covalent interactions rather than covalent bonds. Such supramolecular polymers may assume a variety of geometries by the assembly of monomeric units through non-covalent interactions in *n*-dimensional patterns (linear, branched, dendritic, etc.). Most significant, however, is the high stimuli responsiveness of supramolecular polymers which make them ideal systems to control polymer properties in a straightforward manner.

The existence of supramolecular polymers is widespread, from their biological function as microtubules, microfilaments, viruses, phages and proteins, to their synthetic production as potential coatings, inks, and adhesives. The sensitivity of

these systems to changes in pH, temperature, concentration, and solvent translates to changes in the properties of the bulk material. For example, the sensitivity toward mechanical stress can be capitalized upon with a self-healing rubber composed of molecules containing amido functionality for hydrogen-bonding. This material can undergo multiple cycles of stretching, breaking, and mending.[10] These mechanical properties may be useful in a coating where once applied to a surface, heat can be applied to repair the coating rather than the addition of another layer of material.

Solution viscosity is a particularly important property of a material and the ability to control viscosity poses a challenge to chemists. Supramolecular polymers typically possess low-viscosity melts wherein a small increase in temperature leads to a large decrease in viscosity due to the breaking of weak intermolecular interactions. This decrease in viscosity results in more straightforward processability, such as creation of a surface coating. Covalent polymers, in contrast, require high temperature and pressure to achieve a decrease in viscosity.[9] The ability to modulate the viscosity of a solution by temperature, concentration, or chemical stimulus is valuable to the materials as well as food industries. For example, the mouthfeel of coffee is enhanced by optimizing the viscosity within a certain range by the addition of arabinogalactans.[110] Accordingly, the tunable properties of non-covalent materials renders them prime systems for a wide array of applications.

The properties of supramolecular polymers stem from the structures of their monomeric units. For example, non-covalent association of monomers based on metal-ligand coordination[20,39,111] hydrogen-bonding[19,40,73,112,113] aromatic stacking[41,114], and host-guest interactions[21,22,75,115] have resulted in formation of supramolecular

polymeric systems. Of particular note are the self-complementary ureidopyrimidinone dimers of the A—A type reported by Meijer, Sijbesma, and co-workers that undergo assembly through quadruple hydrogen-bonding interactions to form a homomeric supramolecular polymer. The success of this system is greatly due to the high affinity ($\approx 10^7$ M^{-1}) with which the monomers dimerize, resulting in a high degree of polymerization.[19] Host-guest chemistry has also been shown to generate supramolecular polymers. For example, Harada has incorporated a guest-derivatized cyclodextrin as the A—B monomeric unit to achieve construction of main chain and branched polymers of the $(\cdots A—B\cdots A—B\cdots)_n$ type.[21,75,116] One limitation of this host-guest system is the modest affinities ($K_a \approx 10^4$ M^{-1}) of the A···B interaction which limits the overall degree of polymerization.

The Cucurbit[*n*]uril (CB[*n*]) family of macrocycles is known for its high binding affinities (K_a up to 10^{15})[46,77] and selectivities (K_{rel} up to 10^7)[117] toward aliphatic and aromatic amines. Guests bind to CB[*n*] through the hydrophobic effect to the interior of the CB cavity and cation-dipole interactions between the carbonyl-lined portals of the CB[*n*] and ammonium functionality of the guest. The range of different cavity volumes for CB[5] — CB[8] and CB[10] (82 — 870 $Å^3$) allow for the recognition of a wide variety of guests. These recognition abilities allow CB[*n*] to be tailored to a range of applications including waste-stream remediation[118,119] chemical sensing[42,43], molecular machines[57,120,121], and supramolecular materials[47,122,123]. Of direct relevance to the work reported herein are reports from the Kim and Scherman groups regarding the preparation of supramolecular polymers using the ability of CB[8] to promote 1:1:1 ternary complexes. For example, the Scherman group has

successfully prepared a supramolecular block copolymer from polymers end-functionalized with viologen and naphthalene units.[22] Kim has combined CB[8] with divalent and trivalent building blocks in the construction of higher order supramolecular oligomeric and dendritic complexes.[50,51]

Over the past several years, our group has been interested in the supramolecular chemistry of *nor-seco*-CB[*n*] which by virtue of their new structurally responsive architectures display interesting behavior. For example, (±)-bis-*ns*-CB[6] and bis-*ns*-CB[10] have displayed chiral recognition properties and homotropic allosteric bahavior, respectively. The high selectivity and affinity of CB[*n*] toward ammonium ion guests encouraged us to work on formation of discrete and polymeric complexes comprising bis-*ns*-CB[10] (Figure III-1). Of the *ns*-CB[*n*] isolated thus far, bis-*ns*-CB[10] is unique in that it possesses two identical cavities. Accordingly, bis-*ns*-CB[10] is a prime host for the generation of an $(A—A\cdots B—B\cdots)_n$ type supramolecular polymer (Figure III-2c).

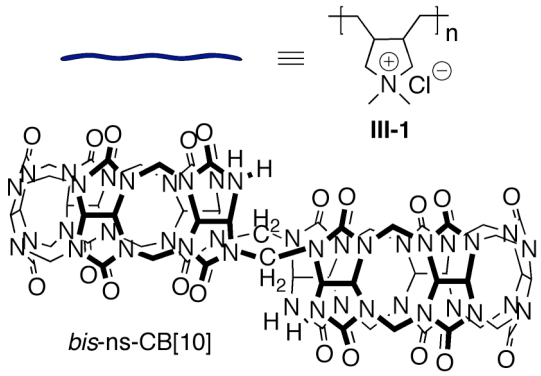

Figure III-1. Schematic depiction of polymer (**III-1**) and the chemical structure of host bis-*ns*-CB[10].

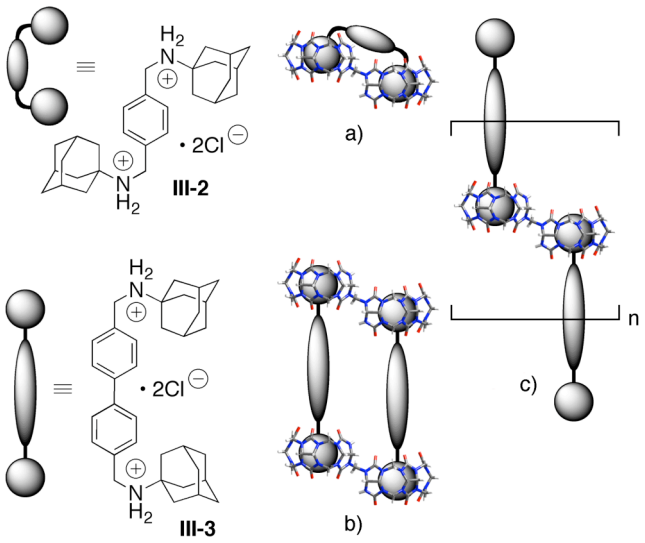

Figure III-2. Schematic representation of adamantanediammonium guests **III-2** and **III-3** with corresponding host-guest inclusion complexes, a) bis-*ns*-CB[10]•**III-2**, and b) bis-*ns*-CB[10]$_2$•**III-3**$_2$, and c) hypothetical linear polymer comprising bis-*ns*-CB[10] and **III-3**.

3.2 Results and Discussion.

Firstly, we will briefly present our previous results that led to the experiments performed herein as well as the design strategy of our current findings. Then we will discuss the experimental data that formulated our final interpretation of this system. And lastly we will close with an explanation of our work and potential applications of this research.

3.2.1 Design Strategy.

Previously we reported studies directed toward the generation of a supramolecular polymer from bis-*ns*-CB[10] and guests **III-2** and **III-3**. Experimentally, we found that divalent guest molecules are capable of forming 1:1 (Figure III-2a) or 2:2 (Figure III-2b) complexes with bis-*ns*-CB[10], where the length of the rigid linker between the two adamantyl groups dictates the molecularity of the resulting complex. We believe a supramolecular polymer did not form due to: 1) the low solubility of bis-*ns*-CB[10] which limited concentrations to the μM range and, 2) the absence of a bulky group on the linker to prevent two guests from side-by-side orientation, apparent in the 2:2 complex (Figure III-2b), or 3) the short length of the linker preorganized the complex to form a closed (2:2) system.[12] We therefore turned our attention to linker length, and hypothesized that if we used a polymeric guest capable of binding inside the cavity of bis-*ns*-CB[10], we could generate a supramolecular polymer, as its extended length would deter formation of discrete complexes (Figure III-2a and 2b). For this purpose, we chose poly(diallyldimethylammonium) chloride, **III-1**, with a molecular weight distribution of 100,000 — 200,000 g/mol. Polymer **III-1** is a polyelectrolyte that assumes a rod-like conformation in dilute aqueous solution and is capable of aggregating through counterion-induced attractions.[124-127] According to SPARTAN modeling, the length of **III-1** spans the range of 270 — 540 nm. This polyelectrolyte has been implemented as a displacer for cation-exchange displacement chromatography of proteins[41] and as a substrate for ultrathin polyelectrolyte multilayer films.[125,129] This

polymeric polycation exhibits excellent solubility in water and its ammonium-tagged repeat units have the potential to bind within the cavities of bis-*ns*-CB[10].

A priori, the interaction between bis-*ns*-CB[10] and **III-1** could proceed by several different geometrical modes of interaction. Figure III-3 represents several of the most plausible modes of interaction. To begin, the degree to which **III-1** self-associates is concentration dependent, as the non-covalent interactions are reversible (Figure III-3a and 3b). The introduction of bis-*ns*-CB[10] to a solution of **III-1** can generate formation of a new assembly. For example, bis-*ns*-CB[10] could bind to the terminal unit of **III-1** and stay put or thread along the main chain. The driving force to thread a molecule of bis-*ns*-CB[10] onto internal pyrrolidinium units of **III-1** would be minimal because all repeat units of **III-1** are identical. This process could potentially be driven by addition of excess bis-*ns*-CB[10] to a solution of **III-1**, creating **III-1**•bis-*ns*-CB[10]$_n$ species. One such result of threading behavior is the construction of a ladder assembly (Figure III-3c) or the kinking of polymer **III-1** (Figure III-3d), similar to a ß-hairpin turn in polypeptide folding. The entropic penalty for formation of both these structures would require high enthalpic gains. If a molecule of bis-*ns*-CB[10] were to bind only to the termini of **III-1**, we envisioned bis-*ns*-CB[10] as a supramolecular polymerizing agent, linking individual polymer strands together (Figure III-3e). The picture could grow increasingly complex, as we consider the concentration, stoichiometries, and dynamic equilibrium of the system. To understand the influence of bis-*ns*-CB[10] on an aqueous solution of **III-1**, we performed viscosity measurements, atomic force miscroscopy (AFM) imaging, and diffusion-ordered NMR spectroscopy (DOSY) experiments.

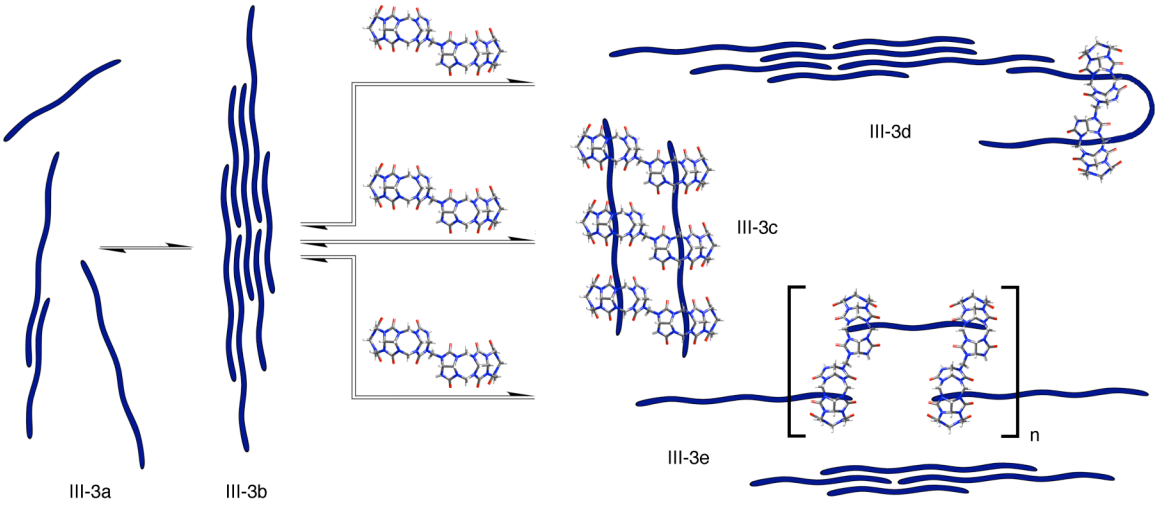

Figure III-3. Illustration depicting the concentration dependent equilibrium between: a) monomeric and, b) aggregated **III-1**. Addition of bis-*ns*-CB[10] may result in either c) ladder formation, d) kinking of individual polymer strands, or e) deaggregation and polymerization.

3.2.2 Viscosity Measurements.

We anticipated that the addition of bis-*ns*-CB[10] to a solution of **III-1** would cause an increase in the solution viscosity, functioning to non-covalently link polymer strands together, and therefore lengthening the polymer. We investigated the viscosity of a solution of **III-1** upon addition of *bis*-ns-CB[10] or CB[7] to ascertain whether a double cavity CB would behave differently from its single cavity relatives (CB[5] — CB[8]) and translate to a difference in solution properties. This hypothetical increase in viscosity should be unique to a solution containing **III-1** and

bis-*ns*-CB[10] compared to a solution containing **III-1** and CB[7], as each of its two cavities of bis-*ns*-CB[10] can encapsulate a terminal pyrrolidine unit of **III-1**.

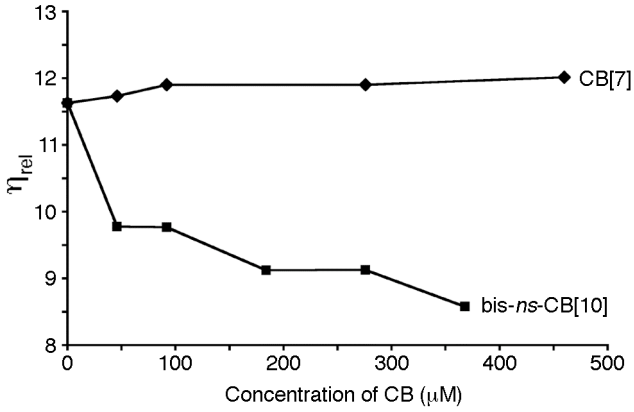

Figure III-4. Plot of relative viscosity of **III-1** (333 μM) versus concentration of CB. ■ = bis-*ns*-CB[10].♦ = CB[7].

Mixtures of **III-1** with CB[6], CB[7], CB[8], or bis-*ns*-CB[10] in water were heated at 50 ˚C for 8 hours. At this time, CB[6] and CB[8] remained insoluble, even at concentrations below 100 μM, confirming an absence of non-covalent interactions between **III-1** and CB[6] and **III-1** and CB[8]. Upon reaching room temperature, homogenous solutions containing CB[7] (46 — 460 μM) and **III-1** (333 μM) or bis-*ns*-CB[10] (46 — 368 μM) and **III-1 (**333 μM) were filtered and viscosity measurements were performed. Figure III-4 shows a plot of η_{rel} versus the concentration of CB. Solutions containing **III-1** and CB[7] did not exhibit significant changes in viscosity relative to a solution containing **III-1** alone. The addition of bis-*ns*-CB[10] to a solution of **III-1**, however, caused a decrease in the relative viscosity. This trend continued with addition of bis-*ns*-CB[10] until the concentration reached 368 μM at which point the solution became heterogeneous. This result was puzzling

as it conflicted with our hypothesis, that addition of bis-*ns*-CB[10] to a solution of **III-1** should increase the hydrodynamic radius of the polymer through host-guest interactions, which should in turn translate to an increase in viscosity. To try to understand this unexpected result, we decided to use other techniques to gain insight into the mode of interaction between **III-1** and bis-*ns*-CB[10].

3.2.3 ^{1}H NMR Experiments.

^{1}H NMR can provide information regarding the geometry and strength of host-guest binding interactions. To provide evidence for the inclusion of a pyrrolidinium unit within the cavity of bis-*ns*-CB[10], ^{1}H NMR spectra were recorded for solutions containing **III-1** alone and with bis-*ns*-CB[10] (Figure III-5). The ^{1}H NMR spectrum of a solution of **III-1** (Figure III-5a) does not display resonances above 1 ppm. Figure III-5b shows the spectrum recorded for a solution containing **III-1** and bis-*ns*-CB[10], displaying upfield shifted polymer peaks, representing an inclusion of the polypyrrolidinium unit within the cavity of bis-*ns*-CB[10]. The ratio of bis-*ns*-CB[10] to **III-1** is 0.08. Therefore, the peaks representing **III-1** bound inside bis-*ns*-CB[10] are less intense when compared to those of the unbound polymer. If we add a competitive guest to a solution containing **III-1** and bis-*ns*-CB[10], we could potentially observe disappearance of the resonances for bound **III-1**, and appearance of resonances for the bound competing guest. This would tell us if the resonances above 1 ppm in Figure III-5b are due to reversible, non-covalent interactions between **III-1** and bis-*ns*-CB[10], and that the competing guest has a higher affinity for bis-*ns*-CB[10] than monomeric units of **III-1**. For this purpose, we

chose *p*-xylylenediamine, **III-4**, as a competitive guest whose affinity for various CB[*n*] has been well documented.[45] Upon addition of **III-4** to a solution containing **III-1** and bis-*ns*-CB[10], the presence of bound polymer peaks disappear (within 6 minutes) and we observe resonances for both free and bound **III-4**.

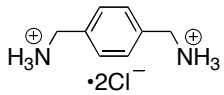

III-4

Figure III-5. Chemical structure of *p*-xylylenediamine dihydrochloride, **III-4**.

Compound **III-4** is a competing guest to polymer **III-1** and bis-*ns*-CB[10] prefers inclusion of **III-4** over **III-1**. An analogous experiment was carried out with CB[7], whereby **III-4** was added to a solution containing **III-1** and CB[7]. Figure III-5d shows the ^{1}H NMR spectra recorded for a solution containing **III-1** and CB[7]. Resonances above 1 ppm are observed and we attribute this to bound pyrrolidinium units within CB[7]. Figure III-5e shows the ^{1}H NMR spectrum recorded for a solution containing **III-1**, CB[7], and **III-4**. Again, the peaks corresponding to bound polymer, **III-1**, disappear and the presence of bound **III-4** within CB[7] is apparent. The results of the ^{1}H NMR experiments show that both bis-*ns*-CB[10] and CB[7] have a greater affinity for **III-4** than for **III-1**. The response of the system to an external stimulus illustrates its dynamic behavior and offers indirect proof that the ^{1}H NMR peaks appearing above 1 ppm arise due to pyrrolidinium units of **III-1** being bound to bis-*ns*-CB[10] or CB[7]. Having confirmed the binding of **III-1** within the cavity of bis-*ns*-CB[10], we wanted to understand how this interaction was able to

cause a decrease in solution viscosity. We considered the bis-*ns*-CB[10] could be inducing a conformational change within the polymer chains, from linear to kinked, which may alter the degree to which it self-associates. Evidence of conformational change could provide insight into the mechanism of binding and offer a plausible reason for the observed viscosity trend.

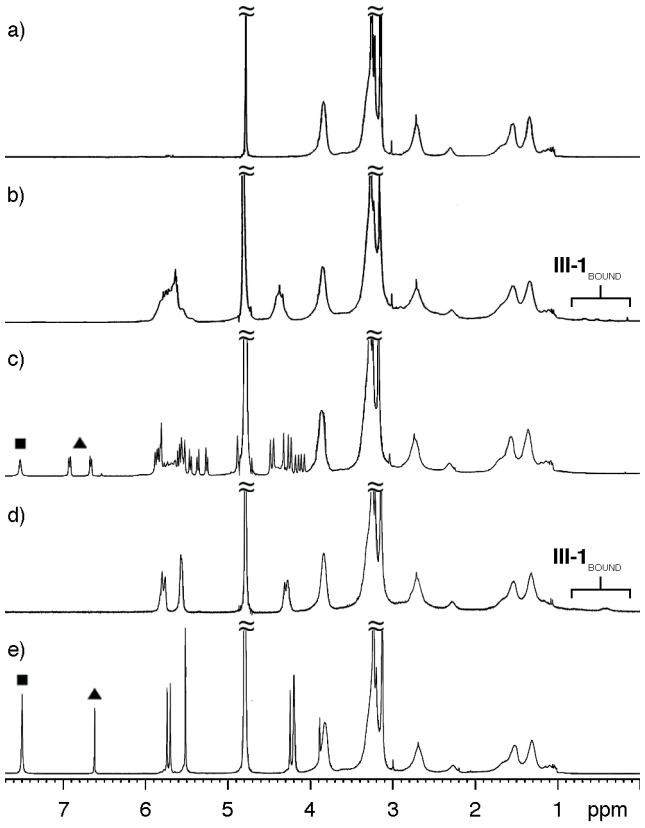

Figure III-6. ^{1}H NMR spectra (400 MHz, D_2O, RT) recorded for solutions of a) **III-1** (30 μM), b) **III-1** and bis-*ns*-CB[10] (232 μM), c) **III-1**, bis-*ns*-CB[10], and **III-4**, d) **III-1** and CB[7] (232 μM), and e) **III-1**, CB[7], and **III-4**. ■, free **III-4**; ▲, bound **III-4**.

3.2.4 Atomic Force Microscopy.

With the challenges inherent in characterizing supramolecular systems, imaging offers the most direct evidence for changes in the topology of a macromolecular assembly. To gain information about the shape of polymer **III-1** alone and in the presence of bis-*ns*-CB[10] we performed AFM imaging (Figure III-6). To ensure that the images generated were representative of the sample as a whole, each sample was imaged in at least five different locations.

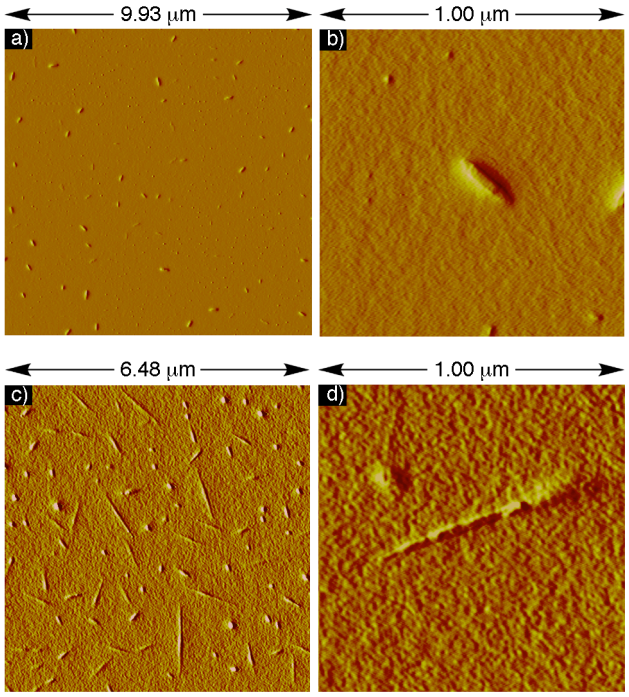

Figure III-7. AFM amplitude images captured of **III-1** (7 μM) from a) 9.93 μm scan area and b) 1.00 μm scan area, and **III-1** (7 μM) with bis-*ns*-CB[10] (7 μM) from c) 6.48 μm scan area and d) 1.00 μm scan area.

Spin-casting solutions of **III-1** (7 μM) onto freshly cleaved mica delivered the amplitude images shown in Figure III-6a and 6b. Figure III-6c and 6d are amplitude images of a dried solution containing **III-1** (7 μM) and bis-*ns*-CB[10] (7 μM). The most obvious difference between solutions of **III-1** and **III-1** with bis-*ns*-CB[10] is the presence of extended linear structures in Figure III-6c. We believe this reflects the formation of a supramolecular polymer constructed from bis-*ns*-CB[10] linking several individual strands of **III-1**. To estimate the size difference between the polymer in Figure III-6a and 6c, the lengths of 10 structures from each image were measured. The average structure length recorded from Figure III-6a was 184 nm and that of 6c was 1000 nm. Upon further analysis of the images, we noticed that the structure in Figure III-6b also appears wider than that in Figure III-6d. We surmised that deaggregation of clusters of **III-1** may translate to an overall decrease in solution viscosity. To ascertain the possibility of bis-*ns*-CB[10] causing deaggregation of clusters of **III-1**, we conducted a bearing analysis. Bearing analysis is a method of analyzing the distribution of surface height over a sample.[130] The collection of feature heights based upon the occurrence of data points at various *z* heights is presented as a histogram. Height images were captured and a bearing analyses performed on the longest structures from both images of **III-1** alone and from **III-1** and bis-*ns*-CB[10]. The average heights differed from 6.8 nm from an image of **III-1** alone to 2.3 nm from an image of **III-1** and bis-*ns*-CB[10].

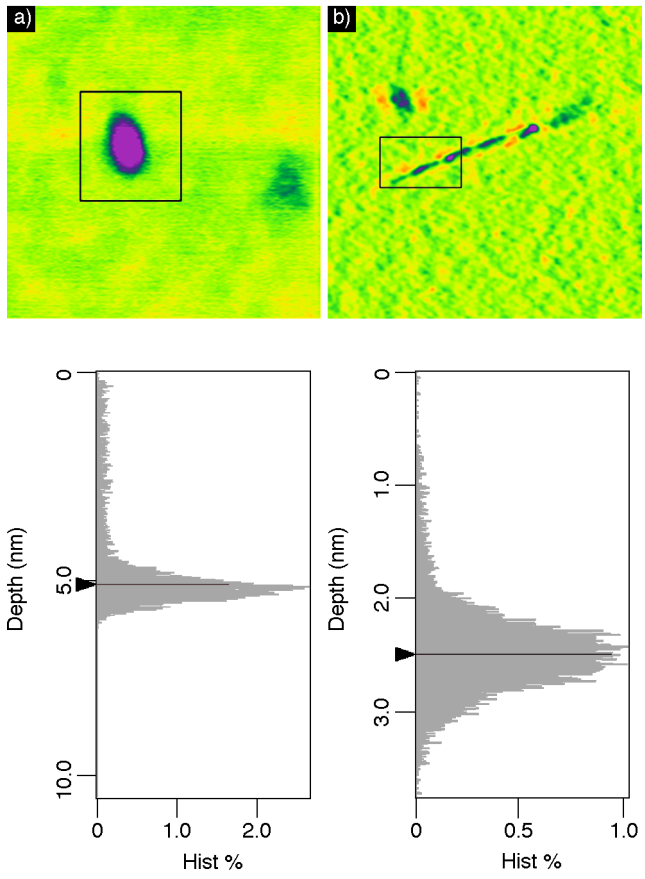

Figure III-8. AFM height images and corresponding bearing analysis histograms for a sample containing a) **III-1** alone and b) **III-1** with bis-*ns*-CB[10]. Boxed region within images is area used for sampling to generate histogram (directly below).

Figure III-7 shows representative bearing analyses where the average depth of a structure from the sample containing only **III-1** is 5.2 nm and that from the sample containing **III-1** and bis-*ns*-CB[10] is 2.5 nm. These measurements provide evidence for the role of bis-*ns*-CB[10] as a deaggregation agent of clusters of polymer strands. To provide evidence for the increase in size of the polymer assembly, we employed diffusion-ordered NMR spectroscopy.

3.2.5 Diffusion NMR.

Diffusion-ordered spectroscopy (DOSY) measures the rate of diffusion of a molecule through solution. In line with our thinking of the role of bis-*ns*-CB[10] as a molecular handcuff (Figure III-3e), the diffusion rate of the polymer should decrease as it is lengthened. If bis-*ns*-CB[10] instead threaded on to **III-1** (Figure III-3c and 3d), the complex should diffuse through solution at approximately the same rate as **III-1** alone. Alternatively, because we observed a decrease in viscosity of a solution containing **III-1** upon addition of bis-*ns*-CB[10], we could also rationalize an increase in the diffusion rates obtained from a solution of **III-1** and bis-*ns*-CB[10] when compared to a solution of **III-1** alone.

$$D_s = \frac{k_B \cdot T}{6 \cdot \pi \cdot \eta \cdot R} \quad \text{(III-1)}$$

According to the Stokes-Einstein equation (Eq. III-1), the diffusion coefficient of a sphere (D_s) is inversely related to the hydrodynamic radius (R) and solvent viscosity (η), where k_B is Boltzmann's constant and T is temperature. Because our polymer, **III-1**, is cylindrical, we resort to evaluating the measurements qualitatively. The diffusion coefficient obtained from a 33 μM solution of **III-1** alone is $D_s = 1.2 \times 10^{-10}$ m^2/s and the value from a solution of **III-1** (33 μM) and bis-*ns*-CB[10] (260 μM) is $D_s = 6.8 \times 10^{-11}$ m^2/s. The theory of diffusion NMR measurements predicts that the value of the $D_{\text{n-mer}}/D_{\text{monomer}}$ ratio reflects a change in size of the assembly.[17] For example, a $D_{\text{n-mer}}/D_{\text{monomer}} = 0.79$ corresponds to a dimeric assembly. Substitution of the D_s value for the *n-mer* (**III-1** and bis-*ns*-CB[10]) over the D_s value

for the *monomer* (**III-1**) we arrive at a value of 0.57. Theory predicts a $D_{n\text{-}mer}/D_{monomer}$ value of 0.59 for a pentameric species and 0.55 for a hexameric species. Though we cannot draw absolute conclusions from this numerical comparison, the $D_{n\text{-}mer}/D_{monomer}$ ratio is an indication of the formation of an assembled oligomeric species comprising **III-1** and bis-*ns*-CB[10] in solution. According to the viscosity data (Figure III-4), a solution containing **III-1** and bis-*ns*-CB[10] is less viscous than a solution containing **III-1** alone. The Stokes-Einstein equation shows that viscosity is inversely proportional to rate of diffusion. Accordingly, we would expect to observe a faster rate of diffusion for a solution containing **III-1** and bis-*ns*-CB[10] than for **III-1** alone. Yet we observe the opposite trend. The hydrodynamic radius (R) is the remaining variable in the Stokes-Einstein equation that effects the rate of diffusion. In order to account for our unexpected observation, the hydrodynamic radius of the polymeric species in a solution containing **III-1** and bis-*ns*-CB[10] is greater than the difference in viscosity from the solution containing **III-1** alone to the solution containing **III-1** and bis-*ns*-CB[10]. This tells us that the hydrodynamic radius of the polymer species in solution has increased. The most plausible explanation, guided by the evidence provided herein, is the viscosity is decreased as a result of bis-*ns*-CB[10] dividing clusters of **III-1**, concomitantly inducing non-covalent polymerization. These DOSY results support the AFM images, accounting for the increase in hydrodynamic radius leading to slower diffusion rates of the extended polymer.

3.3 Conclusions.

In summary, we have shown that bis-*ns*-CB[10] is able to link separate strands of **III-1** together, generating a supramolecular polymer. The observed decrease in viscosity of a solution of **III-1** upon addition of bis-*ns*-CB[10] is best explained with AFM images where bis-*ns*-CB[10]: 1) induces deaggregation of **III-1** and 2) extends the length of polymer. This is supported by an increase in hydronamic radius as evidenced by DOSY NMR spectroscopy.

The formation of a new material opens doors for further properties analysis. This supramolecular polymer may display temperature-dependent properties that could be used, for example, in the preparation of hot melts (applications toward the manufacturing of books, shoes, cartons, envelopes, labels, aircraft, etc.). As shown in this paper, bis-*ns*-CB[10] is a powerful viscosity modulator and therefore may effect the solution viscosity of other systems as well. Due to the reversible nature of the **III-1**$_n$•bis*ns*-CB[10]$_m$ assembly, the system can be tested for its reaction to external stimuli. The potential sensitivity of this material toward external stimuli may find applications in supramolecular photonics and electronics.

3.4 Experimental.

3.4.1 General Experimental.

Starting materials were purchased from commercial suppliers and used without further purification. Poly(diallyldimethylammonium chloride), **III-1**, was

purchased from Sigma-Aldrich and used without further purification. Polymer **III-1** has an average M_W range of 100,000 — 200,000 g/mol. Bis-*ns*-CB[10] was prepared according to the literature procedure.[31] All solutions of **III-1** were allowed to warm at 50 ˚C for 8 hours and then cooled to room temperature and filtered through a PTFE filter (0.2 μm) prior to analysis. Solution viscosities were measured using a Schott-Geräte Ubbelohde microviscometer with a suspended level bulb using a PVS1 (Processor Viscosity System) measuring device. The microviscometer was thermostated in a PV15 water bath at 25.00 (± 0.01) ˚C using a DLK10 thermostat unit (Lauda). NMR experiments were performed on Bruker AV400 and AVIII600 instruments operating at 400 and 600 MHz respectively. Chemical shifts were referenced to the solvent values (δ 4.79 ppm for HOD). ^{1}H NMR spectra were recorded at 25 ˚C (calibration with MeOH) and DOSY experiments were recorded at 40 ˚C (calibration with ethylene glycol). AFM samples were prepared by spin-casting solutions onto a freshly cleaved mica surface. Sample imaging was carried out in air at ambient temperature on an apparatus by Digital Instruments, Inc. in tapping mode. The cantilever-tip systems used were manufactured by Veeco from antimony doped silicon, having an 8 nm tip radius. The height and amplitude images and bearing analysis was performed with NanoScope III software.

IV. Chapter 4: Summary and Future Work.

4.1 Summary.

As chemists learn to control the properties of supramolecular polymers, they are becoming increasingly important to the materials sector of science. In this body of work, host-guest chemistry was employed in the construction of discrete aggregates and polymeric systems. In Chapter 2, we investigated the formation of different complexes as a result of changing stoichiometry and chemical stimulus. In Chapter 3, we described a supramolecular polymer and studied its flow properties and topology.

4.2 Future Work.

The behavior of the systems described in Chapters 2 and 3 have taught us about the requirements necessary to propagate monomeric units in a linear fashion. Incorporation of small oligoammonium ion guests into the construction of higher order complexes have a propensity to form discrete aggregates. One way to discourage the formation of closed systems and encourage polymer formation, may be able to add sterric bulk to the linker of a divalent guest (Scheme IV-1).

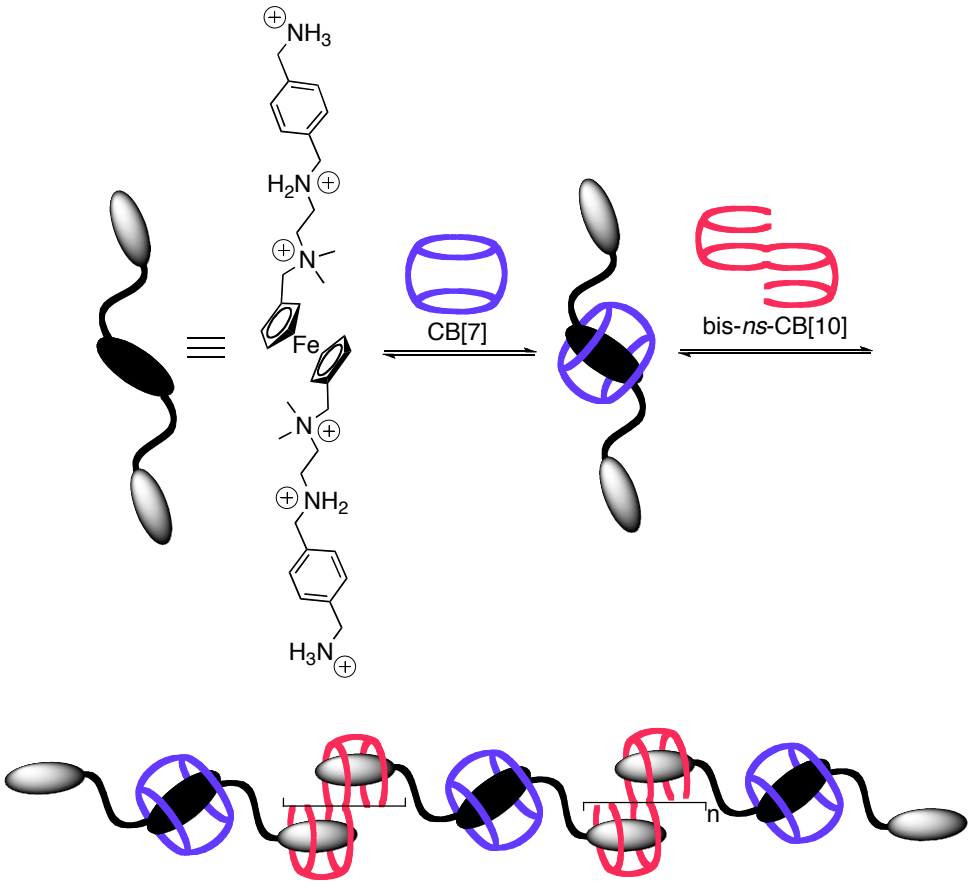

Scheme IV-1. Schematic representation of alternating-CB supramolecular polymer.

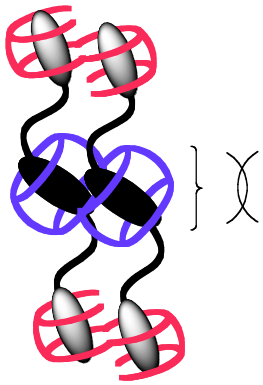

Figure IV-1. Schematic representation of a disfavored closed assembly.

The formation of a pseudorotaxane with CB[7] prior to the addition to bis-*ns*-CB[10] may sterically prevent formation of a 2:2 complex (Figure IV-1), due to the forced close proximity of the adjacent CB[7] macrocycles. To assess its range of applications, the properties of the supramolecular polymer illustrated in Scheme IV-1 would be investigated. An interesting direction to explore may be the thermal responsiveness of the system, considering the stability of the CB macrocycles and their ablity to withstand decomposition until high temperatures have been achieved.

Other possible avenues to take toward the formation of a linearly extended structure would be to change the type of monomeric unit from an A–A plus B–B type system to an A–B type repeat unit. In this manner, the stoichiometry is not the critical variable, but rather the concentration, as the stoichiometry between A and B would be fixed in an A–B type monomeric unit. With the continual advances in CB chemistry, the potential to generate such a monomeric unit is possible. For example, *ns*-CB[6] may react with *o*-pthalaldehyde derivatives containing a CB binding domain to produce a functionalized macrocycle where the top and the bottom are no longer symmetry equivalent. This approach offers a method to curb the problems that arise from imperfect stoichiometric ratios between monomeric units, namely decreasing the DP.

Lastly, functionalized CB that are soluble in organic solution or exhibit excellent solubility in water may preclude the formation of closed systems and promote linear polymeric arrays. Concentration plays a critical role in shifting the equilibrium from rings to chains and perhaps the poor solubility of CBs are hindering the formation of supramolecular polymers. CBs functionalized with alkyl chains or

carboxylic acid groups on the periphery may increase their solubility in organic and aqueous medium, respectively.

Bibliography

(1) Abraham, D.J.; Kellogg, G.E.; Holt, J.M.; Ackers, G.K. *J. Mol. Biol.* **1997***, 272*, 613-632.

(2) Royer, W.E.; Zhu, H.; Gorr, T.A.; Flores, J.F.; Knapp, J.E. *J. Biol. Chem.* **2005**, *280*, 27477-27480.

(3) Benzing, T.; Tjivikua, T.; Wolfe, J.; Rebek, J. *Science* **1988**, *242*, 266-268.

(4) Stuadinger, H. *Chem. Ber.* **1920**, *53B*, 1073-1085.

(5) Stuadinger, H. *Chem. Ber.* **1924**, *57B*, 1203-1208.

(6) Klug, A. *Phil. Trans. Roy. Soc. B* **1999**, *354*, 531-535.

(7) Calhoun, S.L.; Speir, J.A.; Rao, A.L.N. *Virology* **2007**, *364*, 407-421.

(8) Fouquey, C.; Lehn, J.-M.; Levelut, A.-M. *Adv. Mater.* **1990**, *2*, 254-257.

(9) de Greef, T.F.A.; Meijer, E.W. *Nature* **2008**, *453*, 171-173.

(10) Cordier, P.; Tournilhac, F.; Soulié-Ziakovic, C.; Leibler, L. *Nature* **2008**, *451*, 977-980.

(11) ten Cate, T.A.; Sijbesma, R. *Macromol. Rapid Commun.* **2002**, *23*, 1094-1112.

(12) Chen, C.; Dormidontova, E. *Macromolecules* **2004**, *37*, 3905-3917.

(13) Carothers, W. *Trans. Faraday Soc.* **1936**, *32*, 39-49.

(14) Ciferri, A. In *Supramolecular Polymers*; Ciferri, A., Ed.; Marcel Dekker, Inc.: New York, 2000, p 1-59.

(15) Sivakova, S.; Bohnsack, D.A.; Mackay, M.E.; Suwanmala, P.; Rowan, S.J. *J. Am. Chem. Soc.* **2005**, *127*, 18202-18211.

(16) Morris, C.E.M. In *Determination of Molecular Weight*; Cooper, A. R., Ed.; John Wiley & Sons, Inc.: New York, 1989; Vol. 103, p 15-23.

(17) Skejskal, E.O.; Tanner, J.E. *J. Chem. Phys.* **1965**, *42*, 288-292.

(18) Cates, M. E. *Macromolecules* **1987**, *20*, 2289-2296.

(19) Sijbesma, R. P.; Beijer, F.H.; Brunsveld, L.; Folmer, B. J.; Hirschberg, J. H.; Lange, R. F.; Lowe, J. K.; Meijer, E. W. *Science* **1997**, *278*, 1601-1604.

(20) Hofmeier, H.; Hoogenboom, R.; Wouters, M. E.; Schubert, U. S. *J. Am. Chem. Soc.* **2005**, *127*, 2913-2921.

(21) Miyawaki, A.; Takashima, Y.; Yamaguchi, H.; Harada, A. *Tetrahedron* **2008**, *64*, 8355-8361.

(22) Rauwald, U.; Scherman, O. A. *Angew. Chem. Int. Ed.* **2008**, *47*, 3950-3953.

(23) Castellano, R. K.; Rudkevich, D. M.; Rebek, J. *Proc. Natl. Acad. Sci. U.S.A.* **1997**, *94*, 7132-7137.

(24) Behrend, R.; Meyer, E.; Rusche, F. *Justus Liebigs Ann. Chem.* **1905**, *339*, 1-37.

(25) Freeman, W. *J. Am. Chem. Soc.* **1981**, *103*, 7367-7368.

(26) Kim, J.; Jung, I.-S.; Kim, S.-Y.; Lee, E.; Kang, J.-K.; Sakamoto, S.; Yamaguchi, K.; Kim, K. *J. Am. Chem. Soc.* **2000**, *122*, 540-541.

(27) Day, A.; Arnold, A. P.; Blanch, R. J.; Snushall, B. *J. Org. Chem.* **2001**, *66*, 8094-8100.

(28) Day, A. I.; Blanch, R. J.; Arnold, A. P.; Lorenzo, S.; Lewis, G. R.; Dance, I. *Angew. Chem. Int. Ed.* **2002**, *41*, 275-277.

(29) Isaacs, L.; Park, S. K.; Liu, S.; Ko, Y. H.; Selvapalam, N.; Kim, Y.; Kim, H.; Zavalij, P. Y.; Kim, G. H.; Lee, H. S.; Kim, K. *J. Am. Chem. Soc.* **2005**, *127*, 18000-18001.

(30) Liu, S.; Kim, K.; Isaacs, L. *J. Org. Chem.* **2007**, *72*, 6840-6847.

(31) Huang, W. H.; Liu, S.; Zavalij, P. Y.; Isaacs, L. *J. Am. Chem. Soc.* **2006**, *128*, 14744-14745.

(32) Huang, W. H.; Zavalij, P. Y.; Isaacs, L. *Angew. Chem. Int. Ed.* **2007**, *46*, 7425-7427.

(33) Huang, W. H.; Zavalij, P. Y.; Isaacs, L. *Org. Lett.* **2008**, *10*, 2577-2580.

(34) Hwang, I.; Baek, K.; Jung, M.; Kim, Y.; Park, K. M.; Lee, D. W.; Selvapalam, N.; Kim, K. *J. Am. Chem. Soc.* **2007**, *129*, 4170-4171.

(35) Mukhopadhyay, P.; Wu, A.; Isaacs, L. *J. Org. Chem.* **2004**, *69*, 6157-6164.

(36) Liu, Y.; Flood, A. H.; Bonvallet, P. A.; Vignon, S. A.; Northrop, B. H.; Tseng, H.-R.; Jeppesen, J. O.; Huang, T. J.; Brough, B.; Baller, M.; Magonov, S.; Solares, S. D.; Godard, W. A.; Ho, C.-M.; Stoddart, J. F. *J. Am. Chem. Soc.* **2005**, *127*, 9745-9759.

(37) Chakrabarti, S.; Mukhopadhyay, P.; Lin, S.; Isaacs, L. *Org. Lett.* **2007**, *9*, 2349-2352.

(38) Liu, S.; Zavalij, P. Y.; Lam, Y. F.; Isaacs, L. *J. Am. Chem. Soc.* **2007**, *129*, 11232-11241.

(39) Michelsen, U.; Hunter, C. A. *Angew. Chem. Int. Ed.* **2000**, *39*, 764-767.

(40) Simic, V.; Bouteiller, L.; Jalabert, M. *J. Am. Chem. Soc.* **2003**, *125*, 13148-13154.

(41) Gabriel, G. J.; Sorey, S.; Iverson, B. L. *J. Am. Chem. Soc.* **2005**, *127*, 2637-2640.

(42) Praetorius, A.; Bailey, D. M.; Schwarzlose, T.; Nau, W. M. *Org. Lett.* **2008**, *10*, 4089-4092.

(43) Reczek, J. J.; Kennedy, A. A.; Halbert, B. T.; Urbach, A. R. *J. Am. Chem. Soc.* **2009**, *131*, 2408-2415.

(44) lagona, J.; Mukhopadhyay, P.; Chakrabarti, S.; Zavalij, P. Y.; Isaacs, L. *Angew. Chem. Int. Ed.* **2005**, *44*, 4844-4870.

(45) Liu, S.; Ruspic, C.; Mukhopadhyay, P.; Chakrabarti, S.; Zavalij, P. Y.; Isaacs, L. *J. Am. Chem. Soc.* **2005**, *127*, 15959-15967.

(46) Refharsky, M. V.; Mori, T.; Yang, C.; Ko, Y. H.; Selvapalam, N.; Kim, H.; Sobransingh, D.; Kaifer, A. E.; Liu, S.; Isaacs, L.; Chen, W.; Moghaddam, S.; Gilson, M. K.; Kim, K.; Inoue, Y. *Proc. Natl. Acad. Sci. U. S. A.* **2007**, *104*, 20737-20742.

(47) Kim, K.; Kim, D.; Lee, J. W.; Ko, Y. H.; Kim, K. *Chem. Commun.* **2004**, 848-849.

(48) Lee, J. W.; Kim, K.; Choi, S. W.; Ko, Y. H.; Sakamoto, S.; Yamaguchi, K.; Kim, K. *Chem. Commun.* **2002**, *22*, 2692-2693.

(49) Park, K. M.; Kim, S. Y.; Heo, J.; Whang, D.; Sakamoto, S.; Yanaguchi, K.; Kim, K. *J. Am. Chem. Soc.* **2002**, *124*, 2140-2147.

(50) Ko, Y. H.; Kim, K.; Kang, J. K.; Chun, H.; Lee, J. W.; Sakamoto, S.; Yamaguchi, K.; Fettinger, J. C.; Kim, K. *J. Am. Chem. Soc.* **2004**, *126*, 1932-1933.

(51) Kim, S.-Y.; Ko, Y. H.; Lee, J. W.; Sakamoto, S.; Yamaguchi, K.; Kim, K. *Chem.- An Asian J.* **2007**, *2*, 747-754.

(52) Nally, R.; Isaacs, L. *Tetrahedron* **2009**, *In Press*.

(53) Mock, W. L.; Shih, N.-Y. *J. Am. Chem. Soc.* **1989**, *111*, 2697-2699.

(54) Mock, W. L.; Shih, N.-Y. *J. Org. Chem.* **1983**, *48*, 246-257.

(55) Lee, J. W.; Samal, S.; Selvapalam, N.; Kim, H.-J.; Kim, K. *Acc. Chem. Res.* **2003**, *36*, 621-630.

(56) Mock, W. L.; Shih, N.-Y. *J. Org. Chem.* **1986**, *51*, 4440-4446.

(57) Ko, Y. H.; Kim, E.; Hwang, I.; Kim, K. *Chem. Commun.* **2007**, *13*, 1305-1315.

(58) Mohanty, J.; Pal, H.; Ray, A. K.; Kumar, S.; Nau, W. M. *Chem. Phys. Chem.* **2007**, *8*, 54-56.

(59) Wheate, N. J.; Buck, D. P.; Day, A. I.; Collins, J. G. *Dalton Trans.* **2006**, 451-458.

(60) Liu, S.; Zavalij, P. Y.; Lam, Y. F.; Isaacs, L. *J. Am. Chem. Soc.* **2007**, *129*, 11232-11241.

(61) Wang, W.; Kaifer, A. E. *Angew. Chem. Int. Ed.* **2006**, *45*, 7042-7046.

(62) Brunsveld, L.; Folmer, B. J. B.; Meijer, E. W.; Sijbesma, R. P. *Chem. Rev.* **2001**, *101*, 4071-4097.

(63) Lehn, J.-M. *Prog. Poly. Sci.* **2005**, *30*, 814-831.

(64) Zhao, D.; Moore, J. S. *Org. Biomol. Chem.* **2003**, *1*, 3471-3491.

(65) Hofmeier, H.; Schubert, U. S. *Chem. Commun.* **2005**, 2423-2432.

(66) Pollino, J. M.; Weck, M. *Chem. Soc. Rev.* **2005**, *34*, 193-207.

(67) Corbin, P. S.; Lawless, L. J.; Li, Z.; Ma, Y.; Witmer, M. J.; Zimmerman, S. C. *Proc. Natl Acad. Sci. U.S.A.* **2002**, *99*, 5099-5104.

(68) Bouteiller, L. *Adv. Poly. Sci.* **2007**, *207*, 79-112.

(69) Huang, F.; Nagvekar, D. S.; Zhou, X.; Gibson, H. W. *Macromolecules* **2007**, *40*, 3561-3567.

(70) Ishida, Y.; Aida, T. *J. Am. Chem. Soc.* **2002**, *124*, 14017-14019.

(71) Serpe, M. J.; Craig, S. L. *Langmuir* **2007**, *23*, 1626-1634.

(72) Berl, V.; Schmutz, M.; Krische, M. J.; Khoury, R. G.; Lehn, J.-M. *Chem Eur. J.* **2002**, *8*, 1227-1244.

(73) Beck, J. B.; Rowan, S. J. *J. Am. Chem. Soc.* **2003**, *125*, 13922-13923.

(74) Miyauchi, M.; Takashima, Y.; Yamaguchi, H.; Harada, A. *J. Am. Chem. Soc.* **2005**, *127*, 2984-2989.

(75) Miyauchi, M.; harada, A. *J. Am. Chem. Soc.* **2004**, *126*, 11418-11419.

(76) Ohga, K.; Takashima, Y.; takahashi, H.; Kawaguchi, Y.; yamaguchi, H.; Harada, A. *Macromolecules* **2005**, *38*, 5897-5904.

(77) Jeon, W. S.; Moon, K.; Park, S. H.; Chun, H.; Ko, Y. H.; Lee, J. Y.; Lee, E. S.; Samal, S.; Selvapalam, N.; Rekharsky, M. V.; Sindelar, V.; Sobransingh, D.; Inouem Y.; Kaifer, A. E.; Kim, K. *J. Am. Chem. Soc.* **2005**, 1*27*, 12984-12989.

(78) Liu, Y.; Shi, J.; Chen, Y.; Ke, C.-F. *Angew. Chem. Int. Ed.* **2008**, *47*, 7293-7296.

(79) Eelkema, R.; Maeda, K.; Odell, B.; Anderson, H. L. *J. Am. Chem. Soc.* **2007**, *129*, 12384-12385.

(80) Corma, A.; Garcia, H.; Montes-Navajas, P. *Tetrahedron Lett.* **2007**, *48*, 4613-4617.

(81) Choi, S. W.; Ritter, H. *Macromol. Rapid Commun.* **2007**, *28*, 101-108.

(82) Liu, Y.; Ke, C.-F.; Zhang, H.-Y.; Wu, W.-J.; Shi, J. *J. Org. Chem.* **2007**, *72*, 280-283.

(83) Hou, Z.-S.; Tan, Y.-B.; Kim, K.; Zhou, Q.-F. *Polymer* **2006**, *47*, 742-750.

(84) Tan, Y.; Chiu, S.; Lee, J. W.; Ko, Y. H.; Kim, K. *Macromolecules* **2002**, *35*, 7161-7165.

(85) Choi, S.; Lee, J. W.; Ko, Y. H.; Kim, K. *Macromolecules* **2002**, *35*, 3526-3531.

(86) Tuncel, D.; Steinke, J. H. G. *Chem. Commun.* **1999**, 1509-1510.

(87) Meschke, C.; Buschmann, H.-J.; Schollmeyer, E. *Polymer* **1998**, *40*, 945-949.

(88) Lee, J. W.; Ko, Y. H.; Park, S.-H.; Yamaguchi, K.; Kim, K. *Angew. Chem. Int. Ed.* **2001**, *40*, 746-749.

(89) Kim, D.; Kim, E.; Kim, J.; Park, K. M.; Baek, K.; Jung, M.; Ko, Y. H.; Sung, W.; Kim, H. S.; Suh, J. H.; Park, C. G.; Na, O. S.; Lee, D.-K.;Lee, K. E.; Han, S. S.; Kim, K. *Angew. Chem. Int. Ed.* **2007**, *46*, 3471-3474.

(90) de Greef, T. F. A.; Ercolani, G.; Ligthart, G. B. W. L.; Meijer, E. W.; Sijbesma, R. P. *J. Am. Chem. Soc.* **2008**, *130*, 13755-13764.

(91) The solutions for ^{1}H NMR were prepared by stirring an excess of solid bis-*ns*-CB[10] with a solution of known concentration of guest. Integration of the resonances for host and guest allowed a determination of the relative stoichiometry (n:n).

(92) Cohen, Y.; Avram, L.; Frish, L. *Angew. Chem. Int. Ed.* **2005**, *44*, 520-554.

(93) Chakrabarti, S.; Isaacs, L. *Supramol. Chem.* **2008**, *20*, 191-199.

(94) The methylated N-atoms of **II-4** destabilize the bis-*ns*-CB[10]•**II-4** complex due to steric interactions with the ureidyl C=O portals of the host.

(95) Kim's group previously reported a cyclic pentamer formed between CB[8] and a guest containing two binding groups. We suspect that the aggregates described here may be structurally similar. See: Ko, Y. H.; Kim, K.; Kang, J.-

K.; Chun, H.; Lee. J. W.; Sakamoto, S.; Yamaguchi, K.; Fettinger, J. C.; Kim. K. *J. Am. Chem. Soc.* **2004**, *126*, 1932-1933.

(96) Teller, D. C.; Swanson, E.; de Haen, C. *Methods Enzymol.* **1979**, *113*, 103-124.

(97) Bookser, B. C.; Bruice, T. C. *J. Am. Chem. Soc.* **1991**, *113*, 4208-4218.

(98) We would have expected a slower diffusion coefficient for the purely dimeric complex bis-*ns*-CB[10]•**II-8**$_2$ which suggests that 1:1 complex bis-*ns*-CB[10]•**II-8** may also be present in this solution.

(99) We confirmed a spacing of 0.33 *m/z* units which supports our formulation of a 3^+ ion. We also observed an ion of substantial intensity fot the 5^+ state.

(100) The NMR samples are prepared from solid host and a solution of guest. The excess unbound host bis-*ns*-CB[10] remains insoluble and is removed before transferring the solution to an NMR tube for analysis.

(101) For a more complete description of this top-center isomerism and experimental observation of the diastereomers in simpler systems see reference 31. If homotropic allostery is not followed then an additional 12 diastereomers are possible.

(102) Sobransingh, D.; Kaifer, A. E. *Org. Lett.* **2006**, *8*, 3247-3250.

(103) Yuan, L.; Wang, R.; Macartney, D. *J. Org. Chem.* **2007**, *72*, 4539-4542.

(104) Liu, Y.; Li, X.-Y.; Zhang, H.-Y.; Li, C.-J.; Ding, F. *J. Org. Chem.* **2007**, *72*, 3640-3645.

(105) Dawson, R. E.; Lincoln, S. F.; Easton, C. J. *Chem. Commun.* **2008**, 3980-3982.

(106) Chuang, C.-J.; Li, W.-S.; Lai, C.-C.; Liu, Y.-H.; Peng, S.-M.; Chao, I.; Chiu, S.-H. *Org. Lett.* **2008**, *11*, 385-388.

(107) We believe that the dominant diatereomer of bis-*ns*-CB[10]•**II-8**$_2$•CB[6] is the top-top diastereomer depicted. The alternate center-center diastereomer would suffer from increased repulsive interactions between ureidyl carbonyl portals of CB[6] and bis-*ns*-CB[10].

(108) Jiang, W.; Winkler, H. D. F.; Schalley, C. A. *J. Am. Chem. Soc.* **2008**, *130*, 13852-13853.

(109) Stevens, M. P. *Polymer Chemistry*; 3rd ed.; Oxford University Press: New York, 1999.

(110) Curti, D. G.; Gretsch, C.; Labbe, D. P.; Redgwell, R. J.; Schoonman, J. H.; Ubbink, J. B.; Organization, W. I. P., Ed. 2005.

(111) Velten, U.; Rehahn, M. G. S. *Chem. Commun.***1996**, 2639-2640.

(112) Bladon, P.; Griffin, A. C. *Macromolecules* **1993**, *26*, 6604-6610.

(113) Gulik-Krzywicki, T.; Fouquey, C.; Lehn, J.-M. *Proc. Natl. Acad. Sci. U.S.A.* **1993**, *90*, 163-167.

(114) Markovitsi, D.; Bengs, H.; Ringsdorf, H. *J. Chem. Soc., Faraday Trans.* **1992**, *88*, 1275-1279.

(115) Li, G.; McGown, L. B. *Science* **2005**, *38*, 3724-3730.

(116) Hasegawa, Y.; Miyauchi, M.; Takashima, Y.; Yamaguchi, H.; Harada, A. *Macromolecules* **2005**, *38*, 3724-3730.

(117) Isaacs, L. *Chem. Commun.* **2009**, 619-629.

(118) Dantz, D. A.; Meschke, C.; Buschmann, H.-J.; Schollmeyer, E. *Supramol. Chem.* **1998**, *9*, 79-83.

(119) Kornmuller, A.; Karcher, S.; Jekel, M. *Water Res.* **2001**, *35*, 3317-3324.

(120) Lee, J. J. C.; Kim, K.; Kim, K. *Chem. Commun.* **2001**, 1042-1043.

(121) Ong, W.; Gómez-Kaifer, M.; kaifer, A. E. *Org. Lett.* **2002**, *4*, 1791-1794.

(122) Kim, K.; Jeon, W. S.; Kang, J. K.; Lee, J. W.; Jon, S. Y.; Kim, T.; Kim. K. *Angew. Chem. Int. Ed.* **2003**, *42*, 2293-2296.

(123) Sokolov, M.; Virovets, A.; Dybtsev, D.; Gerasko, O.; Fedin, V.; Hernandez-Molina, R.; Clegg, W.; Sykes, A. *Angew. Chem. Int. Ed.* **2000**, *39*, 1659-1661.

(124) Mirenda, M.; Dicelio, L. E.; San Román, E. *J. Phys.: Condens. Matter* **2008**, *112*, 12201-12207.

(125) McAloney, R. A.; Sinyor, M.; Dudnik, V.; Goh, M. C. *Langmuir* **2001**, *17*, 6655-6663.

(126) Grønbeck-Jensen, N.; Mashl, R. J.; Bruinsma, R. F.; Gelbart, W. M. *Phys. Rev. Lett.* **1997**, *78*, 2477-2480.

(127) Guaqueta, C.; Luijten, E. *Phys. Rev. Lett.* **2007**, *99*, 1383021-1383024.

(128) Schmidt, B.; Wandrey, C.; Freitag, R. *J. Chromatogr., A* **2002**, *944*, 149-159.

(129) Mertz, D.; Hemmerlé, J.; Mutterer, J.; Ollivier, S.; Voegel, J. C.; Schaaf, P.; Lavalle, P. *Nano Lett.* **2007**, *7*, 657-662.

(130) Higo, M.; Lu, X.; Mazur, U.; Hipps, K. *Chem. Lett.* **1999**, 679-680.